

Miller Y Comment of the Comment of t

# MODIFICATION OF POLYLACTIDE VIA REACTIVE EXTRUSION

by

Denise Lynn Carlson

## A THESIS

Submitted to
Michigan State University
in partial fulfillment of the requirements
for the degree of

**MASTER OF SCIENCE** 

Department of Chemical Engineering

## **ABSTRACT**

# MODIFICATION OF POLYLACTIDE VIA REACTIVE EXTRUSION

by

#### Denise Lynn Carlson

The branching of polylactide (PLA) by a free radical initiated reactive extrusion process has been accomplished. The addition of between 0.066 and 0.67 % maleic anhydride (MA) onto the PLA backbone was also performed to enhance the interfacial adhesion in PLA blends. Reaction conditions were varied from 160° to 200°C with initiator concentrations between 0.0 and 0.5 %. Characterization was performed using triple detection size exclusion chromatography, melt flow index, and various thermal analysis techniques. A decrease in both molecular weight and melt viscosity indicated that PLA without initiator had extensive thermal degradation. The optimum range for branching, indicated by a high molecular weight and low melt flow index polylactide, was found to be around 170°C to 180°C and 0.1 to 0.25 % initiator. Laser scanning confocal microscopy was evaluated for potential application in assessing polymer blends.



# **ACKNOWLEDGMENTS**

I wish to thank Dr. Li Nie, Dr. Philippe DuBois, and Dr. Ramani Narayan for their input in this research. I also wish to acknowledge Dr. Joanne Whallon for her assistance on the Laser Scanning Confocal Microscope and the Biomaterials group at the Michigan Biotechnology Institute for their help and suggestions. Material for this work was provided by Cargill Central Research, Minneapolis, MN.

# **TABLE OF CONTENTS**

Chapter		Page
		Number
	List of Tables	
	List of Figures	
	Nomenclature	xiv
1.	Introduction	
	1.1 Motivation	1
	1.2 Structure of Thesis	4
2.	Background and Literature Review	
	2.1 Terminology	6
	2.1.1 Molecular Weights	
	2.1.2 Chain Scission	
	2.1.3 Branching and Crosslinking	
	2.1.4 Gelation	
	2.1.5 Grafting	8
	2.1.6 Reactive Extrusion	
	2.2 Molecular Weight Determination	11
	2.2.1 End Group Analysis	
	2.2.2 Colligative Properties	11
	2.2.3 Light Scattering	
	2.2.4 Intrinsic Viscosity	
	2.2.6 Gel Permeation Chromatography	
	2.3 Free Radical Polymerization	
	2.3.1 General Mechanism of FRP	17
	2.3.2 Reactive Extrusion of FRP	
	2.3.3 Maleation	21
3.	Materials	
-	3.1 Polylactide	24
	3.1.1 Commercial Preparation	
	3.1.2 Applications	

	3.2 Lupersol 101	28
	3.3 Maleic Anhydride	
4	Durancius and Chamataniastics	
4.	Processing and Characterization	20
	4.1 Processing	
	4.1.1 Reactive Extrusion	
	4.1.2 Extrusion Conditions	
	4.2 Characterization	
	4.2.1 Gel Permeation Chromatography	
	4.2.2 Intrinsic Viscosity	
	4.2.3 Melt Flow Index	
	4.2.4 Differential Scanning Calorimetry	
	4.2.5 Thermal Gravimetric Analysis	
	4.2.6 Dynamic Mechanical Analysis	
	4.2.7 Titration	
	4.2.8 Scanning Electron Microscopy	
	4.2.9 Extraction	
	4.2.10 Moisture Analysis	46
5.	Free Radical Branching of PLA	
	5.1 Discussion of Results	47
	5.1.1 Effect of Extrusion Temperature	
	5.1.2 Effect of Initiator Concentration	
	5.1.3 Thermogravimetric Analysis	
	5.1.4 Differential Scanning Calorimetry	
	5.1.5 Dynamic Mechanical Analysis	
	5.1.6 Highly Branched Samples	
	5.1.7 Film Results	
	5.2 Proposed Reaction Mechanism	
6.	Maleation of PLA	
	6.1 Discussion of Results	81
	6.1.1 Effect of Extrusion Temperature	81
	6.1.2 Effect of Initiator Concentration	82
	6.1.3 Thermogravimetric Analysis	90
	6.2 Proposed Reaction Mechanism	
7	PLA Blends	
٠.	7.1 Blend Theory	05
	7.1.1 Miscibility	
	7.1.2 Compatibility	
	7.1.2 Companyinty	

	7.2 Materia	ıls	97
		Cellulose Acetate and its Derivatives	
	7.2.2	Polypropylene	98
		Poly(vinyl acetate)	
		Ethylene vinyl acetate copolymers	
		ent and Procedures	
	7.3.1	Solution Casting	100
	7.3.2	Haake Mixer	100
	7.4 Discuss	ion of Results	101
	7.4.1	Blends of PLA with CA, CAP, CAB	101
		Blends of PLA with PP	
		Blends of PLA with PVA	
		Blends of PLA with EVAC Copolymers	
		Blends of PLA with Starch	
8.	Related Wor	rk	
	8.1 LSCM I	Background	107
		Matrix with Protein Filler	
		ed Modified Starch with Talc Filler	
9.	Conclusions	and Recommendations	
	9.1 Conclus	sions	122
		nendations	
Aj	ppendix Ra	w Data	128
Ri	hliography		140

# LIST OF TABLES

Page Number	
Relationship of various polymer properties to molecular weight (MW) and molecular weight distribution (MWD).	1.1
Temperature settings for free radical branching	4.1
Temperature settings for maleation	4.2
Free radical branching of PLA: MP load%, melt viscosity, and TriSEC51	5.1
Decomposition temperatures from thermogravimetric analysis58	5.2
DSC results: 10°C/min to 200°C	5.3
T <sub>G</sub> averages for dynamic mechanical analysis	5.4
Highly brached sample comparison to unextruded PLA72	5.5
Tensile Results for PLA film	5.6
Maleation of PLA: MP load%, melt viscosity, TriSEC, and % maleation	5.1
Maleation decomposition temperatures from thermogravimetric analysis.	5.2
ELVAX properties	7.1
Glass transition temperatures for PLA/PVA blends 103	7 2

A.1	Branched data from TriSEC (triple detector size exclusion chromatography).	129
A.2	Ubbelhode viscometry experiments.	134
A.3	Polylactide film results.	135
A.4	Maleation data from TriSEC.	136
A.5	Titration results of maleated samples.	139

# **LIST OF FIGURES**

	Page Number
2.1	Flow of dilute polymer solution in a capillary
2.2	Schematic of Ubbelhode viscometer
3.1	Commercial preparation of polylactide
3.2	Lupersol 101 [2,5-dimethyl-2,5-di-(t-butylperoxide)]
3.3	Maleic anhydride (MA), [C <sub>4</sub> H <sub>2</sub> O <sub>3</sub> ]
4.1	Baker Perkins twin screw extruder (Composite Materials and Structures Center, MSU).
4.2	Co-rotating twin screw configuration
4.3	TriSEC flow loop
4.4	Orion 960 Autochemistry system. 43
4.5	SEM image formation
5.1	DV chromatograph showing the shift in molecular weight distribution of unextruded (higher M.W.) and extruded (lower M.W.) PLA. (normalized to concentration)
5.2	DV chromatograph showing the shift in molecular weight distribution of PLA extruded at 160°C with increasing L101 content. (normalized to concentration)

5.3	DV chromatograph showing the shift in molecular weight distribution of PLA extruded at 170°C with increasing L101 content. (normalized to concentration)
5.4	DV chromatograph showing the shift in molecular weight distribution of PLA extruded at 180°C with increasing L101 content. (normalized to concentration)
5.5	MFI of extruded samples showing a decrease in MFI with increasing L101 content
5.6	TGA showing decomposition temperature for branched PLA with 0.1% L101.
5.7	TGA for pure PLA compared to extruded PLA with 0.5% L10160
5.8	TGA for free radical branched PLA at 170°C
5.9	TGA for free radical branched PLA at 200°C
5.10	Compilation of DSC results for T <sub>G</sub> comparison
5.11	Storage modulus for several samples as given by DMA67
5.12	Loss modulus for several samples as given by DMA
5.13	Tan delta (tan δ) for several samples as given by DMA
5.14	Mark-Houwink plot of the 170°C series
5.15	A comparison of light scattering chromatographs of PLA (top) and 190°/0.5 (bottom)
5.16	Peroxide decomposition
5.17	Proposed branching mechanism
5.18	Chain scission reactions
6 1	Weight percent maleation as a function of initiator concentration 86

6.2	DV chromatograph of 180°C series showing molecular weight distribution. (normalized to concentration)
6.3	DV chromatograph of 200°C series showing molecular weight distribution. (normalized to concentration)
6.4	MFI of maleated samples.
6.5	Proposed mechanism for the maleation of PLA
7.1	Comparison of PP and PLA
7.2	Poly(vinyl acetate)98
7.3	SEM micrograph of 70% CAP and 30% PLA showing immiscibility 102
7.4	SEM micrograph of 60% PLA and 40% starch blend showing poor interfacial adhesion.
7.5	SEM micrograph of 70% PLA and 30% starch blend with 0.5% L101 showing partial interfacial adhesion
7.6	SEM micrograph of 70% maleated PLA and 30% starch showing good interfacial adhesion
8.1	LSCM image production
8.2	SEM micrograph of potato showing cell wall and starch granules 113
8.3	LSCM photograph of densified potato showing zein penetration 115
8.4	LSCM photograph of densified potato showing diffusion of zein along crack.
8.5	LSCM photograph of densified potato (inner cross-section)
8.6	SEM X-ray peaks for the modified starch with talc blend

8.7	SEM micrograph showing the surface of the modified starch with talc blend.	121
8.8	SEM dot map of the X-ray analysis for Silicon.	121

# **NOMENCLATURE**

CA	. cellulose acetate
CAB	. cellulose acetate butyrate
CAP	. cellulose acetate propionate
CHCl <sub>3</sub>	. chloroform
CH <sub>2</sub> Cl <sub>2</sub>	. methylene chloride
DMA	. dynamic mechanical analysis
DSC	differential scanning calorimetry (or calorimeter)
EVAC	. ethylene vinyl acetate copolymers
FDA	. food and drug administration
FRP	. free radical polymerization
GPC	. gel permeation chromatography (or chromatograph)
HC1	. hydrogen chloride
L101	. lupersol 101
LSCM	. laser scanning confocal microscope (or microscopy)
MA	. maleic anhydride
MeOH	. methanol
MFI	. melt flow index
NaOH	. sodium hydroxide
PE	. polyethylene
PLA	. polylactide (or polylactic acid)
PP	. polypropylene
PS	. polystyrene
PVA	. polyvinyl acetate
RALLS	. right angle laser light scattering
SEC	size exclusion chromatography (or chromatograph)
SEM	. scanning electron microscopy (or microscope)
TGA	. thermogravimetric analysis
THF	. tetrahydrofuran
TriSEC	triple detector size exclusion chromatography

9	. Mark-Houwink parameter
	•
A <sub>2</sub>	
C,c	
	. refractive index increment
$\Delta G_m$	. free energy of mixing
ΔH <sub>m</sub>	. enthalpy of mixing
ΔΡ	. pressure change
ΔS <sub>m</sub>	entropy of mixing
g	- · · · · ·
<b>G</b> '	
G"	
I <sub>o</sub>	
	scattering intensity for solution
	scattering intensity for solvent
	optical constant or Mark-Houwink parameter
L	
	. molecular weight of polymer type "i"
	number average molecular weight
M <sub>peak</sub>	
	viscosity average molecular weight
	weight average molecular weight
N <sub>a</sub>	
	normality of hydrogen chloride
	number of molecules of polymer type "I"
n <sub>o</sub>	refractive index of solvent
	refractive index of solution
N <sub>mor</sub>	normality of morpholine
P(θ)	particle scattering function
Q	volumetric flow rate
R	gas constant
R <sub>g</sub>	
R <sub>θ</sub>	. Rayleigh ratio
r	
r <sub>c</sub>	
t, t <sub>0</sub>	
T	
	glass transition temperature
	ratio of storage to loss moduli
V	<del>-</del>
	volume of hydrogen chloride
V <sub>mor</sub>	
v <sub>i</sub>	molar volume of polymer type "i"

	. scattered volume
α	. viscometer constant
χ	polymer-polymer interaction parameter
φι	volume fraction of polymer type "i"
λ <sub>o</sub>	incident beam wavelength
η	solution viscosity
η <sub>0</sub>	solvent viscosity
η <sub>rel</sub>	relative viscosity
η <sub>sp</sub>	specific viscosity
[η]	intrinsic viscosity
θ	· · · · · · · · · · · · · · · · · · ·
ρ	•

## INTRODUCTION

## 1.1 Motivation

Polylactide (PLA) is an important biodegradable polymer which has been used in such established applications as medical implants [Gilding (1982)], sutures [Conn et al. (1974), Schmitt et al. (1967)], and drug delivery systems [Heller (1985)]. As the need for biodegradable polymers in the context of designing materials for the environment opens up new market opportunities [Narayan (1992)], polylactide polymers are finding commercial use in single-use disposal items. However, one of the limitations for using PLA is its processing instability. Gogolewski (1993) has shown that the degradation of PLA already occurs at 160°C under injection molding. Another shortcoming of PLA is its very low melt viscosity which may limit its blow molding processibility. The free radical branching of PLA could offer the opportunity for enhancement of physical and chemical properties and/or improvements of processibility by increasing the molecular weight in order to compensate for the molecular weight decrease by processing degradation and by increasing the melt viscosity. Table 1.1 shows how various properties are affected by the molecular weight and molecular weight distribution of a polymer.

Table 1.1: Relationship of various polymer properties to molecular weight (MW) and molecular weight distribution (MWD). Key: + property increases, - property decreases, \* little change. [Yau et al. (1979)].

Property	Increase MW	Narrow MWD
Tensile Strength	+	+
Elongation	+	-
Yield Strength	+	-
Toughness	+	+
Brittleness ,	+	-
Hardness	+	-
Abrasion Resistance	+	+
Softening Temperature	+	+
Melt Viscosity	+	+
Adhesion	-	-
Chemical Resistance	+	+
Solubility	-	*

The proposed free radical process is very simple and easy to manage by reactive extrusion in the presence of trace amounts of free radical initiators. Free radical polymerization via reactive extrusion has been done extensively on polypropylene and polyethylene systems leading to controlled degradation [Suwanda et al. (1989)] and branching [Suwanda et al. (1988a)], respectively.

Combining PLA with natural materials and synthetic polymers provides ways of cost reduction and combined properties. Unfortunately, simple PLA composites with natural materials and polyblends have poor properties because of the lack of

interfacial adhesion. Introducing new functional groups onto the polylactide backbone paves the way to prepare composites, laminates, coated items, and blends/alloys with improved properties and cost effectiveness. Functionalizing the matrix polymer and the fiber/filler with highly reactive groups is perhaps the most successful strategy leading to a variety of commercial composites and alloys made by reactive processing. In this study, the addition of maleic anhydride (MA) to the PLA polymer backbone has been accomplished.

The purpose of this research is to investigate the results of the free radical initiated branching of PLA extruded at temperatures ranging from 160°C to 200°C with an initiator concentration between 0.0 and 0.5 percent. Free radical initiated maleation of PLA was also done using 2 percent MA with similar temperature and concentration ranges. The modified PLA samples were characterized by several analytical methods including gel permeation chromatography (GPC), right angle laser light scattering (RALLS), melt flow index (MFI), and thermal gravimetric analysis (TGA). Based on the analytical results, the chemical modification may then be characterized as chain scission, branching, crosslinking or any combination of the three. A proposed reaction mechanism is also included.

## **1.2 Structure of Thesis**

The basic concepts used in this work are not novel, but together they comprise a novel way of processing polylactide including branching and maleation. The first part of this thesis details some of the techniques which were incorporated. Chapter 2 provides background information on polymers in general, including molecular weight analysis which is extremely important for this research. A literature review on polymers which have been processed by free radical polymerization via reactive extrusion is provided as well. Previous applications include polyethylene and polypropylene. A brief description of the materials which were used is located in Chapter 3.

Chapter 4 details the processing and characterization methods which were used.

Specific equipment information as well as sample preparation can also be found.

The heart of the work is contained in Chapter 5, the free radical branching of PLA, and Chapter 6, the maleation of PLA. These chapters discuss the results of all pertinent analytical tests. A proposed reaction mechanism is also provided. Since polylactide resin by itself may be quite expensive for commercial use, PLA blends were also formulated. Chapter 7 briefly describes blend theory and blending

methods. SEM micrographs of several blends are shown with a discussion of these preliminary results.

Related work (Chapter 8) was done on the applications of Laser Scanning Confocal Microscopy (LSCM) for use in polymer blend systems. Traditionally, Scanning Electron Microscopy (SEM) is used to evaluate polymer morphology, but sample preparation may sometimes create artifacts in the sample. However, LSCM provides a noninvasive technique for observing polymer morphology as sample preparation is minimum.

Chapter 9 contains all pertinent conclusions, as well as several recommendations for further work.

# **BACKGROUND AND LITERATURE REVIEW**

# 2.1 Terminology

## 2.1.1 Molecular Weights

In general, a polymer is a heterogeneous material with a wide range of molecular weights. This molecular weight distribution can be characterized by the polydispersity of the polymer. Polydispersity is defined as the ratio  $M_w/M_n$ . A wider distribution of molecular weights gives a larger polydispersity since the contribution of each molecule to the number average molecular weight,  $M_n$ , is proportional to its mass (Equation 2.1), and its contribution to the weight average molecular weight,  $M_w$ , is proportional to the square of its mass (Equation 2.2).

$$M_{n} = \frac{\sum_{i=1}^{\infty} N_{i} M_{i}}{\sum_{i=1}^{\infty} N_{i}}$$
 (2.1)

$$M_{w} = \frac{\sum_{i=1}^{\infty} N_{i} M_{i}^{2}}{\sum_{i=1}^{\infty} N_{i} M_{i}}$$
 (2.2)

$$\mathbf{M}_{v} = \left(\frac{\sum_{i=1}^{\sigma} N_{i} M_{i}^{(1-a)}}{\sum_{i=1}^{\sigma} N_{i} M_{i}}\right)^{1-a}$$
(2.3)

where  $N_i$  is the number of molecules of type i and  $M_i$  is the molecular weight of molecule type i. The viscosity average molecular weight,  $M_v$ , is also given (Equation 2.3), where "a" is a property of the polymer-solvent system with a value typically between 0.5 and 0.8 [Sperling].

## 2.1.2 Chain Scission

Polymer chain degradation, or chain scission, usually occurs when chemical bonds along the polymer backbone break. This degradation causes a reduction in the molecular weight of the polymer which results in an increase in the melt flow index. The molecular weight distribution becomes more random with a polydispersity approaching two. Since polymers with a high molecular weight have a greater number of bonds, they experience preferential chain scission. Therefore, for broad molecular weight distributions, as the molecular weight decreases, the molecular weight distribution narrows.

# 2.1.3 Branching and Crosslinking

Free radical branching of a polymer occurs when two radical centers on the polymer backbone terminate by combination. This long chain branching process can continue until a three-dimensional network is formed. The polymer is then said to be crosslinked consisting of various levels of sol ("free" polymer) and gel (networked polymer).

Long chain branching produces a high molecular weight polymer which has an increased melt viscosity. It is generally undesirable to form a crosslinked polymer via reactive extrusion as the crosslinked gel may damage the extruder.

## 2.1.4 Gelation

The gelation of a polymer is undesirable for processing. At the gel point various phenomena occur: (1) the viscosity diverges to infinity, i.e. there is a transition from a viscous liquid to an elastic solid, (2) the weight average molecular weight diverges to infinity, and (3) an insoluble gel phase appears.

# 2.1.5 Grafting

The grafting of polymer chains is used to enhance the properties of polymer blends. Grafting occurs when the polymer, peroxide (used as the free radical initiator), and the grafting compound are processed in an extruder. In this study, maleic anhydride (MA) has been grafted to the polymer backbone. This process is commonly referred to as maleation. The addition of MA to the polymer enhances the compatibility and interfacial adhesion of various polymer blends. This is discussed in some detail in Section 2.2.3, as well as Chapter 6.

## 2.1.6 Reactive Extrusion

Reactive extrusion refers to an extrusion process whereby the extruder is used as a chemical reactor [Brown and Orlando (1988)]. In reactive extrusion, the extruder may be considered a continuous flow reactor in which the absence of a solvent medium provides an advantage over other reactive processes. Another advantage of a reactive extruder is that several chemical process operations, such as mixing, reacting, and shaping of a material, are combined into one piece of equipment. Other advantages of reactive extrusion over conventional polymerization techniques include: (1) carefully controllable residence time distributions and temperature profiles; (2) the production of variable size batches with very short start-up and change over times; and (3) the extruders ability to easily process high viscosity materials [Pabedinskas et al. (1989)]. Since very viscous materials may be reacted or produced, lower reaction temperatures may be used and a higher degree of branching may be accomplished.

Several types of chemical reactions may be performed by reactive extrusion [Brown and Orlando (1989)].

- Bulk polymerization reactions used to prepare high molecular weight polymer from monomer or low molecular weight polymer.
- Graft reactions resulting in a graft copolymer of a polymer and monomer feed.
- Inter-chain formations of two or more polymers forming a copolymer.
- Coupling reactions of a homopolymer plus a branching agent to increase the molecular weight by chain extension or branching.
- Functionalization reactions in which functional groups are introduced to the polymer backbone.
- Controlled molecular weight degradation in which high molecular weight polymers are reduced to lower molecular weights. Three types of degradation may occur [Rauwendaal (1986)]:
  - Thermal degradation: depolymerization, random chain scission, and unzipping of substituent groups.
  - Mechanical degradation: shear and/or elongational stress.
  - Chemical degradation: such as hydrolysis or oxidation.

Conventional extruders commercially available include single-screw or twinscrew. Twin-screw extruders may be intermeshing or non-intermeshing, corotating or counter-rotating [Rauwendaal (1986)]. The extruder which was used for this research was a co-rotating, intermeshing, twin-screw extruder.

# 2.2 Molecular Weight Determination

Polymer molecular weights may be determined by several experimental methods.

A brief description of some of these approaches follows.

## 2.2.1 End Group Analysis

The polymer is dissolved into a solvent and titrated for functional groups. This technique is very sensitive to impurities and is only good for low molecular weights (<5000 g/mol).

# 2.2.2 Colligative Properties

A number of colligative properties can be measured and a corresponding molecular weight, in this case  $M_n$ , can be calculated. A dilute polymer solution ( $\leq 0.1$  wt%) is used for the following techniques: (1) boiling point elevation, (2) freezing point depression, (3) vapor pressure lowering, and (4) osmotic pressure.

## 2.2.3 Light Scattering

Light scattering is a technique used for determining the weight average molecular weight. Light interacts with a molecule and is scattered. This scattered light is referred to as Rayleigh scattering and has the same wavelengh of that of the incident light beam. The information about the size and molecular weight of a polymer is experimentally determined from the light scattering intensity which is above that of the solvent background. This excess light intensity caused by the polymer molecules in solution is directly related to the M<sub>w</sub> of the polymer and the sample concentration (C).

$$\frac{KC}{R_{\theta}} = \frac{1}{M_{\text{W}} P(\theta)} + 2A_2 C \qquad (2.4)$$

The K term in equation 2.4 is an optical constant

$$K = \frac{2\pi^2 n_o^2}{\lambda_o^4 N_a} * \left(\frac{dn}{dc}\right)^2$$
 (2.5)

where n is the refractive index of the medium,  $\lambda_o$  is the wavelength of the incident beam,  $N_a$  is Avagadro's number, and dn/dc is the refractive index increment. The excess Rayleigh ratio,  $R_\theta$ , gives the normalized scattering intensity with respect to the scattered volume, distance, and incident intensity,  $I_o$ :

$$R_{\theta} = (I_{\theta \text{soln}} - I_{\theta \text{solv}}) * r^2 / I_{\theta} v$$
 (2.6)

The  $A_2$  term is the second virial coefficient which will be set equal to zero for this study. The term  $P(\theta)$  in equation 2.4 is the particle scattering function.  $P(\theta)$  is a

function of the geometry and size of the polymer molecules with respect to the wavelength of the incident light. For random coil polymers,  $P(\theta)$  is the following:

$$P(\theta) = \frac{2}{X^2} [e^{-X} - (1 - X)]$$
 (2.7)

where

$$X = \frac{8}{3} * \left(\frac{\pi n}{\lambda} * R_g * \sin \theta / 2\right)^2$$
 (2.8)

and R<sub>g</sub> is the radius of gyration.

# 2.2.4 Intrinsic Viscosity

Intrinsic viscosity measurements are done in a capillary tube with a dilute solution and result in the viscosity average molecular weight  $(M_v)$ . The flow rate, and hence the shear rate, through the capillary is dependent upon the distance from the capillary edge. In dilute solutions, the polymer coils are expanded and thus different shear rates are felt by the polymer resulting in an increase in frictional drag and rotational forces on the molecule (Figure 2.1). This dynamic work results in an increased solution viscosity.

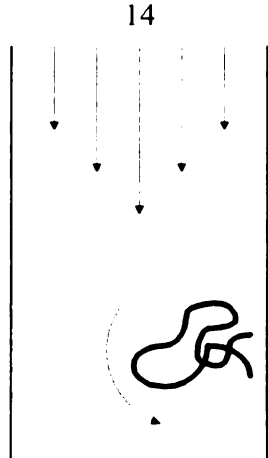


Figure 2.1: Flow of dilute polymer solution in a capillary.

The solvent viscosity,  $\eta_0$ , and the solution viscosity,  $\eta$ , are both measured in the Ubbelhode capillary viscometer (Figure 2.2). The flow through the capillary controls the time for the bulb to drain. The time for the bulb to drain can be related to the viscosity of the solution using Hagen-Poisulle's law for laminar flow:

$$Q = \frac{\pi r_c^4 \Delta P}{8 \eta L} = \frac{dV}{dt}$$

Where

$$\Delta P = 1 \rho g$$

Substituting  $\Delta P$  into Hagen-Poisulle's law and integrating results in

$$t = \frac{\eta}{\rho \alpha} = \frac{v}{\alpha}$$

Where  $\alpha$  becomes an apparatus constant equal to the following:

$$\alpha = \frac{\pi r_c^4 g}{8I} * \left( \int \frac{dV}{I} \right)^{-1}$$

The relative viscosity is the ratio of the solution and solvent viscosities:

$$\eta_{\rm rel} = \eta/\eta_0 = t/t_0$$

The specific viscosity is the relative viscosity minus one:

$$\eta_{sp} = \eta_{rel} - 1$$

The intrinsic viscosity of a solution is defined either as

$$[\eta] = \left[\frac{\eta_{sp}}{c}\right]_{c=0}$$

or as

$$[\eta] = \left[\frac{\ln(\eta_{rel})}{c}\right]_{c=0}$$

A plot of intrinsic viscosity versus concentration of both relationships should result in an extrapolation to the same point at zero concentration. Also, the sum of the slopes of the two lines is related by the Huggins equation,

$$\frac{\eta_{sp}}{c} = [\eta] + k' [\eta]^2 c$$

and the Kraemer equation,

$$\frac{\ln\left[\eta_{rel}\right]}{c} = \left[\eta\right] - k''\left[\eta\right]^{2} c$$

Algebraically,

$$k + k" = 0.5$$

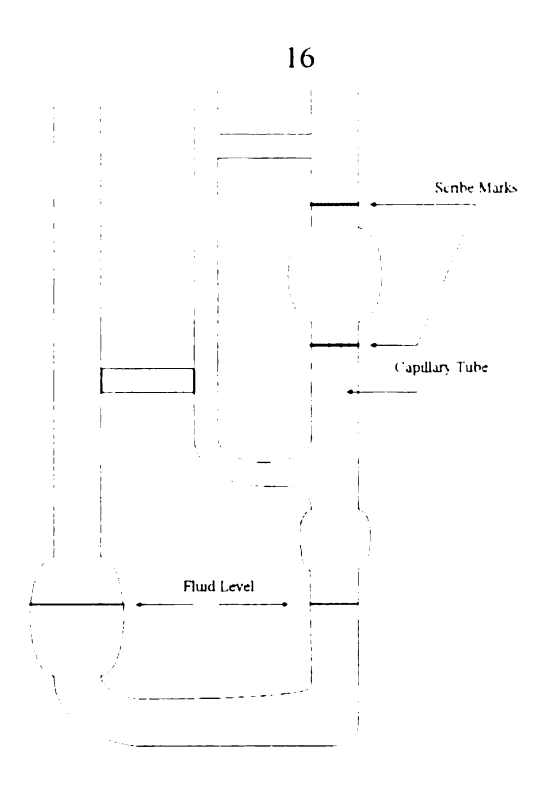


Figure 2.2: Schematic of Ubbelhode viscometer.

## **Practical Considerations**

To effectively use a viscometer for intrinsic viscosity measurements, several practical considerations should be met. A water bath should be used to regulate the solution temperature. The efflux time should be relatively long (generally > 100 seconds) to reduce timing errors and minimize kinetic energy corrections. Small solution concentrations must be used for extrapolation to a concentration of zero, i.e. the relative viscosity  $\eta_{rel}$  should be between 1.1 and 1.6.

#### Mark - Houwink Relationship

An empirical relationship between the intrinsic viscosity and the molecular weight was concluded by Mark and Houwink in 1938:

$$[\eta] = KM_v^a$$

K and a are constants for a specific solvent-polymer pair at a specific temperature.

# 2.2.5 Gel Permeation Chromatography

In GPC, a dilute polymer solution is put through a series of columns. Larger polymer molecules have faster elution times as the smaller molecules are able to sample more of the capillaries in the packing of the columns. Calibration is done with known molecular weight standards to give molecular size versus elution time. The GPC calculates all of the molecular weight moments (M<sub>n</sub>, M<sub>w</sub>, M<sub>v</sub>, etc.) and also gives the peak molecular weight, i.e. the molecular weight which shows up most often.

# 2.3 Free Radical Polymerization

#### 2.3.1 General Mechanism of FRP

Free radical initiated polymerizations are one mechanism of polymer growth in which polymerization reactions occur almost instantaneously. Several polymers

are formed mainly by this mechanism including polyethylene, poly(vinyl chloride), and poly(methyl acrylate) [Flory (1967)]. Free radical polymerizations consist of three steps: initiation, propagation, and termination.

Initiation: Typically an organic peroxide is incorporated as an initiator. Upon heating, the peroxide undergoes homolysis and decomposes to form two radical species, which are then able to react with the monomer or polymer to form another radical species.

ROOR 
$$\xrightarrow{k_d}$$
 2 RO $^{\bullet}$ 

In general,

$$C \xrightarrow{k_c} 2R_c^{\bullet}$$

$$R_C^{\bullet} + M \xrightarrow{k_i} R_1^{\bullet}$$

Propagation: Propagation by the free radical mechanism occurs very rapidly. The radical species reacts with an unreactive monomer or polymer, which in turn, becomes the active center.

$$R_1^{\bullet} + M \xrightarrow{k_{pl}} R_2^{\bullet}$$

$$R_2^{\bullet} + M \xrightarrow{k_{p2}} R_3^{\bullet}$$

$$R_n^{\bullet} + M \xrightarrow{k_{pn}} R_{(n+1)}^{\bullet}$$

It is usually assumed that the reaction rate coefficients of propagation are independent of size and therefore are equivalent.

$$\mathbf{k}_{\mathrm{p}1} = \mathbf{k}_{\mathrm{p}2} = \mathbf{k}_{\mathrm{p}n} = \mathbf{k}_{\mathrm{p}}$$

Termination: Termination occurs by either combination in which the species add to each other or by disproportionation where one of the species forms a double bond.

a) by combination

$$R_n^{\bullet} + R_m^{\bullet} \xrightarrow{k_{tc}} P_{(n+m)}$$

b) by disproportionation

$$R_n^{\bullet} + R_m^{\bullet} \xrightarrow{k_{tp}} P_n + P_m$$

#### 2.3.2 Reactive Extrusion and FRP

Of current interest is reactive extrusion of polymers leading to either controlled molecular weight degradation or to an increase in molecular weight. Two systems of intense interest have been polypropylene (PP) and polyethylene (PE).

A great deal of research and experimentation has been done on controlling the reactive degradation of PP in an extruder [Pabendinskas et al. (1989, 1994 a,b), Fritz et al. (1986)]. The reactive extrusion of PP with a free radical initiator,

usually an organic peroxide, has been shown to lead to chain scission and hence molecular weight degradation [Tzoganakis et al. (1988,1989)]. This free radical initiated degradation provides an easy path for producing necessary molecular weights for specific applications. An increase in the initiator concentration degrades the high molecular weight tail and narrows the molecular weight distribution of PP [Suwanda et al. (1988 a,b), Triacca et al. (1993)]. The changes in flow properties which result from the lower molecular weight are of much interest. As the molecular weight and viscosity decrease, melt flow properties are increased which improves the processibility of PP.

The degradation of PP in an extruder has been modeled by Tzoganaskis et al. (1988) and Suwanda et al. (1988 a,b). Pabedinskas et al. (1994 a,b) have recently tried to model this system with the explicit purpose of developing a process control strategy.

In contrast to the free radical initiated degradation of PP, polyethylene free radical polymerization produces a polymer with an increased molecular weight. The reactive extrusion of linear low density polyethylene (LLDPE) and a free radical initiator leads to a high molecular weight polymer as the initiator concentration is increased [Suwanda et al. (1989)]. An increase of molecular weight should

improve mechanical properties. The polymerized LLDPE showed increases in MFI, yield strength, and yield modulus.

### 2.3.3 Maleation

Reactive extrusion can be used for the functionalization of many polymers. Of specific interest over the past years has been the addition of maleic anhydride to several polymer backbones such as PP and PE. The maleation of these polymers has been generally done to improve the adhesion properties. Introducing new functional groups onto the polylactide backbone paves the way to prepare composites, laminates, coated items, and blends/alloys with improved properties and cost effectiveness. Functionalizing the matrix polymer and the fiber/filler with highly reactive groups is perhaps the most successful strategy leading to a variety of commercial composites and alloys made by reactive processing.

Functional groups such as isocyanate, amine, anhydride, carboxylic acid, epoxide, oxazoline, are often introduced during reactive extrusion with short residence time. Combinations of hydroxyl/isocyanate [Mizuno et al. (1978)], amine/anhydride .

[Lambla et al. (1989), Morita et al. (1987), Udding et al. (1988)], amine/epoxide, anhydride/epoxide, amine/lactam [Akkapeddi et al. (1988)], and amine/oxazoline [Sneller (1985)], provide practical routes for reactive processing. Such coupling

reactions provide interfacial bondings in composites, laminates, and coated items [Krishnan et al. (1992), Argyropoulos et al. (1991)]. In polymer blends and alloys (immiscible) such coupling reactions provide control of phase size and strong interfacial bonding. A variety of functional groups has been introduced onto the surface of natural polymers [Doane et al. (1992), Glasser (1989)].

The free radical initiated reaction of MA with several polyolefins has led to very interesting results. Branching and/or crosslinking occurs in maleated samples of LDPE [Gaylord et al. (1982)], HDPE [Gaylord et al. (1989)], and LLDPE [Gaylord et al. (1992)]. In an ethylene-propylene copolymer rubber (EPR), both crosslinking and degradation occur [Gaylord (1987)].

Degradation occurs in the case of maleated PP [Gaylord et al. (1983b), Callais et al. (1990), Hogt et al. (1988)]. The degradation is greater in the presence of MA plus initiator, than in the presence of only initiator. Grafting of MA, as well as melt flow, is increased with an increase of peroxide content for PP.

The free radical initiated reaction of polystyrene (PS) with various organic peroxide initiators results in degradation and molecular weight reduction. In the presence of MA; however, the extent of degradation is reduced [Gaylord et al. (1983a)].

Homopolymerization of MA may play an important role in the reactions of MA with polyolefins. Cationic intermediates participate in the homopolymerization of MA, but the addition of small amounts of dimethylformamide (DMF) may prevent the reaction [Gaylord et al. (1981)]. Crosslinking which normally occurs in the maleation of LDPE is suppressed with the addition of DMF. Furthermore, the addition of DMF to PP-MA mixtures before reactive extrusion results in MA grafted PP with a higher intrinsic viscosity than a mixture without DMF. Therefore, less degradation occurs with the addition of an anti-MA homopolymerization agent such as DMF.

# **MATERIALS**

# 3.1 Polylactide

The focus of this work is on the modification of polylactide. In this section, the preparation and uses of PLA will be described in some detail. The PLA was provided by Cargill. It has a specific gravity of 1.248. GPC results indicate that PLA has an  $M_n$  of about 122,000 and a polydispersity of 1.4 (see Table 5.1 for complete details).

# 3.1.1 Commercial Preparation

Polylactides are prepared by the ring-opening polymerization of the lactide dimer (Figure 3.1). Naturally occurring lactic acid is dehydrated to form the cyclic diester lactide. This process is also known as internal esterification. Lactic acid is a key biomass intermediate obtained from acetaldehyde or fermentation of hexoses or hexose polymers such as starch or cellulose [Sperling and Carraher (1990)]. Several catalysts may be used for the ring-opening polymerization, including tin(IV) chloride, stannous octoate, and tetraphenyltin [Van Dijk et al. (1983)].

During the past decade, aluminum alkoxides have also been used [Barakat et al. (1993)].

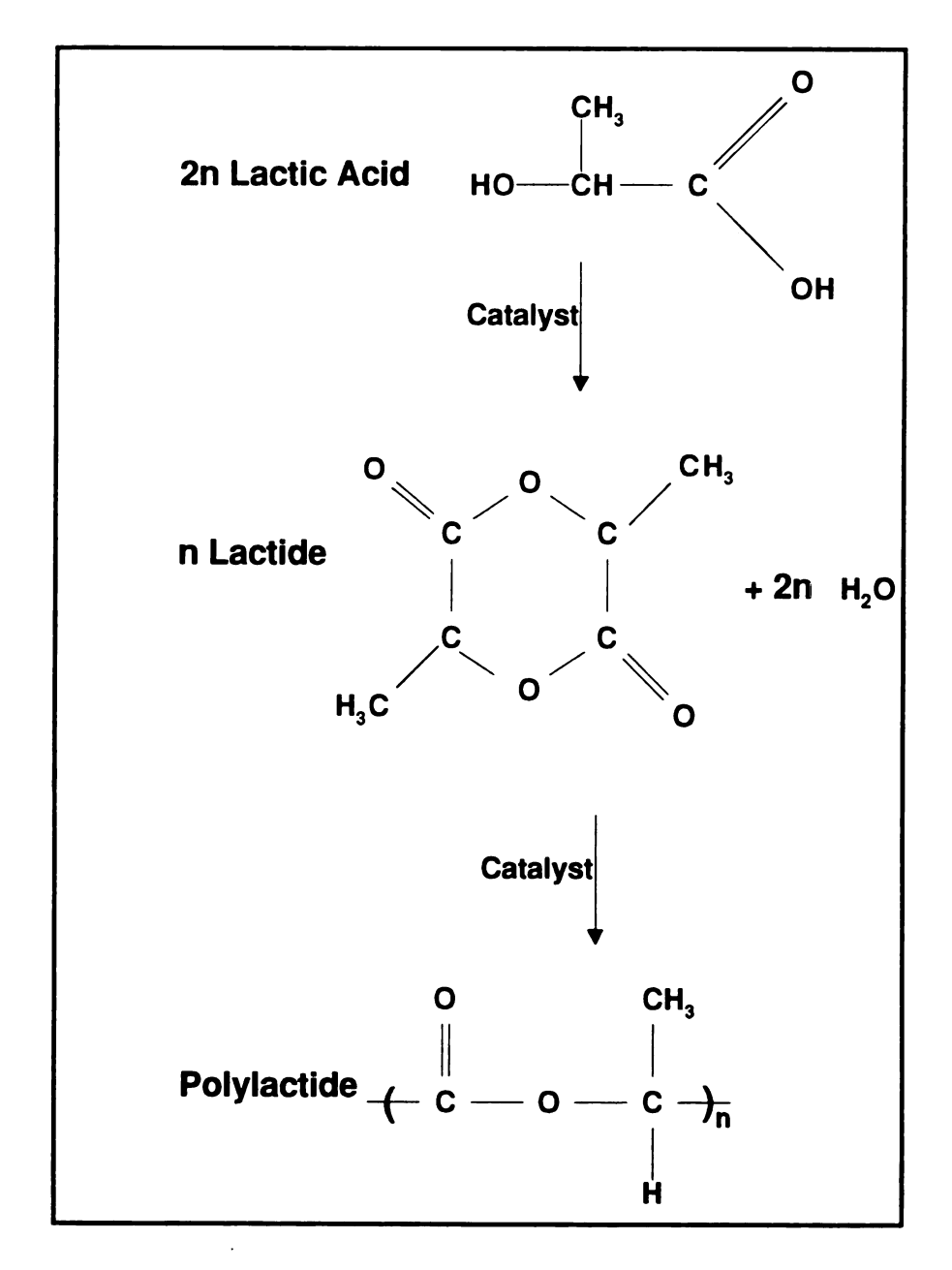


Figure 3.1: Commercial preparation of polylactide.

## 3.1.2 Applications

#### **Sutures**

Polymers of lactic acid have been used commercially for absorbable sutures. Copolymers of lactide and glycolide were synthesized as early as 1963 to produce synthetic absorbable sutures which were an improvement over catgut sutures [Conn et al. (1974), Schmitt et al. (1967)]. Further advances of PLA sutures include dimensional stability and improved tensile strength [Schneider (1974, 1972), Yves (1970)]; however, processing via extrusion may cause a loss in inherent viscosity [Schneider (1971)].

### **Drug Delivery Systems**

Biodegradable polymers have been found to be very efficient in the controlled release of therapeutic drugs. Lactide polymers were the first synthetic biodegradable polymers to be used in this application [Heller (1985)]. Polylactide has also been used as a semi-permeable biocompatible local delivery device for the treatment of periodontal disease [Goodson (1988), Damani (1993)].

# **Medical Implants**

Polylactide has been used to coat a sintered tricalcium phosphate implant [Eitenmuller et al. (1986)]. The PLA coating is of a certain thickness so as to

control the adsorption time of a therapeutically active ingredient which is contained in the porous implant.

### **Biodegradable Packaging: Status**

The current applications for PLA are in the medical and pharmaceutical industries which are low volume markets able to accommodate high resin costs. However, as the need for biodegradable packaging and biodegradable items increases it becomes necessary to find a less costly way of producing PLA. Several companies are currently working on the research and development of the commercial production of PLA. Argonne National Laboratories is developing a technology for polymerizing lactic acid produced by the fermentation of potato waste. Batelle and Golden Technologies are in a joint venture for developing PLA technology for packaging applications. Cargill and Ecochem are producing lactic acid from corn and cheese whey, followed by the ring-opening polymerization to high molecular weight PLA.

# **3.2 Lupersol 101**

Lupersol 101 (L101) is a difunctional di-tertiary alkyl peroxide. The free radicals generated from dialkyl peroxide decomposition are initiators in bulk and suspension vinyl polymerizations. L101 was chosen as the initiator for several reasons. A low half life has been reported by the manufacturer as 1 minute at 180°C and 13 seconds at 200°C which may result in more or complete decomposition of the peroxide at the operating temperatures and residence times. L101 is also recognized by the FDA as a food additive (Code of Regulations; Title 21 "Food and Drugs" part 170 under "Food Additives").

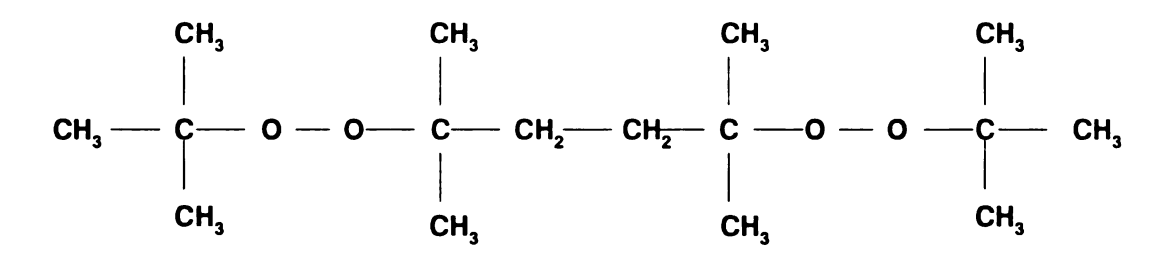


Figure 3.2: Lupersol 101 [2,5-dimethyl-2,5-di-(t-butylperoxide)]

# 3.3 Maleic Anhydride

Maleic anhydride (MA), shown in Figure 3.3, was purchased from Aldrich Chemical Company. Maleic anhydride is a toxic chemical considered as corrosive and as a sensitizer. Care must be taken in handling to avoid breathing in the dust particles of MA as well as the fumes from extrusion. Also, MA may be absorbed through the skin so gloves must be worn. MA has a melting point between 54°C and 56°C and a boiling temperature of around 200°C, which is the maximum temperature at which any of the experiments were run.

Figure 3.3: Maleic anhydride (MA), [C<sub>4</sub>H<sub>2</sub>O<sub>3</sub>]

Maleic anhydride can be used as a coupling agent providing bonds both to a filler containing hydroxyl groups (esterification) and to the polymer matrix (through peroxide addition) [Dalvag et al. (1985)].

## PROCESSING AND CHARACTERIZATION

# 4.1 Processing

#### 4.1.1 Reactive Extrusion

The thrust of this work is the free radical branching of PLA via reactive extrusion. Therefore, extrusion is the most important step of all the experiments. It is thus necessary to describe in some detail the reactive extruder and extrusion experiments.

The extruder used was a Baker-Perkins co-rotating intermeshing twin screw extruder. Figure 4.1 shows a schematic of the extruder. The diameter of each screw is 3 cm, the length is 42 cm. There are two feed ports on the barrel, two barrel valves, and a venting port. The material was fed at the first feed port while the other feed port and venting port were kept closed. Each screw has two sets of six mixing paddles and a Camel back discharge screw at the end. The die which was used had two 3 mm in diameter holes. The temperature was measured at three points on the barrel, at one point on the die, and at four points inside the barrel (melt temperature), defining the conditions in zone 1, zone 2, zone 3, and the die

(zone 4). The barrel could be cooled by adjusting the flow rate of the cooling water supply which was manually controlled by four valves.

The extruder shafts are composed of slip-on screws, kneading paddles and orifice plug segments. The configuration of these elements was as depicted on Figure 4.2. The transversely neighboring paddles are always kept at 90 degrees to each other, while the axially kneading paddles can take on a number of orientations depending on the amount of forwarding action desired in each mixing zone. The amount of cross-sectional area available for axial flow is controlled by the barrel valves and orifice plugs. The barrel valves are triangular shaped vanes positioned over the orifice plugs which are discs with a diameter close to that of the barrel.

#### **4.1.2 Extrusion Conditions**

PLA and Lupersol 101 (L101) (also maleic anhydride, if maleation was desired) were mixed in zip-lock plastic bags before extrusion on the Baker Perkins corotating intermeshing twin-screw extruder. The extruder was purged (cleaned) with polyethylene before and after each run. When the PE coming out of the die was clear, it was assumed the no other material was in the extruder. The material was run directly after the purging with PE. Samples of 350 - 400 grams of PLA were used for purging and sample collection. Screw speed was set at 100 rpm with a constant feed rate of 5 percent. In the beginning of the extrusion, the

extrudate is a mixture of PE and the material, so the mixture was discarded and sample was not collected until the material appeared to be pure PLA (change in color from white/clear to light brown or tan). This usually occurred after 150 - 200 grams of material was collected. Approximately 100 - 150 grams of the material was collected for further testing. Collection of the material was stopped when the load of the extruder, which remained fairly constant throughout the reaction, started to decrease. Although there was still some material left in the extruder, it had been subjected to a longer residence time and would not have the same properties as the collected material.

Tables 4.1 and 4.2 show the temperature settings for the free-radical branching of PLA and the maleation of PLA, respectively. The temperatures in the first zone are kept lower as the materials need to be moved ahead without melting in this zone. In the case of maleation, a lower temperature setting at the feeding zone (compared to branching only) was necessary to prevent PLA co-aggregation in the hopper. The melt temperatures in zones 1 and 3 ran lower than the set points for all of the materials; however, the melt temperature in zone 2 always ran higher than the set point. Tables 4.1 and 4.2 show these discrepancies.

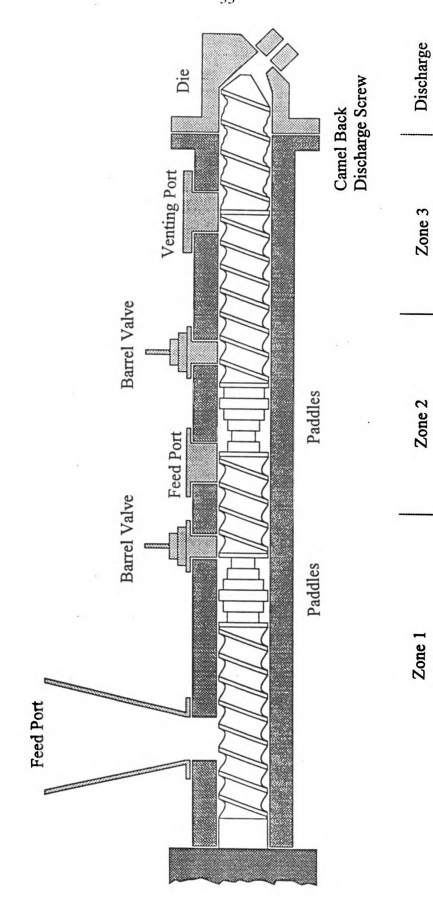


Figure 4.1: Baker-Perkins twin screw extruder (Composite Materials and Structures Center, MSU).

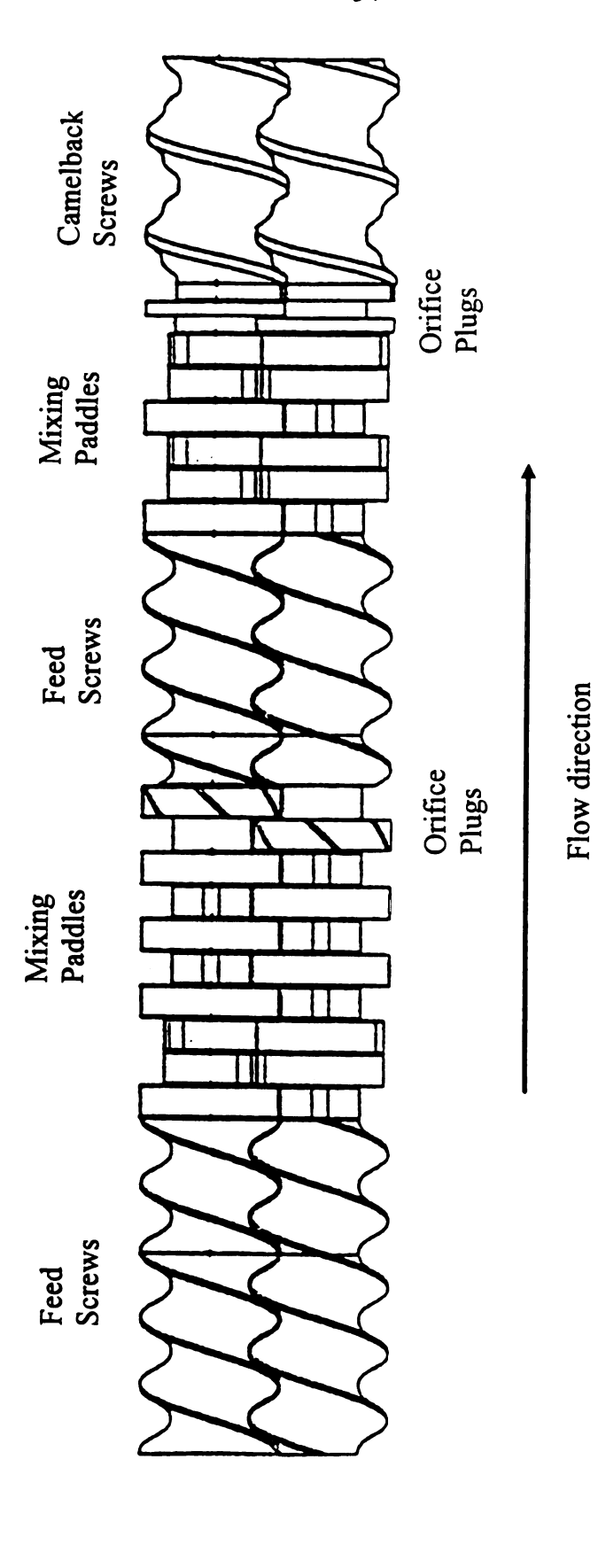


Figure 4.2: Co-rotating twin screw configuration.

Table 4.1: Temperature settings for free radical branching.

		Temperature (C)				
Temperature (°C)	Temperature Type	Zone 1	Zone 2	Zone 3	Die	
160	Set	180	155	160	160	
	Melt	145	165	156	186	
170	Set	180	163	185	160	
A .	Melt	145	174	173	162	
180	Set	180	170	190	160	
	Melt	152	186	181	166	
190	Set	180	185	200	160	
	Melt	149	197	192	167	
200	Set	200	190	210	155	
	Melt	158	202	199	177	

Table 4.2: Temperature settings for maleation.

		Temperature (°C)					
Temperature (°C)	Temperature Type	Zone 1	Zone 2	Zone 3	Die		
180	Set	170	170	190	160		
	Melt	148	184	180	162		
200	Set	170	190	210	155		
	Melt	146	201	199	175		

# 4.2 Characterization

### 4.2.1 TriSEC Analysis

Molecular weights and molecular weight distributions were determined using a TriSEC (triple detector size exclusion chromatograph) operating in THF at 25°C. The samples were dissolved in degassed THF and then filtered with a 0.45 micron filter before injection to remove undissolved contaminants which may block the system. The TriSEC system consists of: (1) Viscotek model 600 RALLS (right angle laser light scattering) detector, (2) differential viscometer/refractometer, and (3) size exclusion chromatograph. A random coil configuration for the polymer was assumed. The total injection volume was 242 μl with a flow rate of 1 mL/min.

Figure 4.3 is a schematic of the TriSEC detector flow loop which is a closed loop operating system. Pure solvent is continuously passed through the apparatus. The solvent is degassed and then pumped into the GPC column oven. The solvent is first heated in the oven before it goes through the GPC columns. When a sample is run, it is injected into the oven, heated to the specified temperature, and then allowed to enter the GPC column. Once the solution has exited the column, it goes to the RALLS detector and then onto the parallel configuration of the differential viscometer/refractometer. If a sample is being run, the solution is collected in a waste container; otherwise, the pure solvent is recycled.

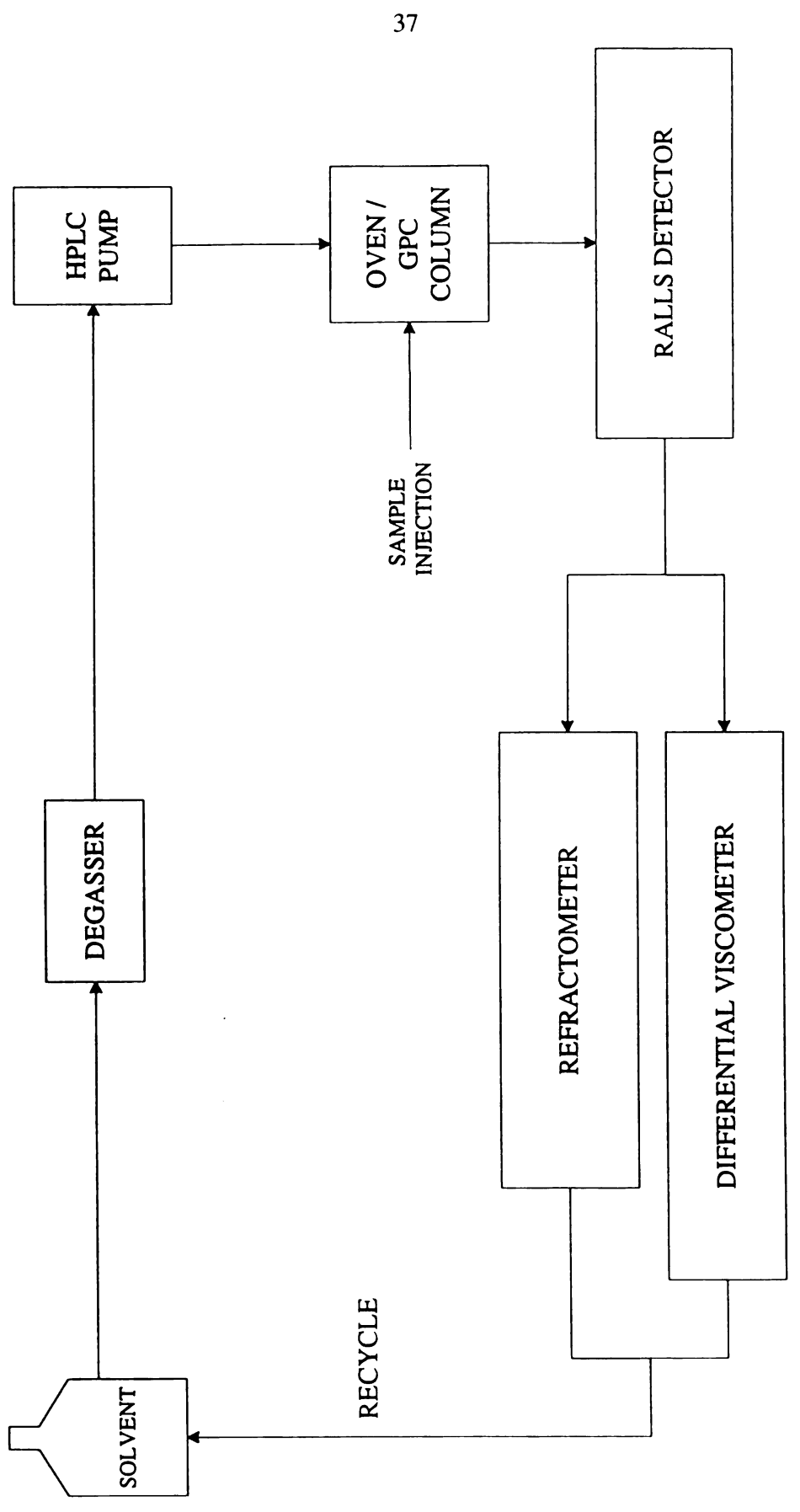


Figure 4.3: TriSEC flow loop.

**RALLS:** Light scattering theory is discussed in some detail in section 2.2.3. A scattering angle of 90° and an incident wavelength of 670 nm was used

**Differential viscometer/refractometer:** A Viscotek 200 model was used.

**SEC:** Two (2) Plgel bimodal mixed bed columns were used. A universal calibration was done with polystyrene standards.

#### Analysis

At least 3 injections of each sample were done. Each injection resulted in a different refractive index (n). The refractive indices for each sample were averaged and a new sample concentration was back calculated. Molecular weight analysis was then done. The computer software uses an iterative algorithm to correlate all three detector values.

## 4.2.2 Intrinsic Viscosity

Intrinsic viscosity measurements were done in a Ubbelhode viscometer (see Chapter 2, Figure 2.2 for a detailed diagram) kept in a water bath at 30°C. The PLA samples were dissolved in THF then filtered with a 120 mesh stainless steel filter (to remove large contamination). These polymer solutions were compared to pure THF (see section 2.2.5 for a detailed description of the basic experimental concepts). A minimum of 4 timings were taken and then averaged for the final

result. This test was done to validate the viscometry results obtained from the TriSEC detector.

#### 4.2.3 Melt Flow Index

A Ray-Ran melt flow indexer was used to characterize melt viscosity. Material was first pelletized before analysis. ASTM standard test D-1238 was used at the conditions of 190°C and a 2.16 kg load.

## **4.2.4 Differential Scanning Calorimetery**

The glass transition temperature,  $T_G$ , of PLA and modified PLA samples was studied using a DuPont 910 differential scanning calorimeter.  $T_G$  was taken at the midpoint of the step transition. Analysis was done at  $10^{\circ}$ C/min up to  $200^{\circ}$ C under nitrogen atmosphere.

# **4.2.5** Thermogravimetric Analysis

A thermogravimetric analyzer (DuPont TGA module 951 and Hi-Res TGA 2950) was used to measure the change in weight of the sample due to decomposition. Analysis was done at 20°C/min to about 20% volatilization. High resolution was done so that when the sample begins to rapidly degrade the heating time slows down, allowing for a more accurate measurement.

### 4.2.6 Dynamic Mechanical Analysis

A Carver laboratory press was used to prepare the samples by a cycle of heating at 140°C for 5 minutes, pressing at 12000 lbs for 2 minutes, and cooling under pressure to room temperature. Samples were molded into 3" squares, 0.125" thick, which were further cut into 0.5" strips using a high-speed wet saw. A DuPont 983 dynamic mechanical analyzer was used to measure the loss and storage moduli.

Dynamic mechanical analysis was done on several samples which were processed the same way so a comparison could be made. Material was pelletized before compression molding to ensure a more even distribution. The compression molding cycle consisted of a 5 minute heating period, where the sample was allowed to melt before pressurization; a two minute heated pressurized segment at a force of 12000 lb.; and a pressurized cooling segment in which the sample was allowed to cool to room temperature before removal. The mold used was a 3" x 3" x 0.125" square sheet of steel which had overflow grooves to ensure even thickness and sample density. The samples were then cut into 0.5" x 3" pieces using a water cooled saw. PLA may degrade at the high temperatures generated by the friction of the saw and undergo hydrolysis with the water especially at the elevated temperature. Since DMA is done on the bulk properties and these phenomena occur only at the cutting edges, these degradation effects have been

neglected. A comparison of PLA to the modified PLA samples may still be accomplished as all samples have undergone the same preliminary processing.

Polymers such as PLA are viscoelastic materials having characteristics of both viscous liquids and elastic solids. A viscous liquid under stress will dissipate energy but not store it, while an elastic solid has the capacity to store mechanical energy but can not dissipate it [Murayama (1978)]. When a polymer undergoes deformation, part of the energy is stored as potential energy and part is dissipated as heat which shows as mechanical damping. The storage modulus G' is related to the storage of energy as potential energy and its release in periodic deformation. The loss modulus G" is associated with the dissipation of energy as heat when the material is deformed. The damping peak or internal friction is defined as

$$\tan \delta = G''/G'$$

In DMA, the commonly used frequency range is from 10<sup>-2</sup> Hz to 10<sup>6</sup> Hz [Murayama (1978)]. A frequency of 1 Hz was chosen for these experiments. An amplitude of 0.5 mm was chosen after lower amplitudes of 0.3 and 0.4 mm proved to be insufficient.

#### 4.2.7 Titration

The extent of maleation for samples grafted with maleic anhydride can be determined by titration. Since the initial percent of maleic anhydride reacted is

quite low, 2 percent, it can be assumed that the actual percent grafted onto the PLA backbone is very small. A direct titration of these samples would probably be inaccurate as a small discrepancy such as a contaminant could result in a large error; therefore, a back titration of the sample is necessary. A back titration consists of adding a known excess of base and then titrating the base with acid. The base reacts with both the maleated sample and the acid. The amount of anhydride attached to the PLA backbone can then be determined.

In general, visual titration can be used to determine the indicator end point or potentiometric titration can be done to determine the equivalence point of the sample. A potentiometric titration has been done using an Orion 960 Autochemistry System (Figure 4.4). The autotitrator does a potentiometric analysis and measures the volume of HCl added along with the corresponding mV and pH readings. A first derivative analysis is used to determine the equivalence point of the sample.

The following is the titration method which was used. It is a modified version of Johnson and Funk's (1955) method: (1) remove unreacted maleic anhydride (MA) by drying in a vacuum oven at 130°C for 24 hours; (2) dissolve ~ 1 gram of sample (containing a maximum of 2% MA) in 20 ml of THF-MeOH (5:1); (3) after 1 hour or when samples are completely dissolved, add 2.0 ml of morpholine solution

(0.05 N in MeOH); (4) let mixture react for 10 minutes; (5) titrate samples with 0.01 N HCl using the autotitrator.

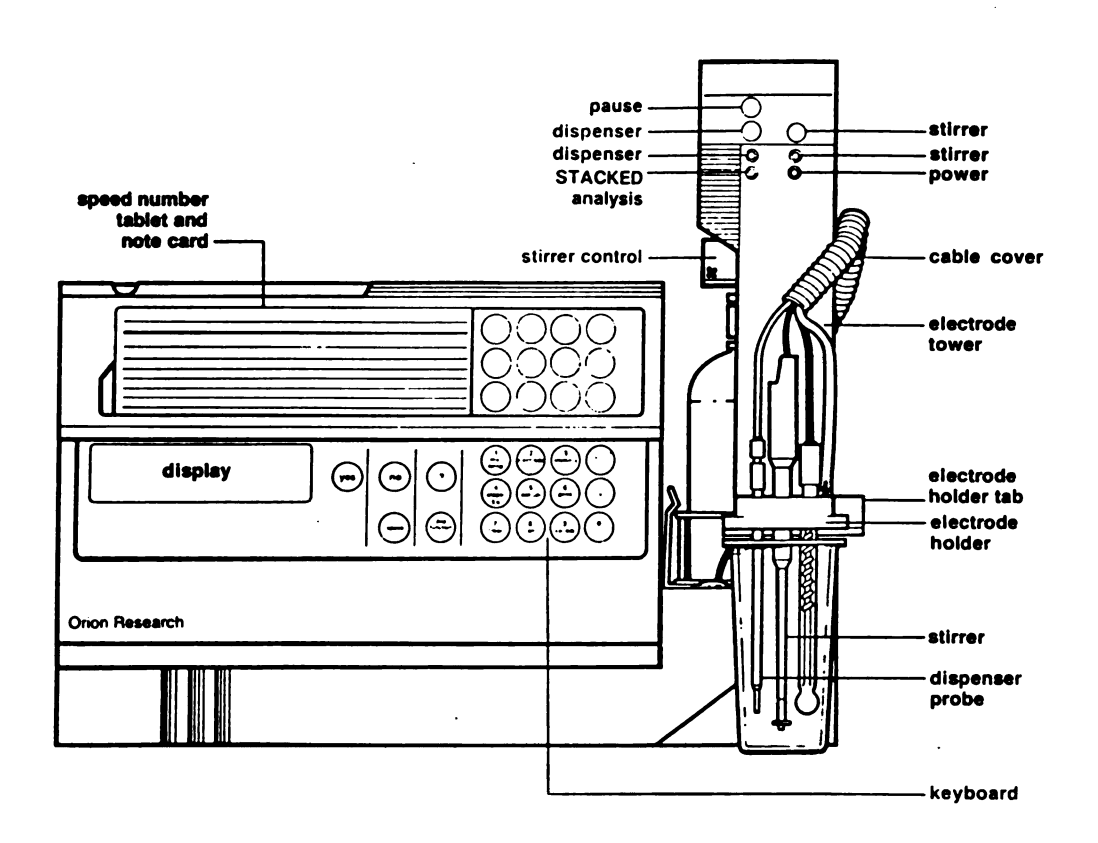


Figure 4.4: Orion 960 Autochemistry system.

The HCl solution was titrated against a known NaOH standard. The morpholine solution was then titrated against the HCl to get a blank reading. The potentiometric titration procedure developed by Siggia and Hanna (1951) uses an excess of aniline instead of morpholine, but they react very similarly as they are both secondary amines. Also, ethylene glycol - isopropyl alcohol (1:1) is used as the solvent for the amine, replacing MeOH.

The calculation for determining the percent anhydride (i.e. the percent of grafted MA) is as follows:

% anhydride = 
$$(V_{mor} * N_{mor} - V_{HCI} * N_{HCI}) * \frac{98.06g / mol}{W_{sample}} * 100$$

V = volume in liters

N = normality (mol/equivalent)

W = weight in grams

## **4.2.8 Scanning Electron Microscopy**

Image Formation: A scanning electron microscope (SEM) is used to observe the surface morphology of a sample. JEOL JSM-35C and JEOL JSM-6400 SEM were both used in this study. The normal SEM image is formed when secondary electrons are given out by the atoms of the sample as a result of inelastic scattering by an electron beam (Figure 4.5). An Everhart-Thornley detector is used to detect the

electrons. The production of secondary electrons is very sensitive to the changes in topography of the sample. Because secondary electrons are detected from only the top layer of a sample, the projecting areas of the sample seemingly give out a large number of these electrons and thus appear brighter. In areas where these electrons can not escape, such as crevices, fewer secondary electrons are detected and thus these areas appear darker in the final image. A resolution of 4 to 6 nm is possible with this technique.

Sample Preparation: The samples for SEM are typically 2 to 4 mm in size. Samples from solution cast films are just cut into small pieces. Larger samples from extrusion or mixing in the Haake mixer are prepared by fracturing at room temperature. All samples were mounted on aluminum stubs and gold coated with a sputter coater.

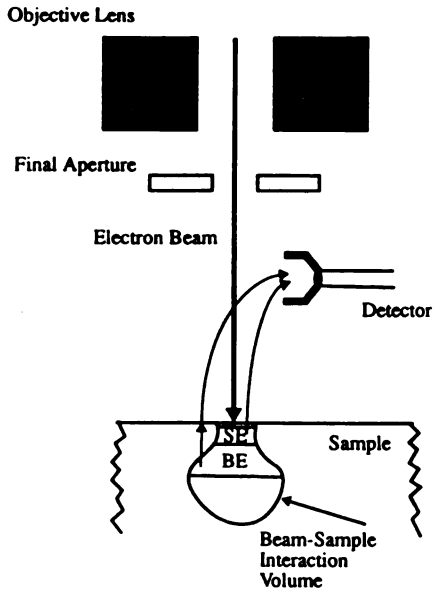


Figure 4.5: SEM image formation.

#### 4.2.9 Extraction

An extraction experiment was done on samples which were highly branched and appeared to be cross-linked. ASTM standard D2765-90 for crosslinked ethylene plastics was modified for use with PLA samples. Approximately 0.3 grams of branched/crosslinked PLA was placed in a metal pouch made of 120 mesh stainless steel. The pouch was then placed in 200 ml of methylene chloride for 24 hours. The sol content of the material would be able to exit the pouch, while any crosslinked fraction would remain trapped inside. Results of this extraction experiment show that no macromolecular crosslink exists; however, the possibility of microgeleation can not be neglected.

## 4.2.10 Moisture Analysis

Moisture analysis was done using an O'Haus MB200 moisture analyzer. PLA is very sensitive to water which will cause it to degrade (accelerated degradation in the extruder). The experiment was run at 105°C for 15 minutes. It was determined that the starting PLA contained less than 0.3% moisture (weight basis). The PLA which was used for processing is vacuum dried at 50°C for at least 5 hours prior to extrusion resulting in 0.1% moisture. Moisture analysis done with up to 2 days of drying also result in 0.1% moisture. This small amount of moisture; however, may still cause thermohydrolysis in the extrusion process.

# FREE RADICAL BRANCHING OF PLA

This chapter is divided into two sections. The first section is comprised of a detailed discussion of the experimental results pertaining to the free radical branching via reactive extrusion of PLA. The second section details a proposed reaction mechanism for the branching.

### 5.1 Discussion of Results

## 5.1.1 Effect of Extrusion Temperature

A trade-off exists between having an extrusion temperature low enough to reduce thermal degradation, but high enough to ensure that all of the initiator has reacted. Temperatures between 160°C and 200°C were evaluated. In the absence of initiator, drastic degradation is readily apparent even at 160°C as shown by the decrease of the number average molecular weight, M<sub>n</sub>, of PLA from 121,600 to 88,800 (entries 1 and 2 in Table 5.1, also Figure 5.1) as well as the increase in MFI from 12.76 to 123.3 g/10 min. These results are comparable with observations reported by Gogolewski (1993) who found that the injection molding of polylactides at temperatures between 130°C and 215°C resulted in a peak molecular weight decrease greater than 50%. Furthermore, these results are also

comparable to those reported by Jamshida (1988) who examined the thermal degradation of P(1)LA using DSC.

Increasing the temperature from 160 C to 190 C does not sharply modify M<sub>n</sub> (compare entries 2, 6, 9, and 12 in Table 5.1) which is maintained between 76,000 and 89,000, nor does it affect the weight average intrinsic viscosity, IV<sub>w</sub>. Based on these results, it is apparent that the extrusion process has a strong debilitating effect on the integrity of PLA as shown by the decrease in M<sub>n</sub> and intrinsic viscosity, as well as the increase in MFI. In order to inhibit this behavior, we have branched PLA by a free-radical process.

### **5.1.2 Effect of Initiator Concentration**

At  $160^{\circ}$ C: The addition of only 0.05% L101 was able to improve the extrusion properties of PLA by increasing  $M_n$  from 88,800 to 125,500 and decreasing the MFI from > 50 g/10 min to 5.39 g/10 min (entries 2 and 3 in Table 5.1). Further addition of L101 (i.e., from 0.05 up to 0.26); however, provided no additional property improvements (entries 2-5 in Table 5.1, also Figure 5.2).

At 170°C and 180°C: Increasing the initiator content leads to an increase in M<sub>n</sub>, M<sub>peak</sub>, and the MP load % (screw torque); as well as a decrease in the MFI (entries 6-8 and 9-11 in Table 5.1, also Figures 5.3 and 5.4). Molecular weight

distributions are kept between 1.3 and 1.5 with the exception of the highly branched  $170^{\circ}/0.5$  sample. At  $170^{\circ}$ C and 0.1% L101, the extruded PLA is characterized by properties similar to the initial, not extruded PLA (entries 1 and 7 in Table 5.1). For example, compare the intrinsic viscosity for PLA at 1.04 with that of the  $170^{\circ}/0.1$  sample at 1.08. The molecular weight values are very good in comparison with the mean values reported by Gogolewski after injection molding  $(M_n << 100,000)$ .

As previously stated, an initiator concentration of 0.5% at 170°C (entry 8 in Table 5.1) leads to highly branched PLA as can be seen in the high MP load %, the elastomeric properties exhibited upon extrusion, and the high molecular weight polydispersity of 550. Also, the sample was quite difficult to filter for SEC analysis: several filters had to be used for the dilute sample solution. An extraction experiment has been done showing no large scale cross-linking; however, microgel may be present along with the branching. A more detailed description of highly branched samples will be discussed in Section 5.1.6.

At 190°C: An increase in the initiator concentration results in an increase in M<sub>peak</sub> and M<sub>n</sub> (entries 12-14 in Table 5.1). Branching effectively occurs as shown by the increase in both M<sub>n</sub> and MP load %, as well as a decrease in MFI. The highly branched, possibly microgel, state observed with 0.5% L101 (entry 14 in Table

5.1) is proof of the fact that branching is still occurring at this high temperature, even though chain scissions are generally more prevalent at high temperatures and high initiator concentrations.

 $\underline{200 \text{ C}}$ : At 200 C branching is counter-balanced by chain scission leading to an approximately constant  $M_{peak}$  and  $M_n$ , in addition to a constant MFI between 10 and 13 g/10 min (entries 15-17 in Table 5.1).

Based on the above observations, it clearly appears that between 170°C and 190°C branching occurs as evidenced by increases in M<sub>peak</sub>, M<sub>n</sub>, and extruder torque. Branching is also shown by an exponential decrease in MFI with initiator concentration (Figure 5.5). At temperatures T >190°C, in addition to branching, chain scissions by free radical processes appear probable along with other transesterification reactions (intra- and inter- molecular) leading to a decrease in molecular weight. Comparisons between undried and dried PLA in MFI experiments show that some initiator traces are still present inside the PLA sample and can further react at 190°C during the MFI test which may lead to new branching. In any case, the traces of peroxide always favor a decrease of MFI which is one of the objectives of this research.

Table 5.1: Free radical branching of PLA: MP load %, melt viscosity, and TriSEC analysis. (Standard deviations for TriSEC data are located in Appendix A.1)

ID #	PLA samples		MP load%	MFI (g/10 min) <sup>1</sup>		TriSEC			
	T (°C)	wt% L101		undried	dried <sup>2</sup>	M <sub>peak</sub>	M <sub>n</sub>	$M_{w}/M_{n}$	IV <sub>w</sub>
1	PLA <sup>3</sup>		-	12.8	-	134,500	121,600	1.41	1.044
2	160	0.00	59-63	> 50	•	91,900	88,800	1.30	0.82
3	160	0.05	58-60	5.4	9.3	137,900	125,800	4.63	1.33
4	160	0.14	54-56	4.9	7.8	132,100	124,600	1.81	1.14
5	160	0.26	50-52	4.1	6.4	139,500	130,400	2.54	1.17
6	170	0.00	64-68	> 50	-	91,300	76,200	1.50	0.84
7	170	0.10	69-73	17.2	-	126,000	125,300	1.31	1.08
8	170	0.50	78-85	-	-	180,800	133,900	550 <sup>5</sup>	1.534
9	180	0.00	59-61	31.9	39.2	85,900	81,000	1.30	0.83
10	180	0.10	70-72	13.9	15.8	108,500	104,700	1.33	0.98
11	180	0.25	72-74	7.0	12.0	130,900	129,000	1.48	1.01
12	190	0.00	52-56	> 50	•	88,500	82,900	1.30	0.79
13	190	0.10	66-69	19.7	-	115,800	114,500	1.33	1.02
14	190	0.50	71-75	-	-	162,300	153,600	520 <sup>5</sup>	1.72
15	200	0.00	49-51	13.1	55.6	102,900	102,600	1.21	0.92
16	200	0.10	56-58	10.4	29.6	112,000	105,500	1.30	1.11
17	200	0.25	59-61	10.7	17.3	117,600	114,000	1.41	0.97

<sup>1</sup> ASTM standard (D1238) at 190°C with 2.16 kg load

<sup>2</sup> Samples vacuum dried overnight at 130°C (removal of residual peroxide)

<sup>3</sup> Sample not extruded

<sup>4</sup> Ubbelhode viscometry experiments result in IV = 1.16 for PLA and IV = 1.46 for 170°/0.5 (Table A-2 in the Appendix)

<sup>5</sup> Sample highly branched

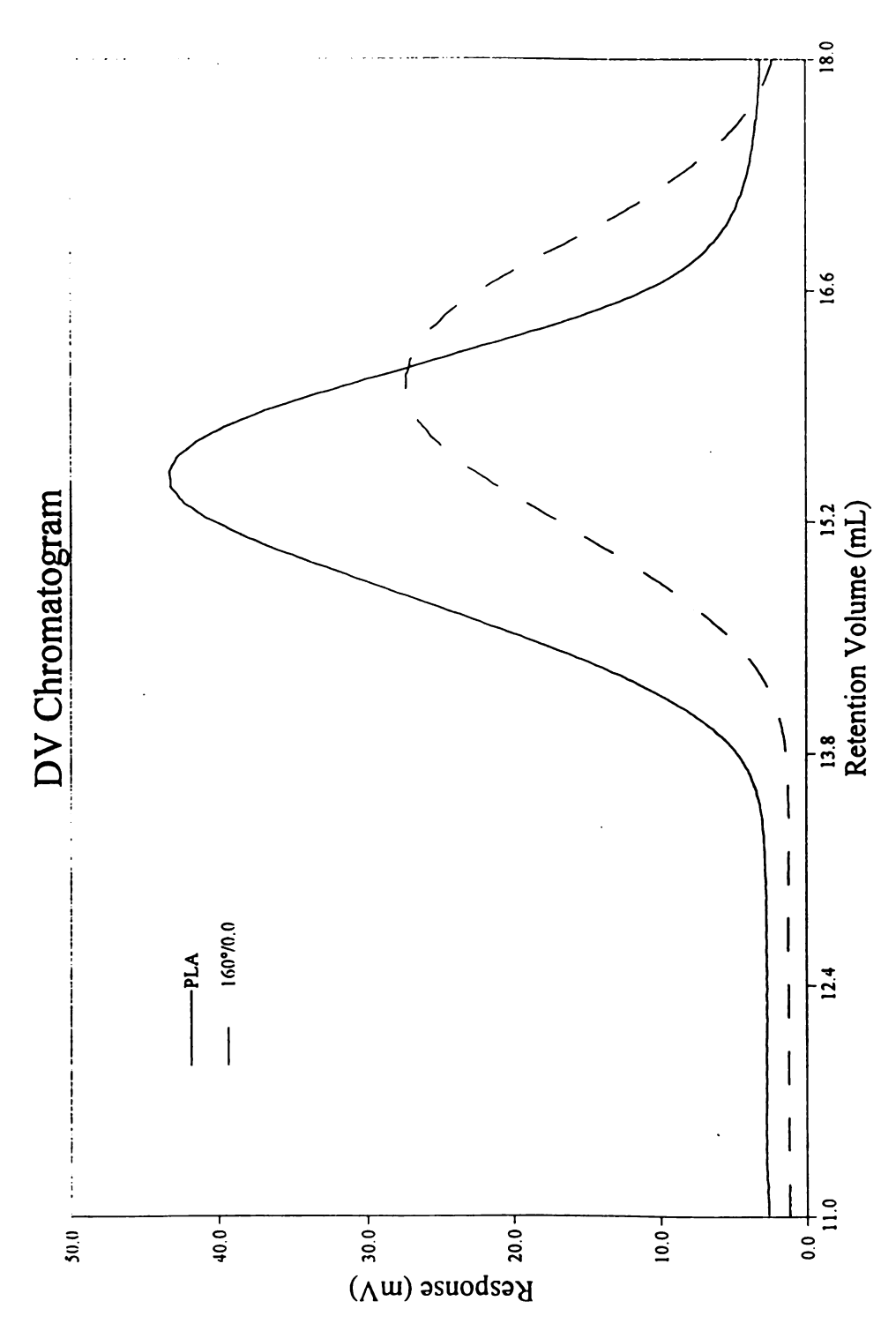


Figure 5.1: DV chromatogram showing the shift in molecular weight distribution of unextruded (higher M.W.) and extruded (lower M.W.) PLA. (normalized to concentration)

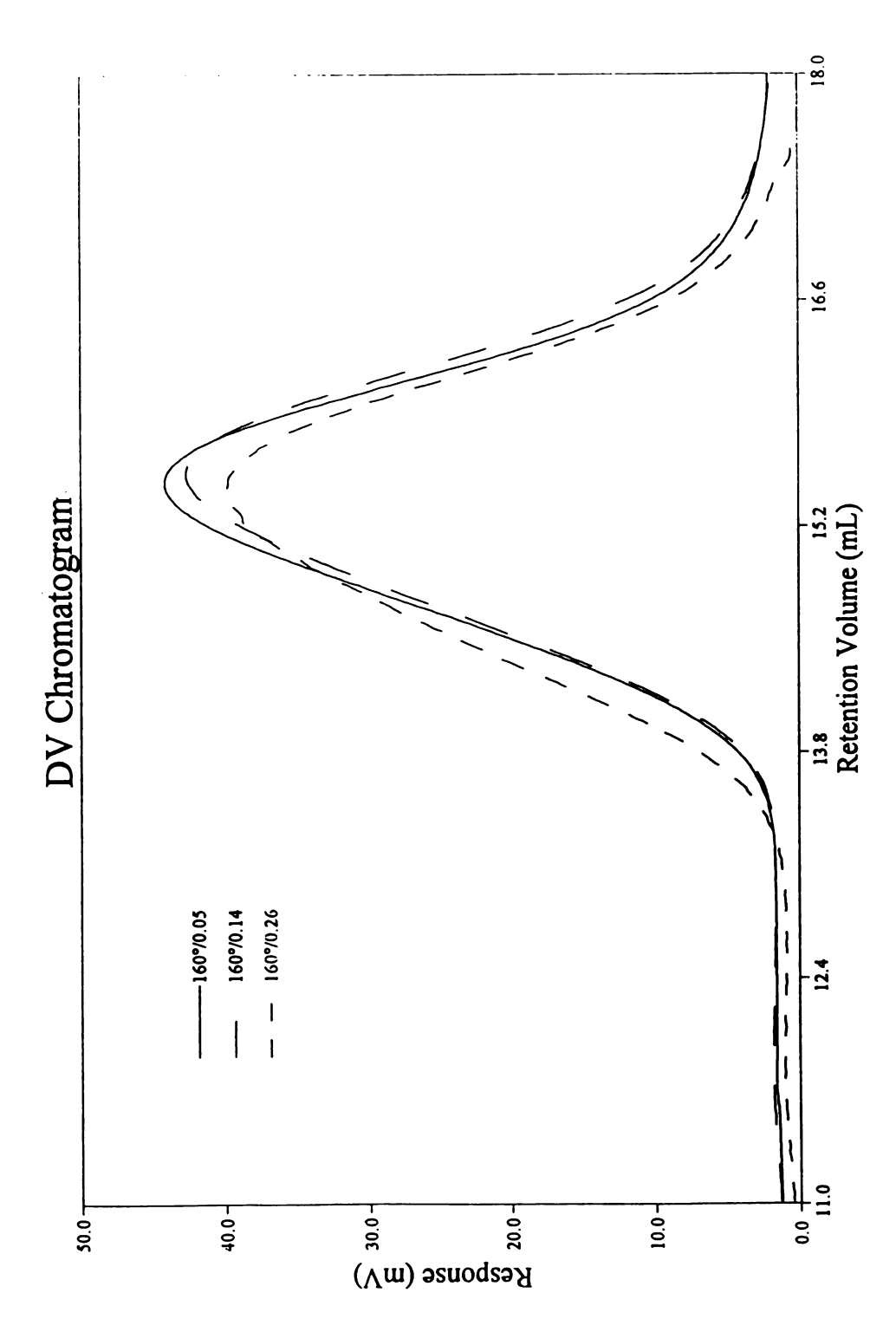


Figure 5.2: DV chromatogram showing the shift in molecular weight distribution of PLA extruded at 160°C with increasing L101 content. (normalized to concentration)

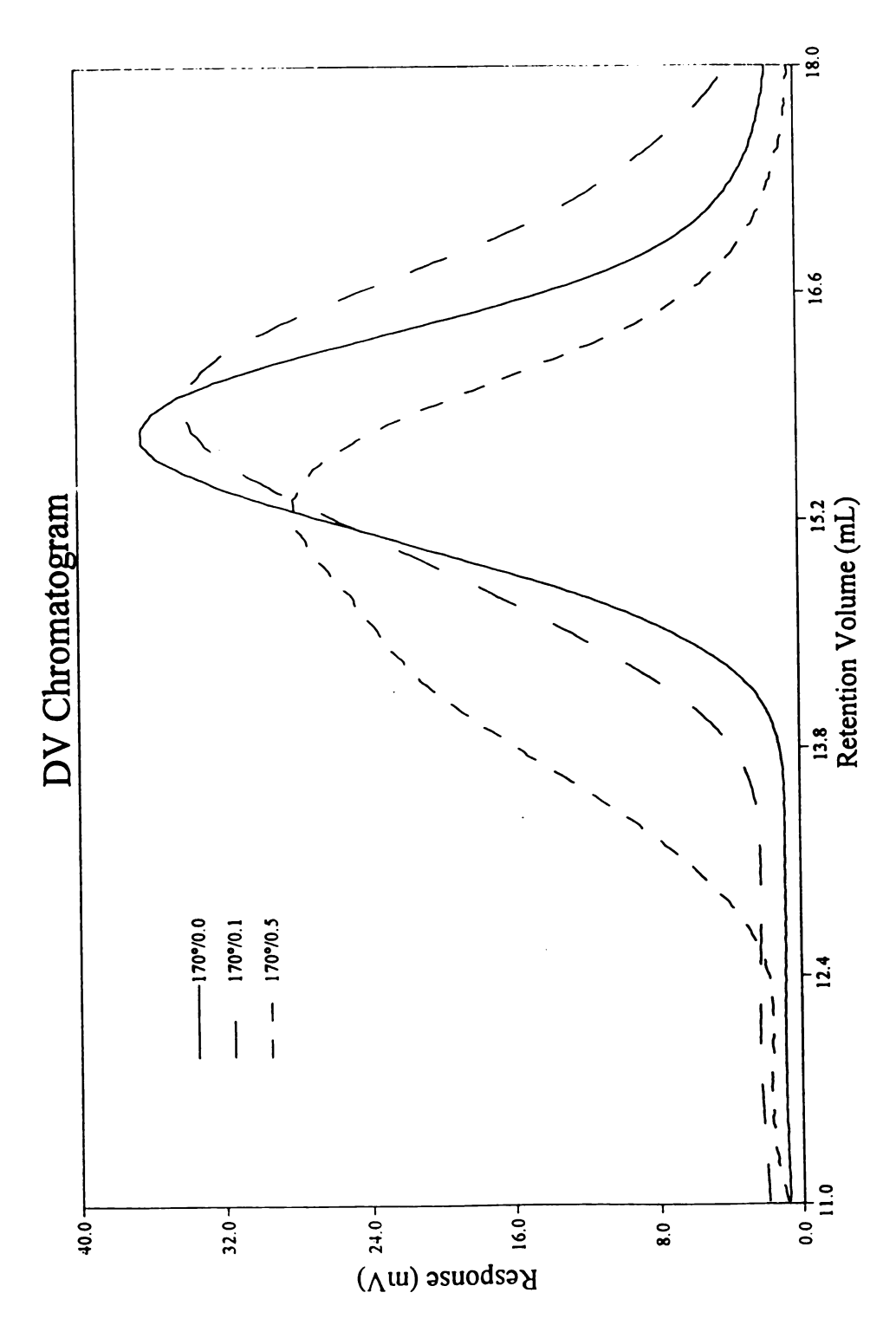


Figure 5.3: DV chromatogram showing the shift in molecular weight distribution of PLA extruded at 170°C with increasing L101 content. (normalized to concentration)

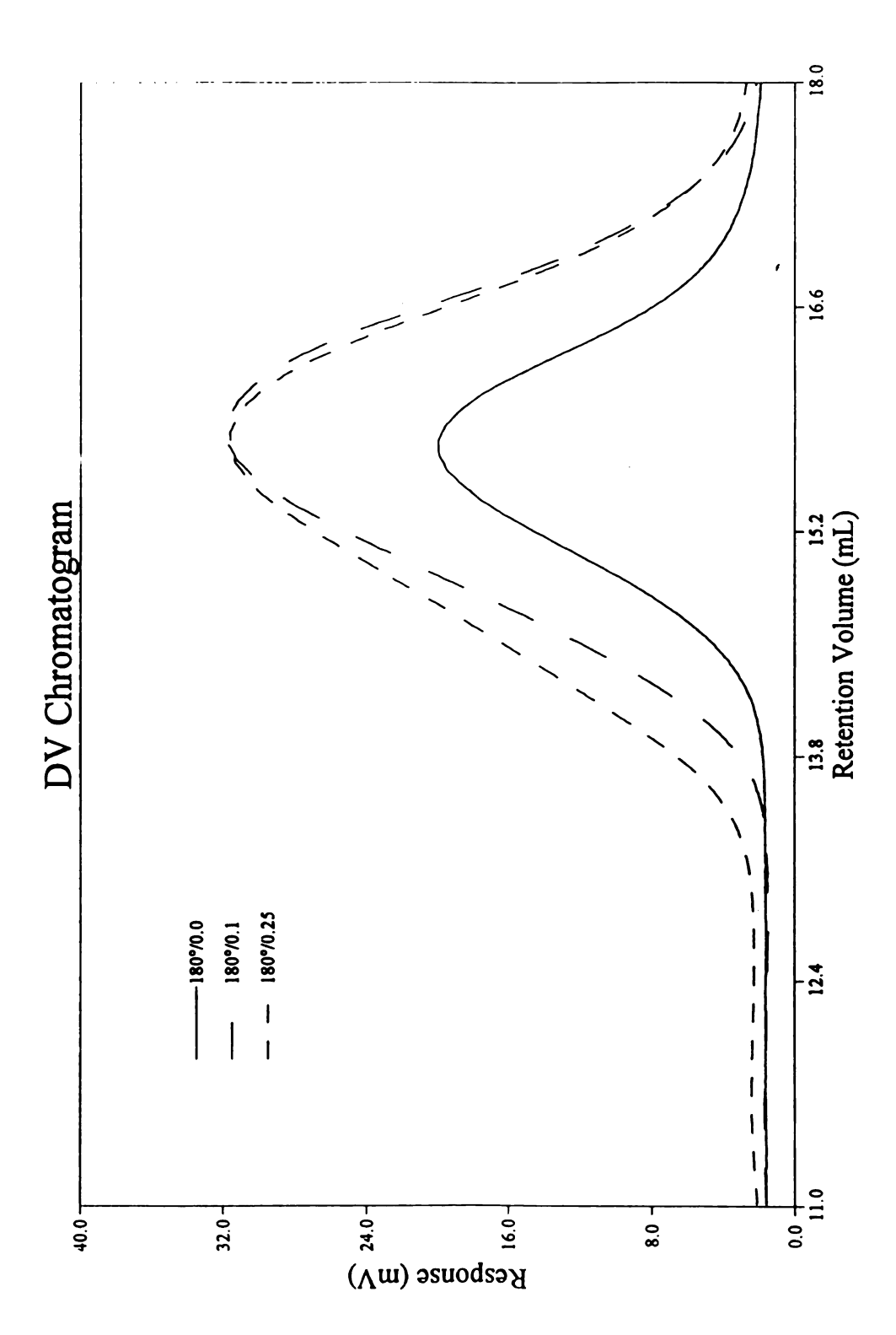


Figure 5.4: DV chromatogram showing the shift in molecular weight distribution of PLA extruded at 180°C with increasing L101 content. (normalized to concentration)

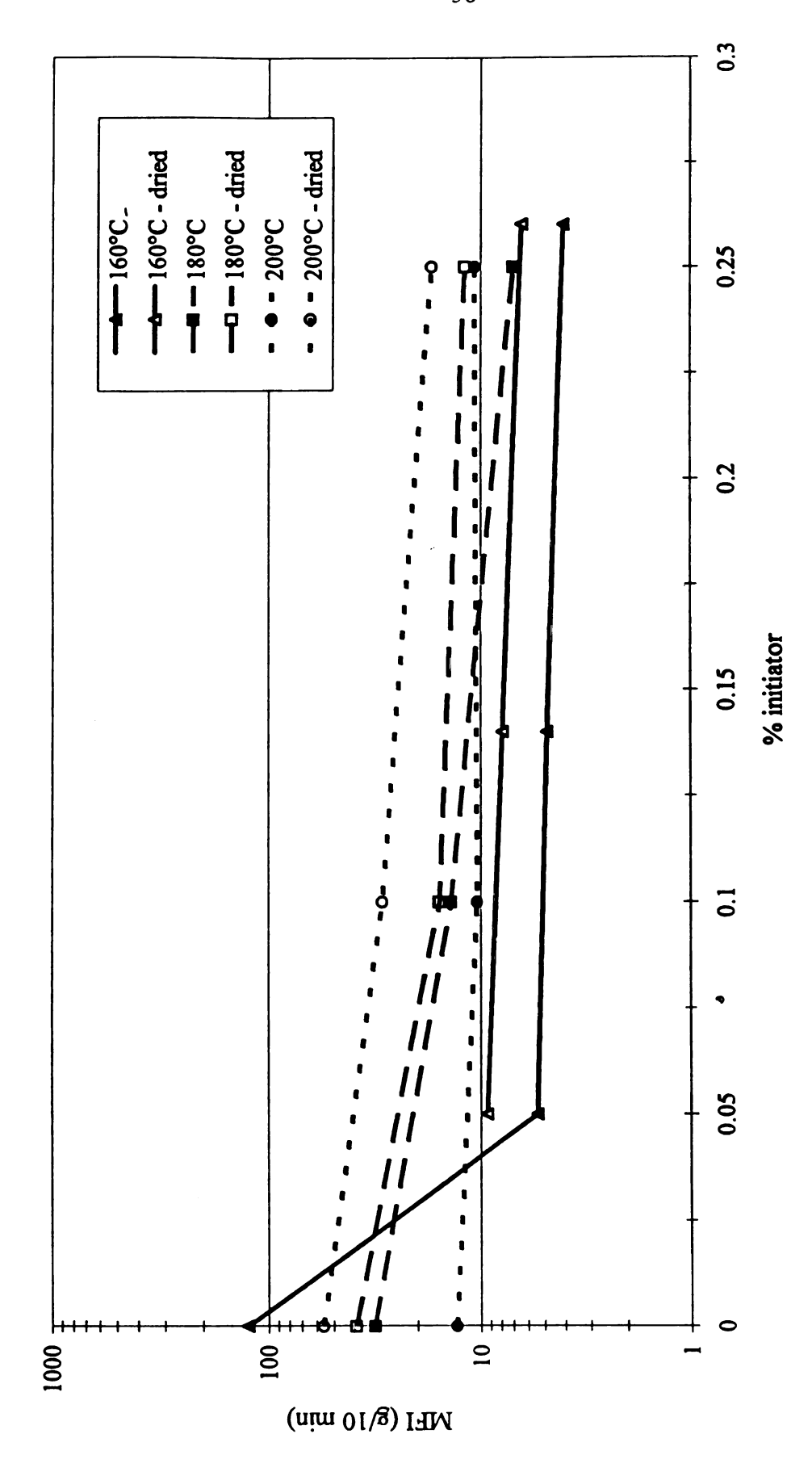


Figure 5.5: MFI of extruded samples showing a decrease in MFI with increasing L101 content.

### 5.1.3 Thermogravimetric Analysis

TGA measures the change in weight of a sample due to volatilization, reaction, or absorption from the gas phase [Rauwendaal (1986)]. An increase in the decomposition temperature results in a more thermally stable product. At an initiator content of 0.1%, an increase in the extrusion temperature results in an increase in the decomposition temperature and a more thermally stable polymer as compared to unextruded, unreacted PLA which degrades more readily (entries 1, 5, 8, 10, 13 in Table 5.1, also Figure 5.6). Jamshida (1988) has proposed thermal degradation by a back-biting mechanism starting from the end groups of the PLA chain. At 0.1% L101, PLA is branched leading to a decrease of the total number of end groups; therefore, the probability of thermally degrading side reactions occurring by this mechanism might be reduced.

At an initiator content of 0.5%; however, the higher extrusion temperature has a somewhat lower decomposition temperature, indicating that the product at 170°C is more thermally stable than that at 190°C (entries 6 and 11 in Table 5.2; also Figure 5.7). An explanation of this may be as follows: a higher temperature tends to produce a lower gel content [Hamielec et al. (1990)] so the lower temperature is more cross-linked and may be more difficult to degrade. In addition to the fact that higher temperatures tend to produce less cross-linked materials resulting in more end groups available for degradation, higher temperatures seem to be more

favorable to chain scissions by free radical processes or intramolecular transesterification leading to the formation of oligomers. Oligomers have been shown to promote the degradation and also the thermal instability of PLA [Jamshida et al. (1988)].

Products extruded at 160 C show little change in decomposition temperature at an increasing initiator content (entries 2-4 in Table 5.2). The decomposition temperatures are lower than that of pure, unextruded PLA (entry 1 in Table 5.2) which is characterized by longer chains. Once again, the extrusion at 160 C causes degradation with a sharp decrease in M<sub>n</sub> as reported by Gogolewski (1993).

Table 5.2: Decomposition temperatures from thermogravimetric analysis.

ID#	Temperature (C)	wt% L101	Onset Value (°C)	Max. Value (C)
1	Pure PLA	-	320.0	321.2
2	160	0.05	319.4	320.5
3	160	0.14	319.1	320.1
4	160	0.26	318.8	319.7
5	170	0.1	323.8	325.1
6	170	0.5	322.1	323.3
7	180	0.0	315.4	$316.5^2$
8	180	0.1	322.0	323.2
9	180	0.25	324.3	325.5
10	190	0.1	323.9	325.2
11	190	0.5	321.1	322.3
12	200	0.0	326.4	328.0
13	200	0.1	326.5	328.0
14	200	0.25	319.5	320.5

- 1 Maximum rate of decomposition
- 2 Temperature still declining

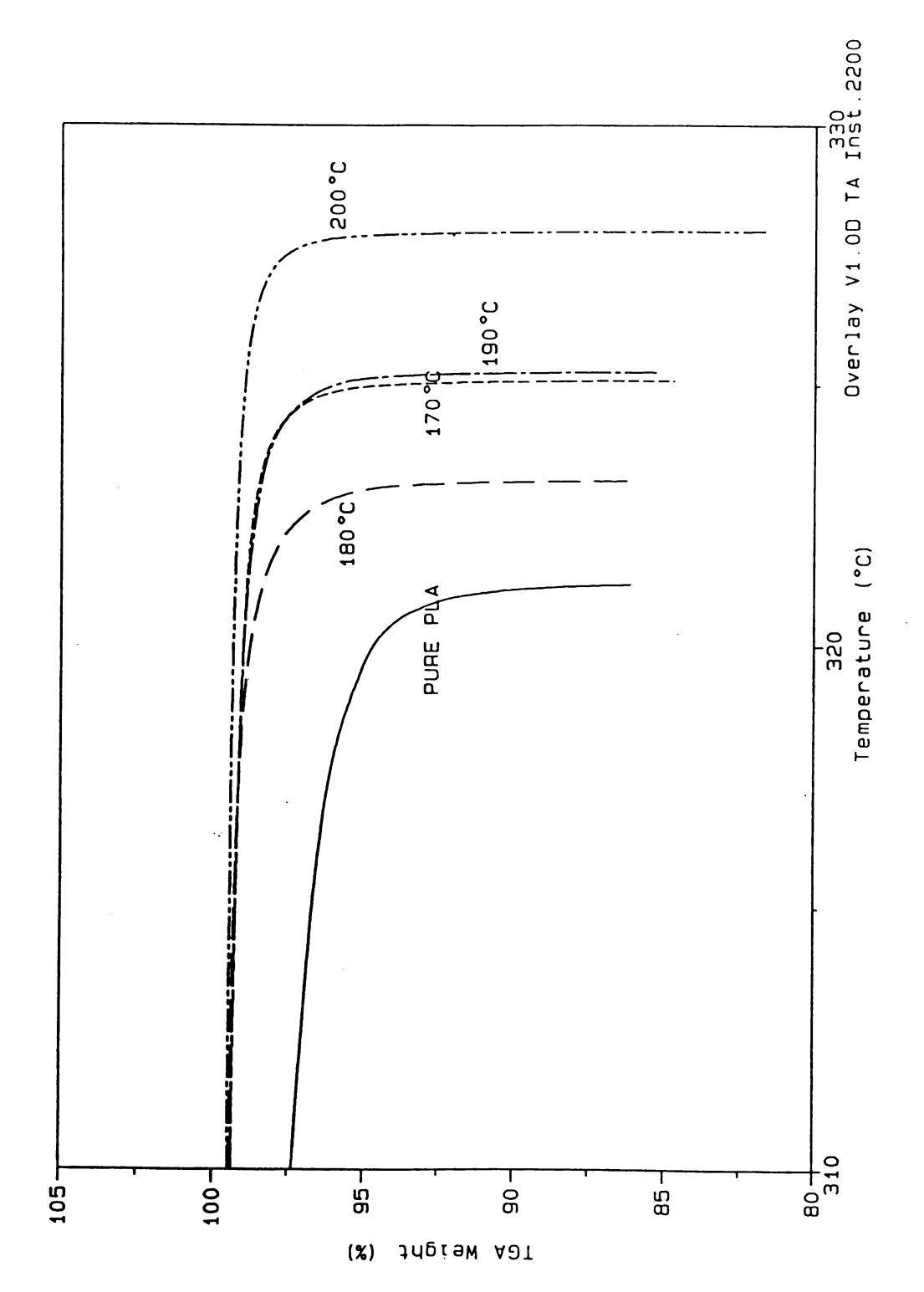


Figure 5.6: TGA showing decomposition temperature for branched PLA with 0.1% L101.

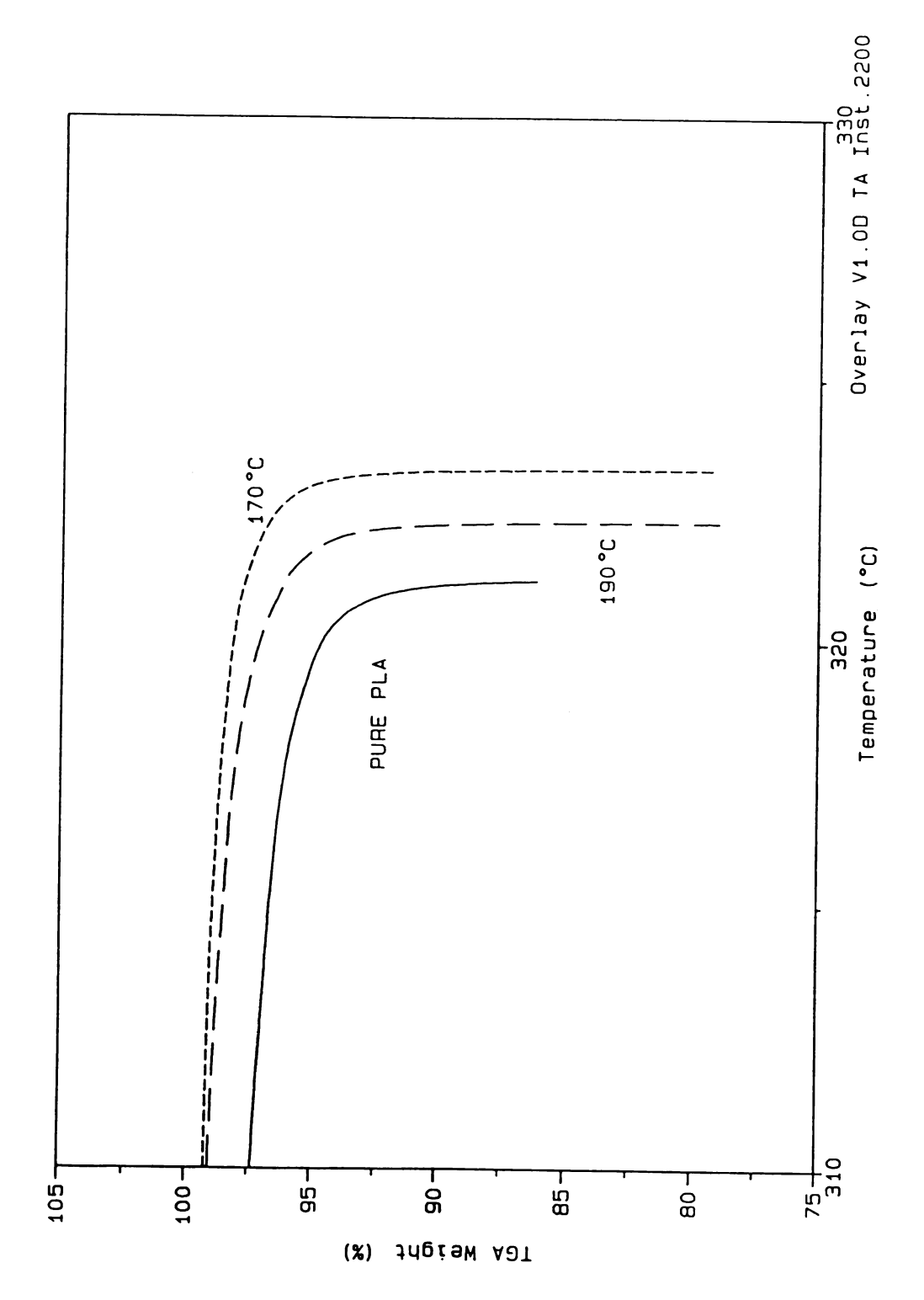


Figure 5.7: TGA for pure PLA compared to extruded PLA with 0.5% L101.

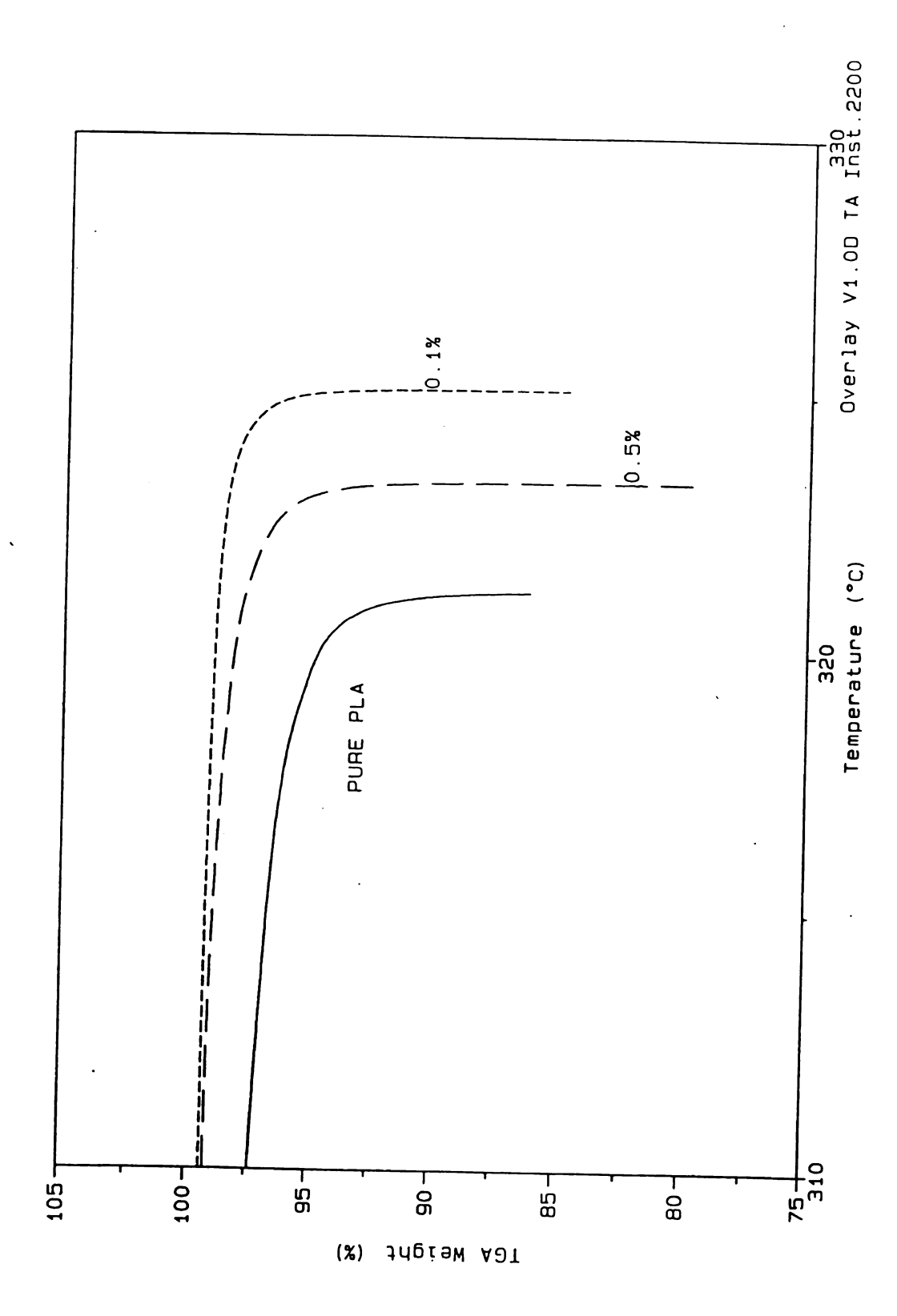


Figure 5.8: TGA for free radical branched PLA at 170°C.

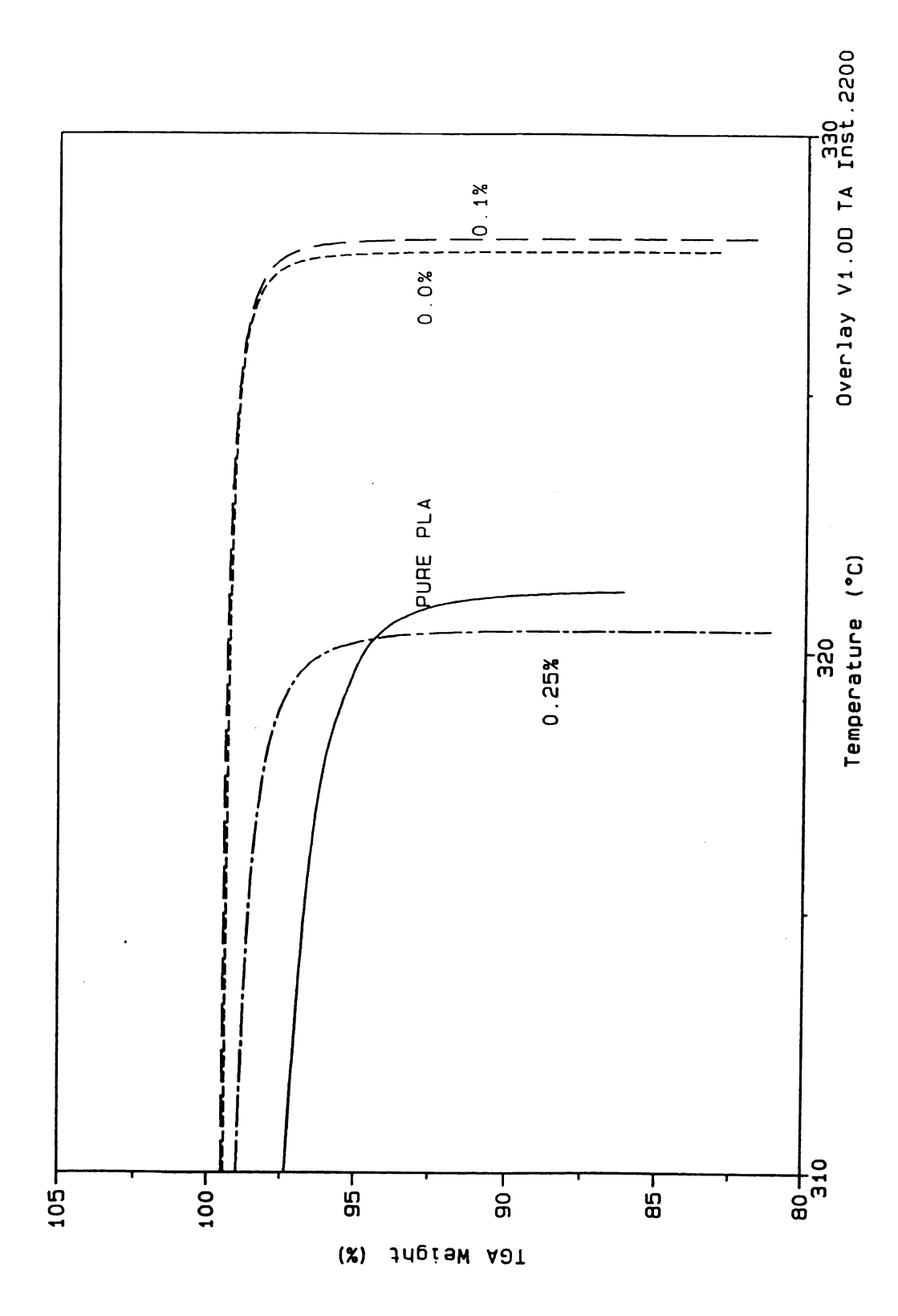


Figure 5.9: TGA for free radical branched PLA at 200°C.

At 180 C, when increasing the initiator concentration from 0.0 to 0.25% L101, the thermal stability increases which indicates that branching also increases (entries 7-9 in Table 5.2). With no initiator present, the sample extruded at 180°C is not as stable as unmodified PLA indicating that degradation has probably occurred (compare entries 1 and 7 in Table 5.2). This could be a result of hydrolysis, i.e. more hydroxyl groups are present resulting in easier degradation.

At temperatures of 170°C and 190°C, samples with an initiator concentration of 0.5% (entries 6 and 11 in Table 5.2) are less thermally stable than those with an initiator concentration of 0.1% (entries 5 and 10 in Table 5.2); however, both are more stable than unextruded PLA. At so high of initiator concentration one can assume, next to the proposed microgel formation of PLA, that a large amount of chain scissions occur resulting in the formation of short chains which are less stable. Figure 5.8 shows the TGA for the PLA system extruded at 170°C. A plot for the 190°C system is very similar.

Figure 5.9 (entries 1 and 12-14 in Table 5.2) clearly confirms the results obtained in Table 5.1 at a extrusion temperature of 200°C, i.e. even if there is some branching which occurs, there are also chain scissions which become extremely important as the L101 content is increased. For example, the stability of PLA

extruded at 200 C in the presence of 0.25%L101 is even worse than that of pure, unextruded PLA.

# **5.1.4 Differential Scanning Calorimetry**

The reactive extrusion of PLA with L101 did not affect the glass transition temperature, T<sub>G</sub>, which was maintained in the range of 58°C to 62°C for all samples, reacted and unreacted (Table 5.3, also Figure 5.10). A crystalline region was noted at about 117°C to 123°C for all samples. These results were somewhat surprising as a change in the T<sub>G</sub> was expected. When the molecular weight increases, the density of the end groups decreases which leads to a decrease in the free volume, and hence, an increase in the T<sub>G</sub> should result. In general, branching normally decreases the T<sub>G</sub>, as the free volume is increased, while crosslinking increases the T<sub>G</sub>, as the number of end groups is decreased.

Table 5.3: DSC results: 10°C/min to 200°C

Temperature (°C)	%L101	$T_{G}(C)$	endothermic transition (°C)
Pure PLA	-	59.2	122.6
170	0.1	59.1	121.61
180	0.1	58.6	121.3
190	0.1	58.6	121.1
200	0.1	58.0	120.9
160	0.0	62.2	117.7
170	0.5	62.0	117.4

<sup>1</sup> A third transition was apparent at 114°C.

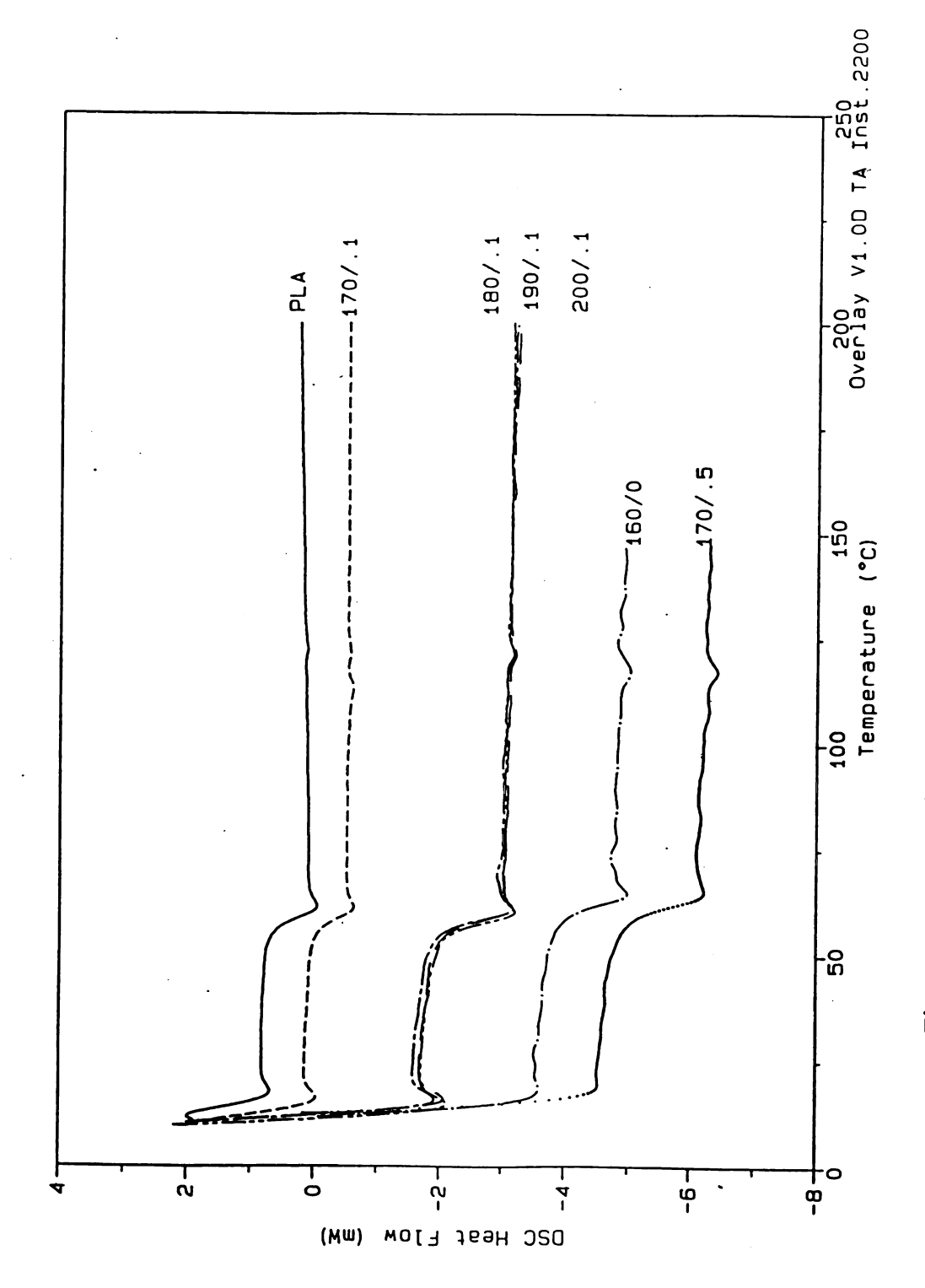


Figure 5.10: Compilation of DSC results for T<sub>G</sub> comparison.

# 5.1.5 Dynamical Mechanical Analysis

DMA confirmed the results found by DSC: no noticeable change in T<sub>G</sub> was apparent. At the glass transition temperature, T<sub>G</sub>, the storage modulus, G', shows a rapid decrease (Figure 5.11), while the loss modulus, G'', and the tan delta (ratio of loss modulus to storage modulus) exhibit maximums (Figures 5.12 and 5.13 respectively). Table 5.4 shows the average T<sub>G</sub> results given by DMA. PLA 110 is pure PLA which has been compression molded at 110°C, while PLA 140 has been molded at 140°C. The T<sub>G</sub> associated with G' is generally accepted as the value which is reported for polymeric materials.

Table 5.4: T<sub>G</sub> averages for dynamic mechanical analysis.

Temperature (C)	%L101	G'	G"	tan δ
PLA 110	-	61.78	69.98	75.36
PLA 140	-	61.46	69.38	75.1
190	0.1	60.88	68.25	74.71
200	0.1	61.32	69.06	74.82
170	0.5	59.92	69.71	75.36
190	0.5	59.83	68.23	74.62

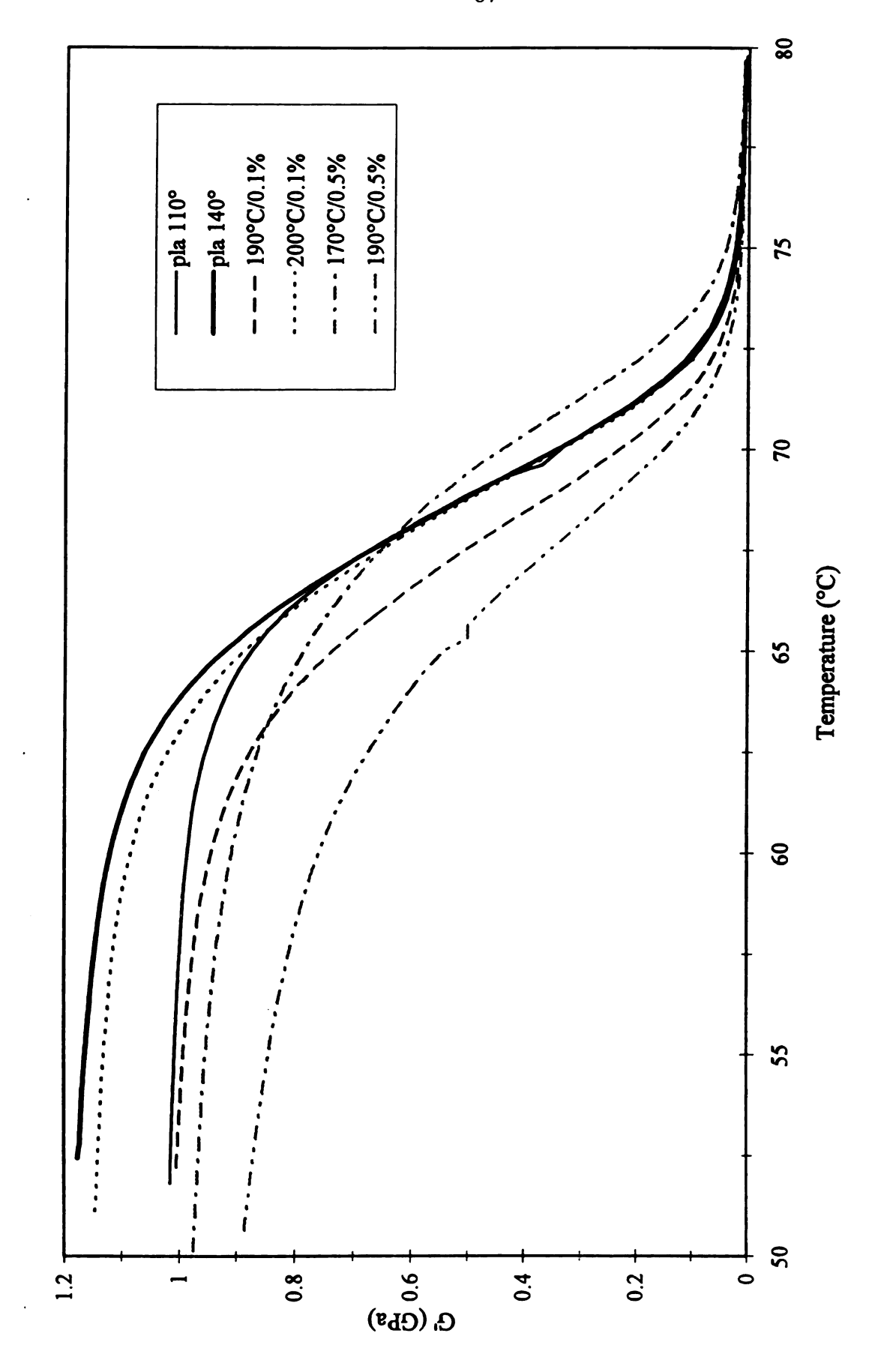


Figure 5.11: Storage modulus for several samples as given by DMA.

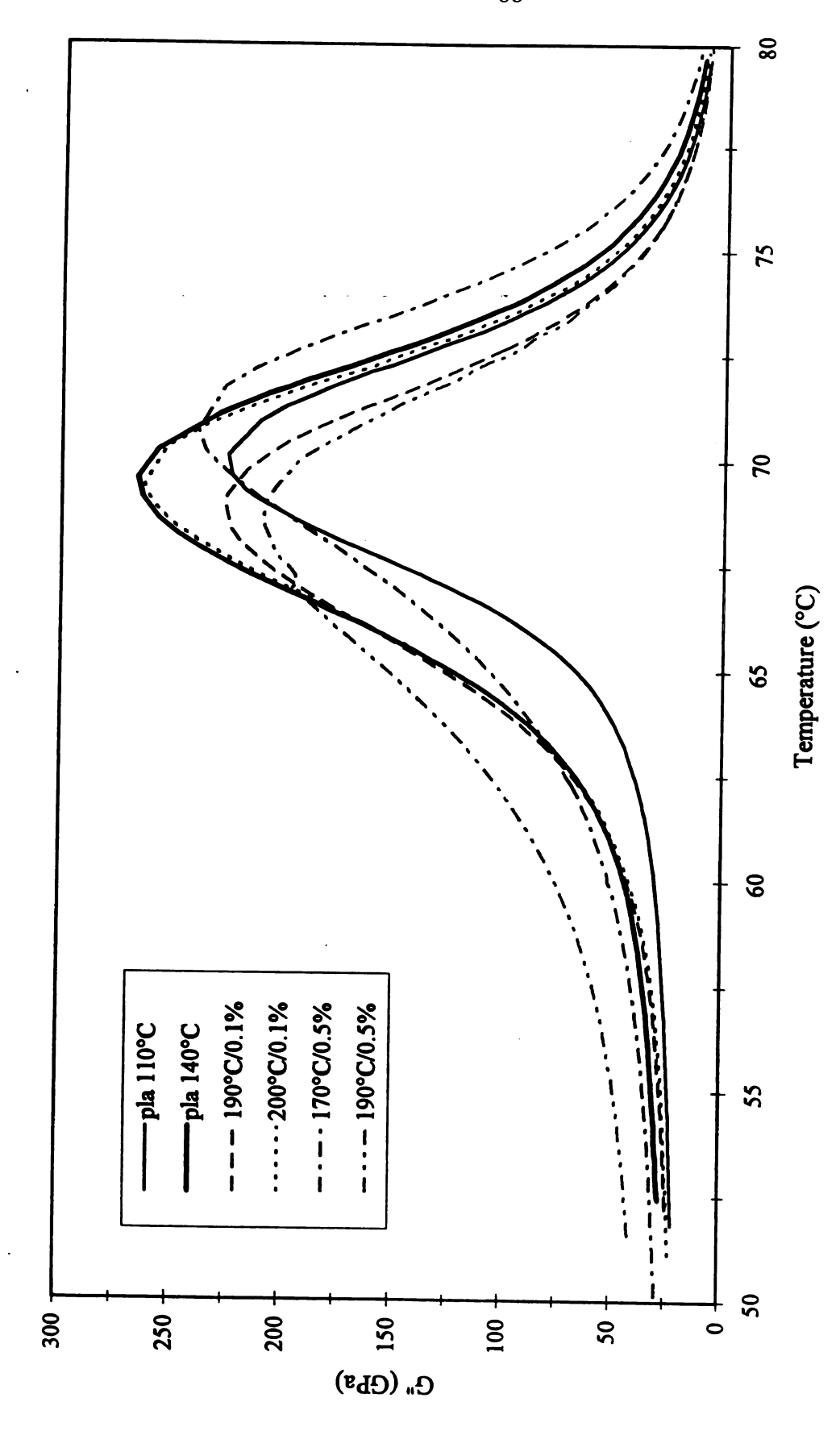


Figure 5.12: Loss modulus for several samples as given by DMA.

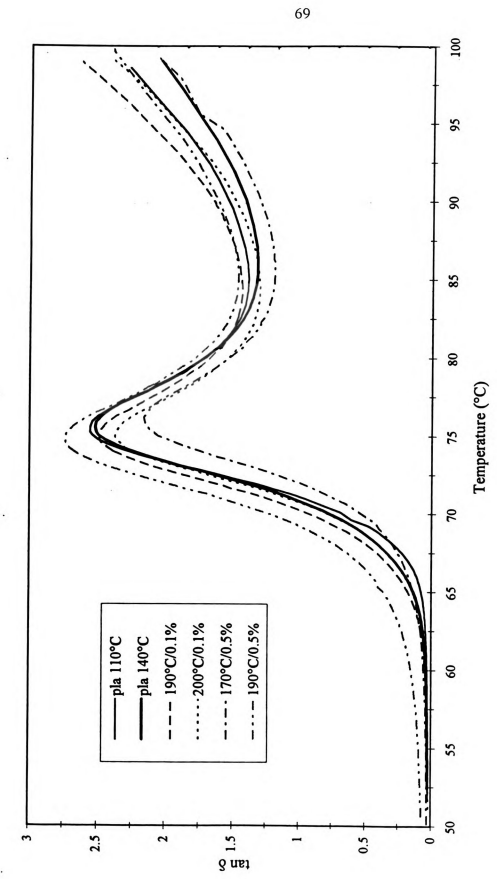


Figure 5.13: Tan delta (tan 8) for several samples as given by DMA.

# **5.1.6 Highly Branched Samples**

This section is specifically devoted to the 170°C and 190°C samples with 0.5% initiator concentration. Besides having a large weight average molecular weight and a high polydispersity, the highly branched samples have other outstanding characteristics. The weight average radius of gyration (Rg<sub>w</sub>) for all the other samples was between 14 and 20 nm (see TriSEC data in Table A-1 of the Appendix), but the Rg<sub>w</sub> for 170°/0.5 and 190°/0.5 were 649 nm and 936 nm, respectively.

As previously stated in Section 5.1.2, these highly branched samples were more difficult to filter in comparison with the other samples. A material balance was done indicating that approximately 20% of the 170°/0.5 sample and about 10% of the 190°/0.5 sample were entrained in the 0.45 micron GPC filter. This material is either microgel, contaminants, or both.

The Mark-Houwink parameter "a" is a polymer confirmation parameter (see Section 2.2.4). For random coil molecules, "a" usually has a value between 0.5 for a poor solvent and 0.8 for a good solvent. Typical "a" values for the PLA polymers which were not highly branched were between 0.64 and 0.77 (Table A-1 in the Appendix). For polymers containing long chain branching, the "a" value can fall below 0.5, depending on the degree of branching [Viscotek (1992)]. The

values for 170°/0.5 and 190°/0.5 are 0.47 and 0.46, respectively, further confirming that these polymers may have long chain branching.

Figure 5.14 is a Mark-Houwink plot of the 170°C series. A linear Mark-Houwink (M-H) plot is generally found in linear standards. For a given polymer, samples which have the highest slope and intercept on a M-H plot represent the least branched structures. As seen in Figure 5.14, the 170°/0.5 sample is considerably lower than the other samples indicating a highly branched structure. The 170°/0.5 molecular weight is also greater than that of the other samples as the log (M.W.) line extends farther than that for the other samples. A M-H plot of the 190°C series showed similar results. A comparison of PLA and 170°/0.1 in Figure 5.14 shows that the M-H plot for both samples is similar in agreement with an earlier statement that these samples are almost equivalent.

The percent of polymer with a molecular weight above 1,000,000 Daltons was also determined. Pure PLA and all other samples which were not thought to be highly branched had less than 1% of their total molecular weight above 1,000,000. 170°/0.5 has 11.14% and 190°/0.5 has 8.31% above 1,000,000 indicating long chain formation. Table 5.5 summarizes these findings in comparison with unextruded PLA.

Table 5.5: Highly branched sample comparison to unextruded PLA.

Sample	Rg <sub>w</sub> (nm)	"a"	% above 1,000,000
PLA	17.85	0.72	< 1
170°/0.5	649	0.47	11.14
190°/0.5	936	0.46	8.31

Figure 5.15 shows a comparison of the light scattering chromatographs of pure PLA and of the 190°/0.5 sample. Clearly obvious is the bimodal peak in the 190°/0.5 sample which indicates that there is a considerable amount of high molecular weight polymer present in the sample in comparison to pure PLA in which there is no such peak. This phenomenon was seen in both the 170°/0.5 and the 190°/0.5 cases.

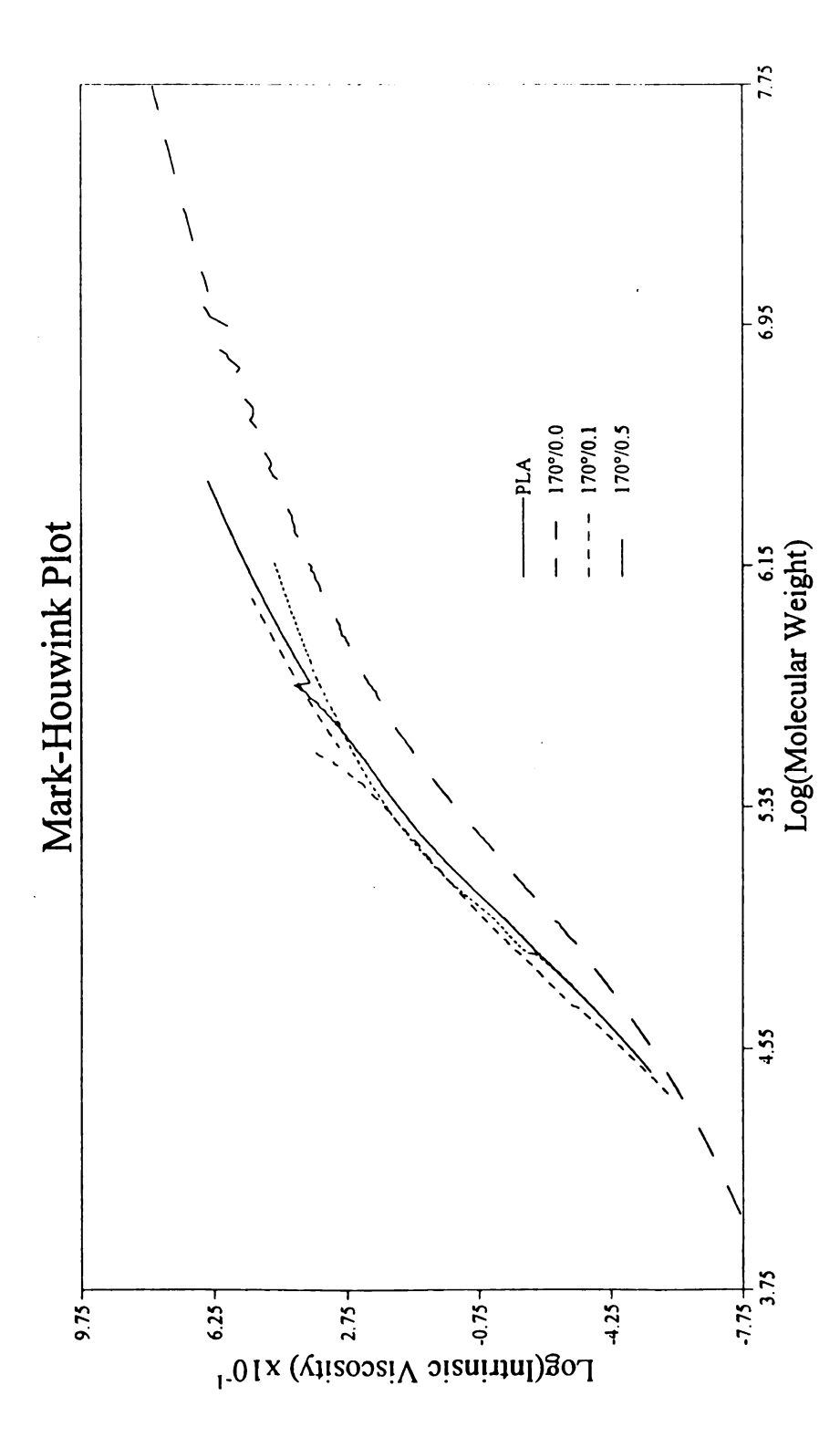
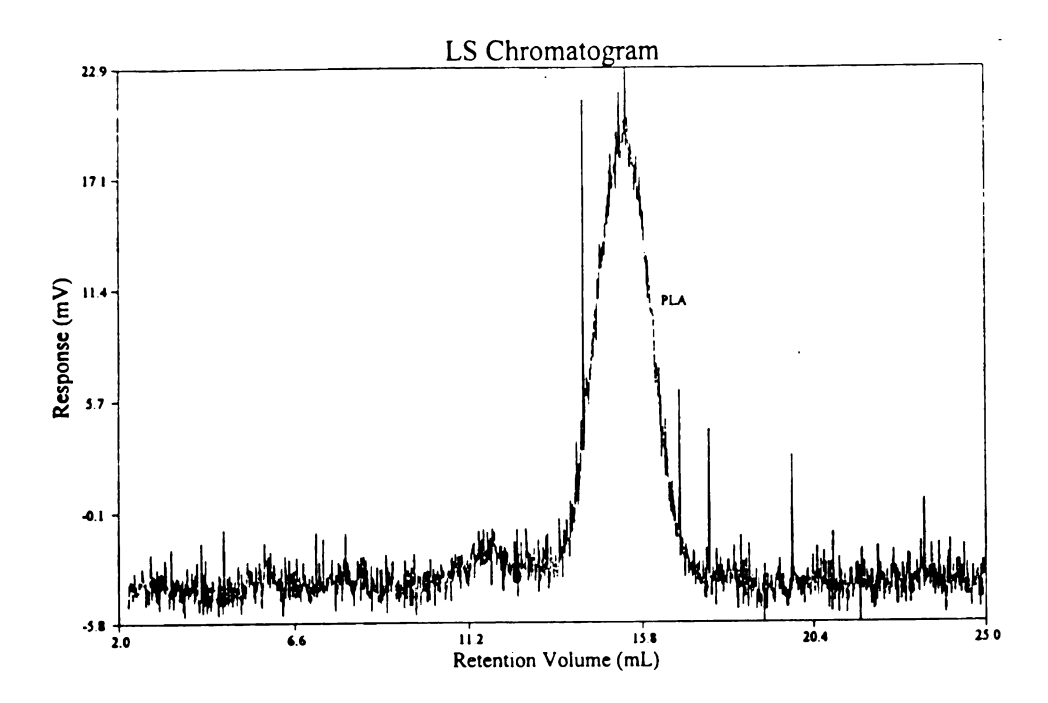


Figure 5.14: Mark-Houwink plot of the 170°C series.



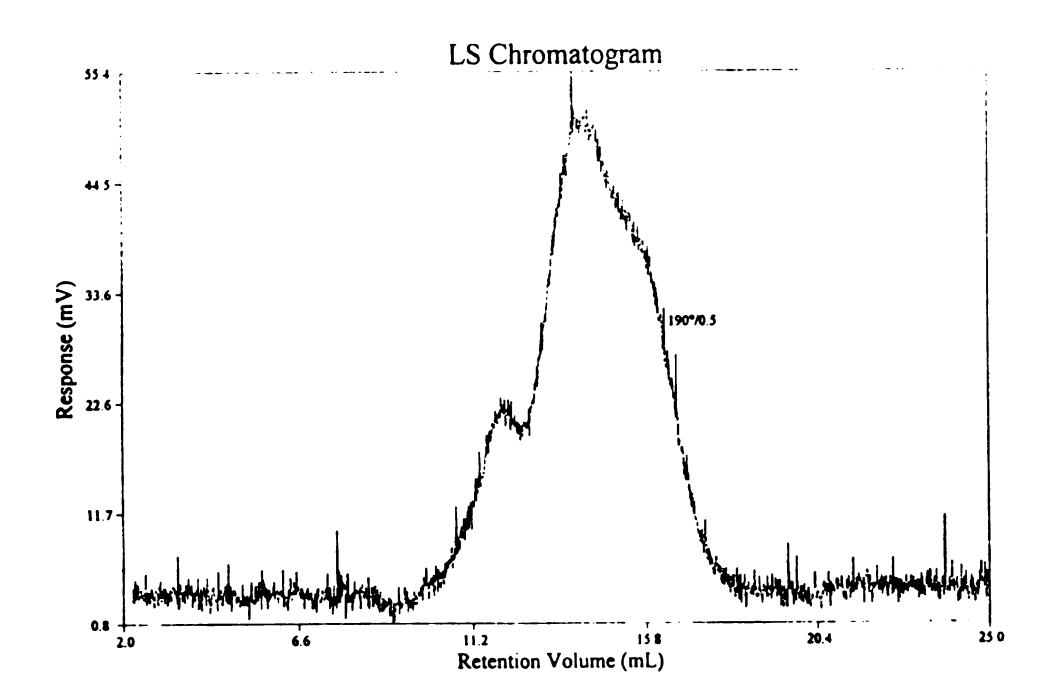


Figure 5.15: A comparison of light scattering chromatographs of PLA (top) and 190°/0.5 (bottom).

## 5.1.7 Film Results

An initial study of PLA film extrusion was done at in this investigation. A small single screw film extruder with an 18'x 3/4" barrel was used to extrude samples of pure PLA and PLA with initiator. As this was a preliminary study to evaluate the feasibility of film extrusion, only an extrusion temperature of 170°C was used. Three different compositions were extruded: (1) pure PLA, (2) PLA and 0.1% L101, (3) PLA and 0.5 L101. With 0.5 % free radical initiator, the resulting product was highly branched and did not extrude to a usable film.

Table 5.6 shows the film properties of PLA and PLA with 0.1% L101. Tensile tests for strength, elongation and tensile modulus were conducted on a UTS machine SFM-20 using ASTM D882 for thin films. Table A-3 in the Appendix lists the operating conditions as well as the data for all experimental runs.

Table 5.6: Tensile results for PLA film.

Property	PLA	PLA with 0.1% L101
Film thickness	0.005	0.003
Maximum psi	2980 +/- 190	2680 +/- 130
% elongation at break	3.6 +/- 1.3	4.1 +/- 2.0

# 5.2 Proposed Reaction Mechanism

The formation of a free radical is the first step in the following proposed reaction mechanism. Figure 5.16 shows the decomposition of L101 which may generate several free radicals. The beta scission is a secondary reaction which may occur. Once the free radical initiator is formed, branching may take place.

Figure 5.17 details the proposed reaction mechanism. First, hydrogen radical abstraction of the PLA polymer chain must take place. Radical coupling of these newly formed reactive polymer backbones may then occur resulting in the formation of a branched species. Chain scission of the polymer backbone may also occur resulting in the formation of a radical species which may also combine with another radical species to result in a branched polymer.

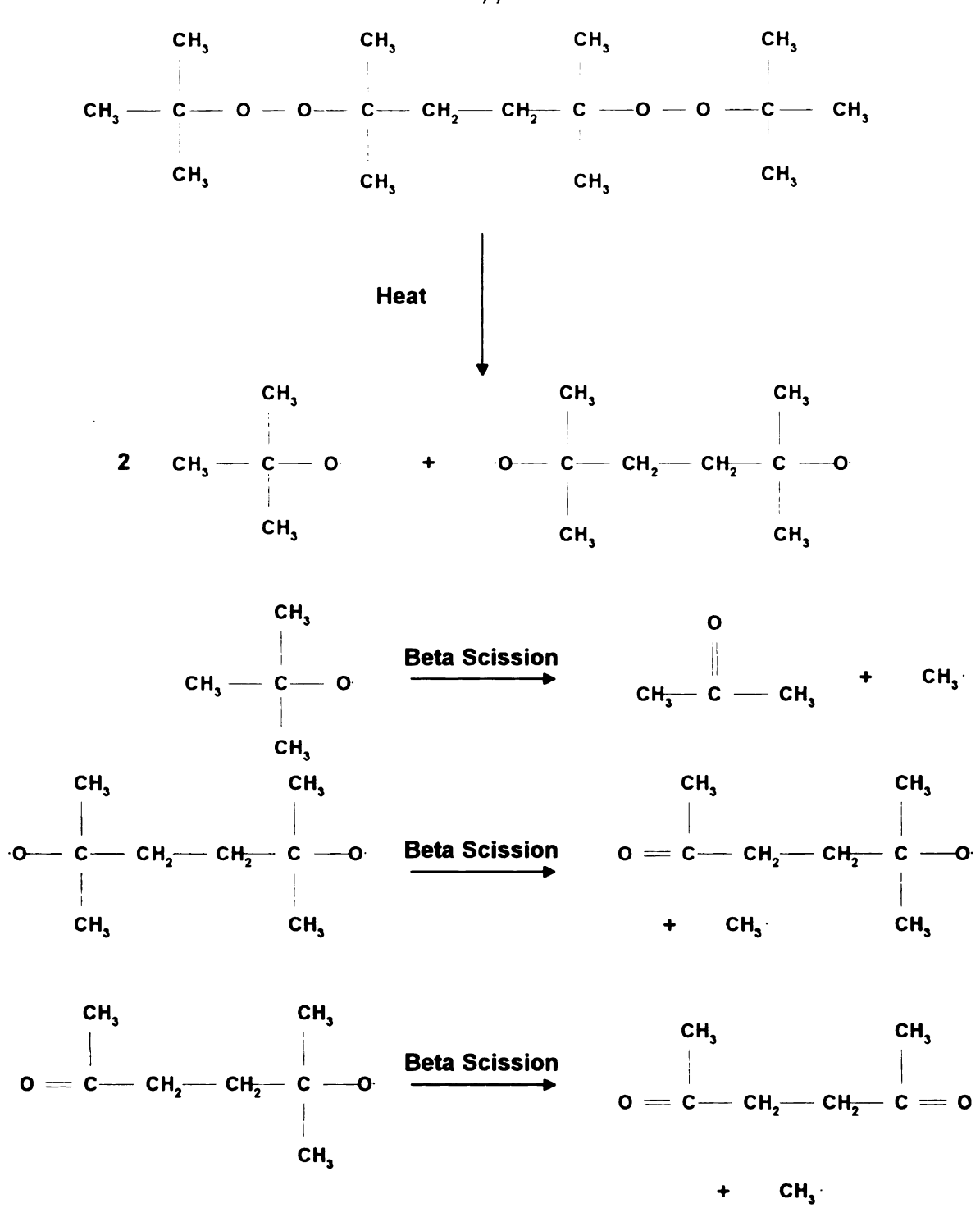
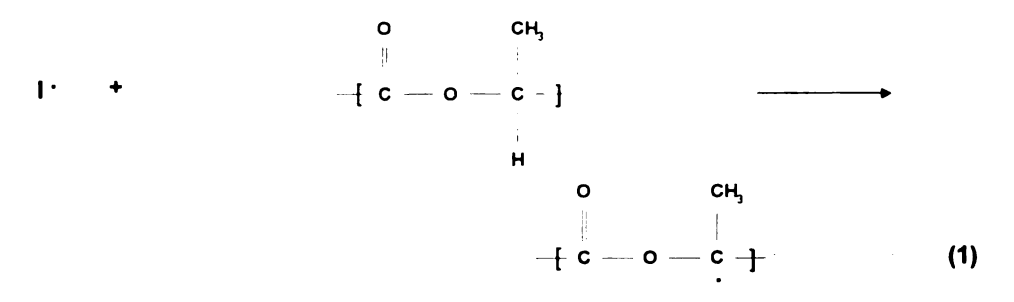
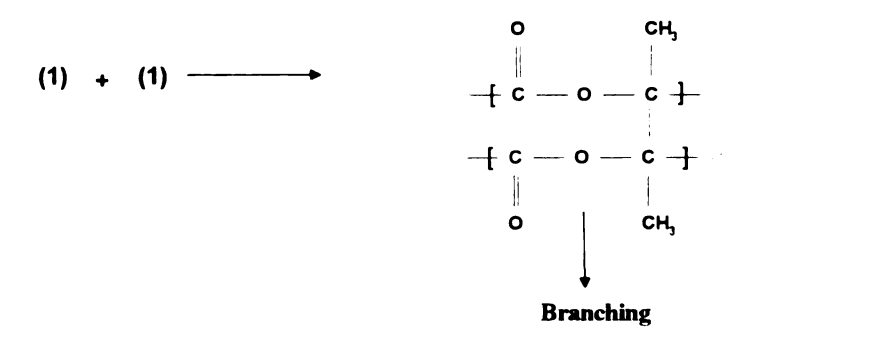


Figure 5.16: Peroxide decomposition.

#### Hydrogen radical abstraction



#### Radical coupling



#### Chain Scission

Figure 5.17: Proposed branching mechanism.

Even if chain scissions could be promoted by free radical processes as proposed in Figure 5.17, they can also be promoted by intramolecular transesterification [McNeill (1985)] (also called backbiting) and thermohydrolysis. Figure 5.18 shows both back-biting and thermohydrolysis reactions and the products which they may produce.

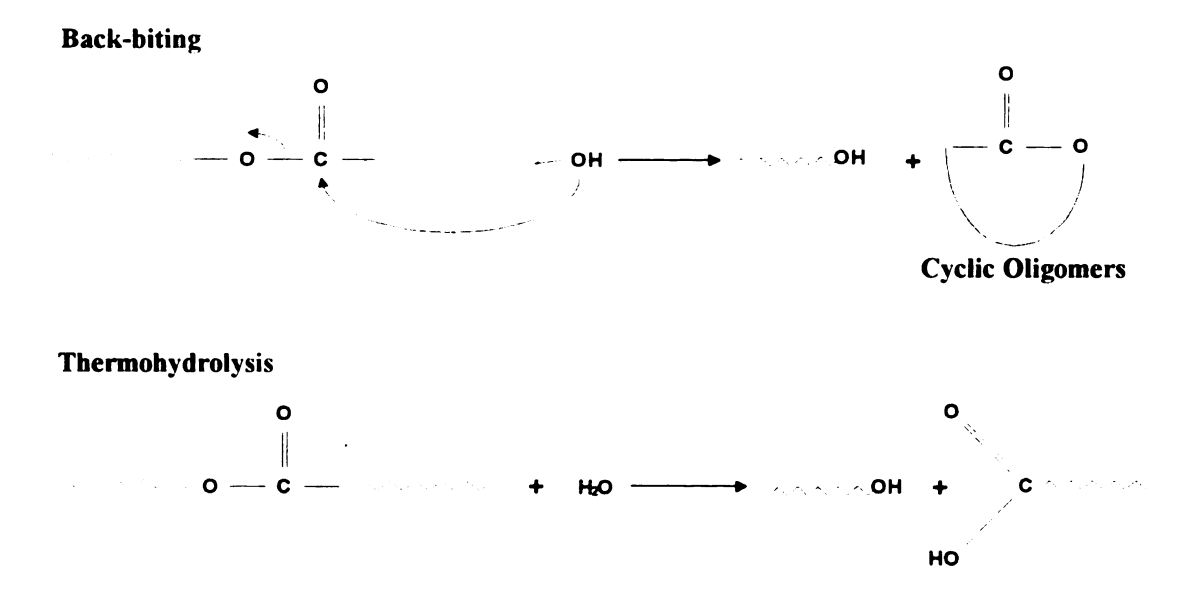


Figure 5.18: Chain scission reactions.

When chain scission occurs, oligomers are formed and there is an increase in the hydroxyl and carboxylic end groups, both of which are favorable to promote thermal decomposition [Jamshidi (1988)]. This is in agreement with the TGA results discussed in Section 5.1.3. When branching occurs, the thermal stability is increased because there is a decrease in both end group and oligomer formation.

In conclusion, there are two competing factors in the free radical extrusion of PLA: (1) branching, which favors large molecular weights, and (2) chain scission or hydrolysis, which favors small molecular weights. In this section, a proposed mechanism has been provided for both of these options. Actual characterization of the true mechanisms would be difficult, if not impossible.

# MALEATION OF PLA

## 6.1 Discussion of Results

The grafting of maleic anhydride to the polylactide backbone was done in an attempt to produce functional groups which would improve the interfacial adhesion of polylactide polymer blends (see Chapter 7). A concentration of 2 percent maleic anhydride was used for all experiments.

# **6.1.1 Effect of Extrusion Temperature**

Based on the free radical branching results given in Chapter 5, the extrusion temperature was not expected to play a large role in the maleation of PLA. Two temperatures were selected (180°C and 200°C) for this study with an initiator concentration ranging from 0 to 0.5% L101. Figure 6.1 shows that for the same initiator concentration, there is little or no difference in the grafting content of MA at the temperatures which were used.

# **6.1.2 Effect of Initiator Concentration**

At 180°C: With no peroxide, the addition of 2% MA has virtually no effect on the extruded PLA. M<sub>n</sub> and M<sub>peak</sub> are approximately the same as the PLA which has been extruded only (compare entry 1 in Table 6.1 with entry 9 in Table 5.1). The addition of 0.1% L101 slightly increases both M<sub>n</sub> and M<sub>peak</sub>. Further addition of L101, 0.25 and 0.5 %, has a slight negative effect on the molecular weight of the samples (see entries 2-4 in Table 6.1). This decrease in molecular weight may be due to the competition between branching (which increases as initiator concentration increases and also increases molecular weight) and grafting of MA (which also increases as initiator concentration increases, but results in little or no molecular weight change).

Figure 6.1 shows that an increase in free radical initiator results in an increase in the percent of maleic anhydride which is grafted (% maleation). Only small amounts of anhydride grafted to a polymer backbone are needed to improve the interfacial adhesion in a polymer blend system. Figure 6.2 is the TriSEC evolution which shows that the changes which occur in the shift of the molecular weights are very subtle and that the molecular weight distribution (the width of the peaks) remains fairly constant.

At 200°: Results similar to the 180°C series are seen at 200°C. The sample with 0.1% L101 has slightly higher M<sub>n</sub> and M<sub>peak</sub>, while the samples with 0.25% and 0.5% L101 are slightly lower (see entries 5-7 in Table 6.1). Figure 6.3 is the analogous TriSEC evolution which also shows (1) subtle shift in molecular weights, and (2) a fairly constant molecular weight distribution.

## General Comments

Table 6.1 also shows the reduction of MP load % at increasing amounts of peroxide. The presence of maleic anhydride appears to cause the chain scission of PLA. A melt flow analysis was done at both temperatures (see Figure 6.4 and Table 6.1) indicating that the addition of increasing quantities of initiator result in higher melt flow indexes (i.e., lower melt viscosity). The observation of increased melt viscosity in the presence of peroxide alone and of reduced melt viscosity in the presence of both peroxide and maleic anhydride is not what is found in the modification of polyolefins. For example, in the modification of polyethylene, the addition of peroxide causes branching and gelation, the presence of maleic anhydride promotes further branching and gelation [Hogt (1988)]; and in the modification of polypropylene, the addition of peroxide cause scission of PP, the presence of maleic anhydride causes further scission of PP chain [Callais et al. (1990)].

Results of the TriSEC analysis further show that the addition of peroxide and MA does increase the chain scission of PLA. Table 6.1 also shows that the weight average intrinsic viscosity,  $IV_w$  of the maleated samples is between 0.73 and 0.95; whereas, the  $IV_w$  for pure PLA is 1.04 (much higher). A further indication of reduced chain size, probably by chain scission, is the decrease in the radius of gyration for the maleated samples (Rg between 13.6 and 15.4 nm) relative to the pure PLA sample (Rg = 17.85 nm) (see Table A.4 in the Appendix).

Table 6.1: Maleation of PLA: MP load %, melt viscosity, TriSEC, and % maleation. (Standard deviations for TriSEC data are located in Appendix A.4. All samples extruded with 2 wt. % MA -- PLA basis)

#01	PLA samples	ımples	MP load %	MFI		SEC	C)		wt% maleation
	T (Ĉ)	wt % L101		(g/10 min)	Mpcak	M <sub>n</sub>	Mw/Mn	IV <sub>w</sub>	
1	180	00.00	28-60	27.8	86,900	81,200	1.25	0.92	990.0
2	180	0.10	61-64	0.09	100,900	008'366	1.27	0.95	0.227
3	180	0.25	19-65	83.6	96,200	000'68	1.30	0.84	0.475
4	180	05.0	85-95	83.4	92,500	85,100	1.31	0.77	0.653
\$	200	01.0	61-63	32.8	103,000	100,100	1.25	0.88	0.280
9	200	0.25	55-57	62.9	81,400	76,500	1.30	0.88	0.464
7	200	0.50	50-52	134.9	90,200	83,200	1.30	0.73	0.672

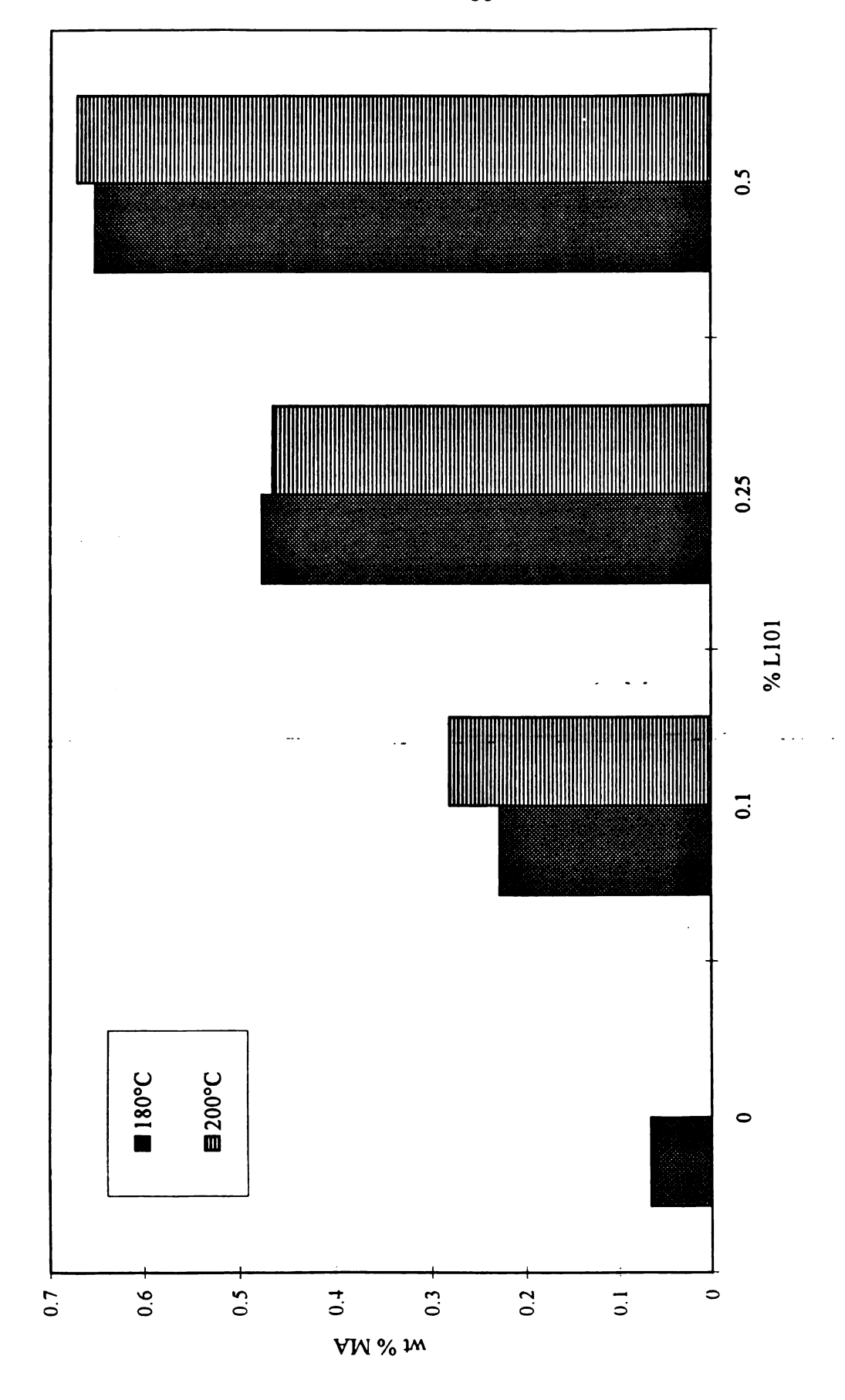


Figure 6.1: Weight percent maleation as a function of initiator concentration.

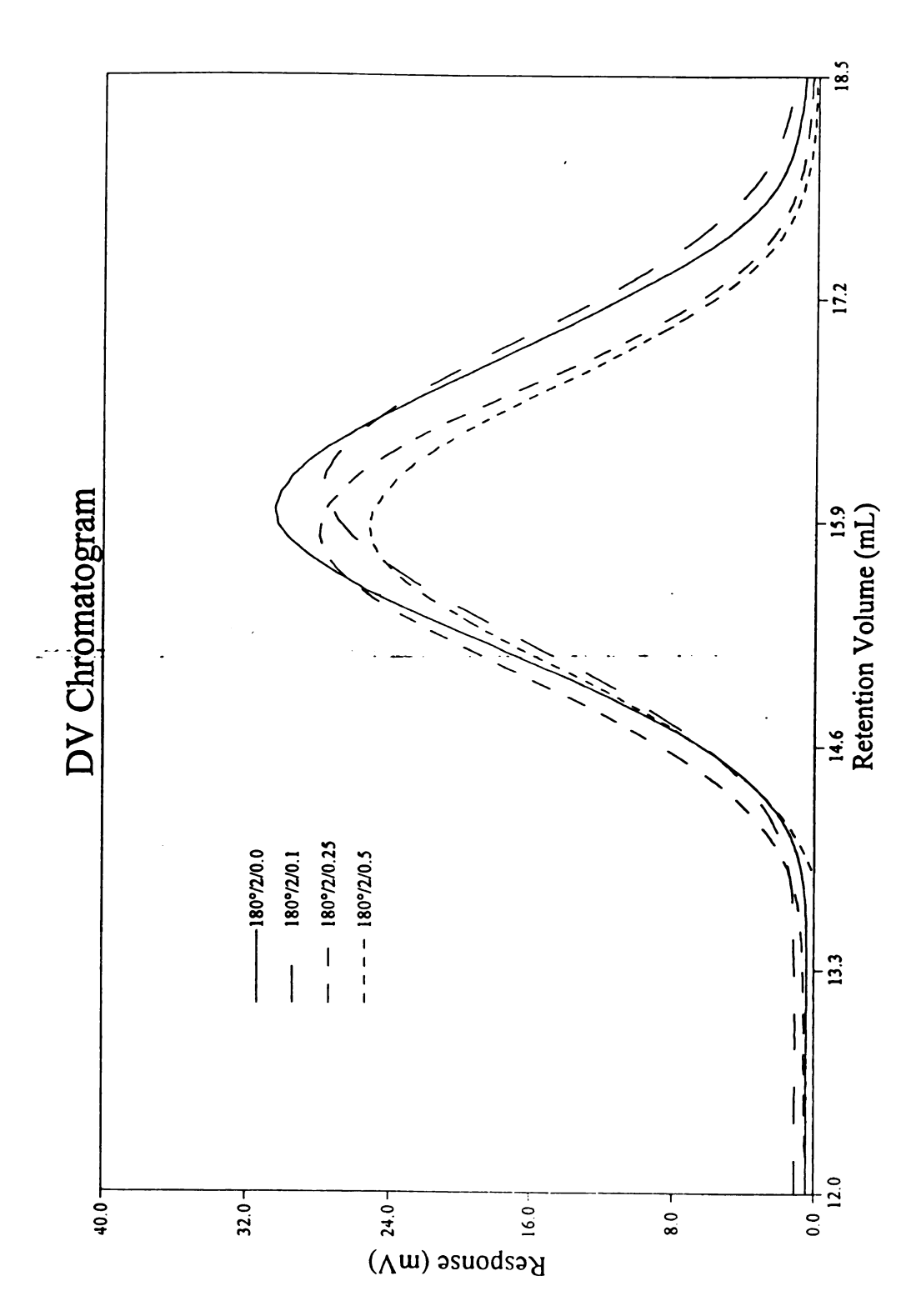


Figure 6.2: DV chromatogram of 180°C maleated series showing molecular weight distribution. (normalized to concentration)

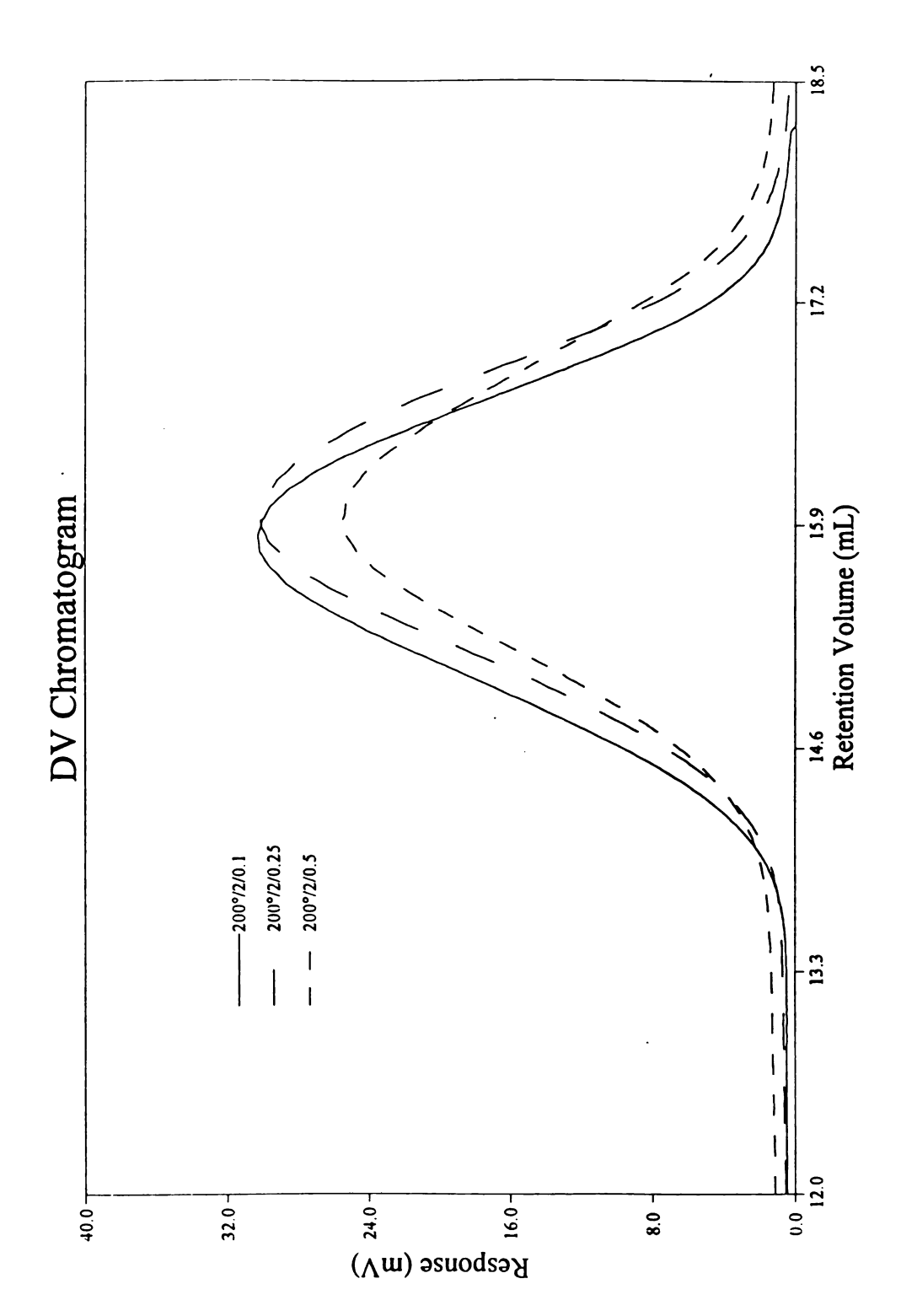


Figure 6.3: DV chromatogram of 200°C maleated series showing molecular weight distribution. (normalized to concentration)

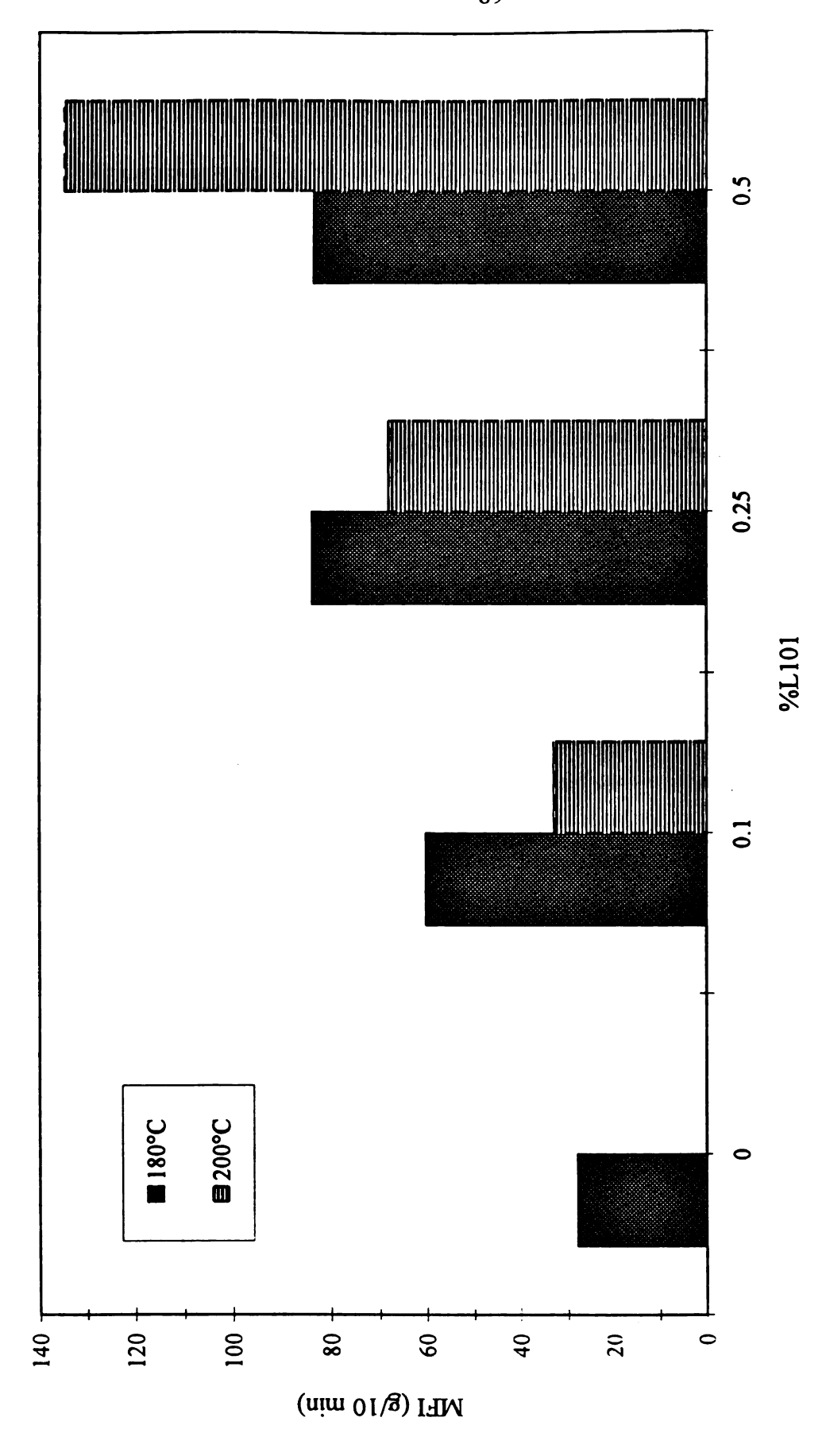


Figure 6.4: MFI of maleated samples (with 2% maleic anhydride).

### 6.1.3 Thermogravimetric Analysis

As stated in Section 5.1.3, an increase in the decomposition temperature results in a more thermally stable product. The maleated samples have decomposition temperatures which range from 2-7°C below that of PLA (see Table 6.2). This is to be expected as the maleated samples, in general, are of lower molecular weight. An exception to this is the 180°/0.1 sample which has a slightly higher decomposition temperature. This is explained by the fact that the 180°/0.1 sample is of a higher molecular weight than the other samples.

Table 6.2: Maleated decomposition temperatures from thermogravimetric analysis.

ID#	Temperature (°C)	wt% L101	Onset Value (C)	Max. Value (°C)
1	180	0.0	311.7	316.4
2	180	0.1	317.3	322.5
3	180	0.25	313.8	318.3
4	180	0.5	309.2	314.6
5	200	0.1	314.9	319.0
6	200	0.25	314.5	319.1
7	200	0.5	309.2	314.9

# **6.2 Proposed Reaction Mechanism**

The formation of a radical is the first step in the maleation of polylactide. The radical formation is the same is it was for the branching of PLA (see Figure 5.16). Once the radical is formed, hydrogen abstraction can occur producing a polylactide which may react with the maleic anhydride radical. The resulting polymer radical may then combine with another radical (MA, peroxide, or polymer radicals or hydrogen) to complete the reaction (see Figure 6.5).

The homopolymerization of maleic anhydride is considered by many to be another significant reaction when grafting MA onto polymer backbones [Gaylord et al. (1983b, 1989)]. Recently; however, Russell (1995) discussed a thermodynamic argument based on the ceiling temperature of poly(maleic anhydride) in which the formation and grafting of poly(maleic anhydride) during maleation in the melt (at temperatures greater than 160°C) would not occur. In the maleation of PLA, the high shear stress in the extrusion process may inhibit the homopolymerization of MA. In any case, the homopolymerization of MA without grafting is assumed to be unlikely for the conditions which were used.

Another possible reaction is beta scission of the polylactide backbone by the free radical leading to an ene-formation which may react with MA (see Figure 5.17, chain scission). A similar process was proposed by De Roover et al. (1995) for

the maleation of PP; however, their experimental observations showed that very severe conditions were needed to favor the ene-reaction with MA including: (1) very low PP molecular mass, (2) very high concentration of MA, (3) high temperature and pressure, and (4) long reaction times. FTIR analysis did not support their (De Roover et al.) theory that an ene-reaction with MA brought about by beta scission occurred. For the maleation of PLA, only 2 % MA is added to the reaction (low concentration) and the reaction time is under 2 minutes; therefore, the possibility of an ene-reaction of PLA has been ruled out. The ketone formed by the beta scission of PLA (which corresponds to the ene-formation of PP) would be structurally unfavorable for the grafting of maleic anhydride.

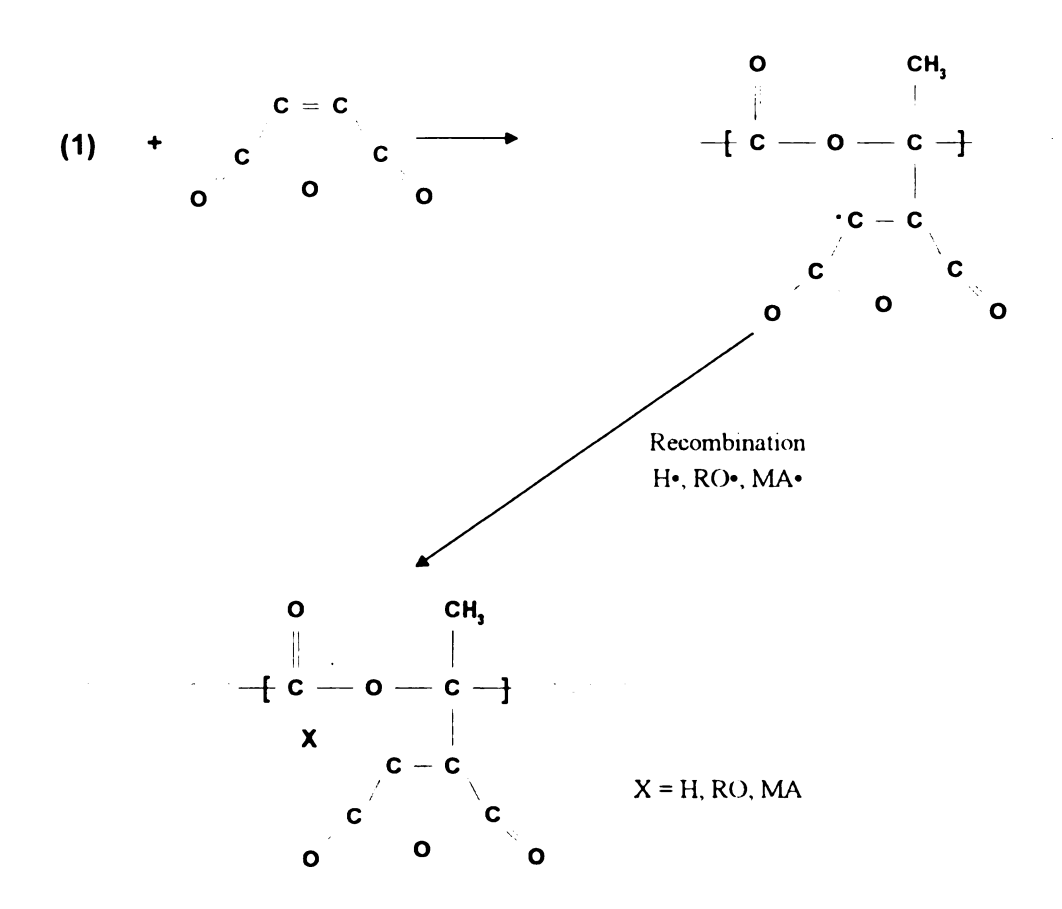


Figure 6.5: Proposed mechanism for the maleation of PLA.

As in the case for the branching of PLA, chain scission of the polylactide chain may also occur (see Figure 5.17 (chain scission)) with the resulting radical becoming available for reaction with MA. Similarly, thermohydrolysis and backbiting may still happen (see Figure 5.18) leading to further degradation of the polylactide chain.

Again, the above reaction is a proposed mechanism for the grafting of maleic anhydride onto the polylactide polymer backbone. Gaylord and others have been working on the maleation mechanism (with PP and PE) for several years now with no explicit results. Actual characterization of the true mechanism for PLA maleation would be difficult, requiring a much more in depth study.

# POLYLACTIDE BLENDS

A polymer blend consisting of two or more polymeric materials can be tailored to industrial needs. Polymer blends have several advantages over polymers including cost and time for development (7-10 years for a new polymer, 2-4 years for a new blend) [Meier (1991)]. Combining polylactide with natural materials and synthetic polymers provides a way of cost reduction and combined polymer properties. The objective of this part of the study is to find miscible or compatible blends of PLA with other polymers.

# 7.1 Blend Theory

## 7.1.1 Miscibility

Polymer blends may be miscible, partially miscible, or immiscible. When a mixture of polymers forms a single thermodynamically compatible phase, a miscible blend is formed. A single glass transition temperature is indicative of a miscible or partially miscible blend. Electron microscopy of a miscible blend will show polymer homogeneity. Miscible blends also exhibit combined physical properties. Films of miscible blends are generally transparent.

Immiscible blends are characterized by high interfacial tension and poor adhesion between phases. Macrophase separation generally occurs resulting in poor material properties such as tensile strength and elongation.

Whether or not two polymers are miscible depends on the free energy of mixing,  $\Delta G_m$ 

$$\Delta G_{\rm m} = \Delta H_{\rm m} - T \Delta S_{\rm m}$$

where  $\Delta H_m$  is the enthalpy of mixing, T is the temperature, and  $\Delta S_m$  is the entropy of mixing. For the polymer blend to be miscible,  $\Delta G_m$  must be negative. The entropy and enthalpy of mixing are defined by Flory-Huggins as the following [Meier (1991)]:

$$\frac{\Delta S_m}{VR} = -\frac{\phi_1}{V_1} \ln \phi_1 - \frac{\phi_2}{V_2} \ln \phi_2$$

$$\frac{\Delta H_m}{VRT} = \phi_1 \phi_2 \frac{\chi_{12}}{\bar{v}}$$

where V is the volume, R is the gas constant,  $\phi_i$  is the volume fraction of polymer i,  $\overline{V}_i$  and  $\overline{V}_i$  are the molar volumes, and  $\chi$  is the interaction parameter.

For high molecular weight polymers, the entropy of mixing is very small so the free energy of mixing is determined by the enthalpy of mixing which is positive for most systems. Specific interactions such as acid-base and hydrogen bonding

can occur which enables  $\Delta H_m$  to be negative and hence the polymer blends will be miscible.

## 7.1.2 Compatibility

Polymer blends are considered compatible if a desired or beneficial result occurs when the polymers are mixed. Compatible blends are not necessarily miscible. Compatibilized blends are immiscible blends which have been altered by methods such as surface modification, grafting, or the addition of a compatibilizing agent. This modification lowers the interfacial tension and increases the adhesion between the polymers resulting in a product which has specific properties desired by industry. The modification of polylactide with maleic anhydride was performed to improve the adhesion of PLA to various polymers and fillers.

# 7.2 Materials

# 7.2.1 Cellulose Acetate and its Derivatives

Cellulose acetate (CA), cellulose acetate propionate (CAP), and cellulose acetate butyrate (CAB) were chosen because of reports from literature on the miscibility of polyesters with CA, CAP, and CAB. These materials were provided by Eastman Kodak.

## 7.2.2 Polypropylene

Polypropylene was selected because of its similarity to PLA in its methyl group. PP has a density of about  $0.85 \text{ g/cm}^3$  and a  $T_G$  of  $-17^{\circ}$ C.

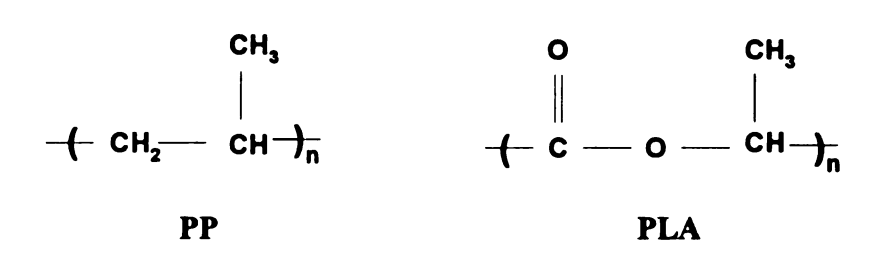


Figure 7.1: Comparison of PP and PLA.

# 7.2.3 Poly(vinyl acetate)

PVA was selected because of its structural similarity to PLA, its good theoretical background for miscibility, and its potential application in drug delivery systems.

The high molecular weight PVA was provided by the Aldrich Chemical Company.

It has a density of 1.191 g/cm<sup>3</sup>.

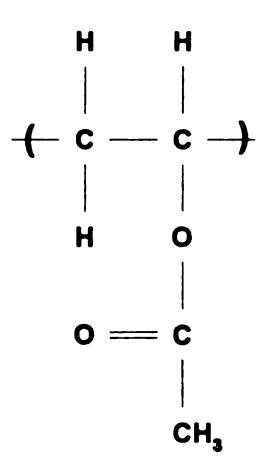


Figure 7.2: Poly(vinyl acetate)

# 7.2.4 Ethylene Vinyl Acetate (EVAC) Copolymers

These random copolymers were selected for the same reasons as PVA (listed above). The EVAC copolymers were provided by DuPont under the trade name of ELVAX. Table 7.1 lists the vinyl acetate content of the EVAC copolymers which were used along with some distinguishing characteristics.

Table 7.1: ELVAX properties.

ELVAX	% vinyl acetate	principle use/characteristic
150	33	adhesion to nonporous surfaces, used in solvent applied coating and hot melt adhesion
350	25	high MW, high melt viscosity, used for maximum toughness and greater specific adhesion
450	18	low melt viscosity, improves hardness and grease resistance
650	12	high MW, high melt viscosity, used for high temp. performance

# 7.3 Equipment and Procedures

# 7.3.1 Solution Casting

Solution casting provides a fairly easy and rapid way of determining polymer blend miscibility. As stated earlier, a miscible blend will, in general, be transparent with no evidence of phase separation.

Approximately 1 gram of polymer (combined total weight of the sample) is dissolved into 20 ml of solvent, in this case methylene chloride. This solution is stirred for about 48 hours before it is transferred into a glass petri dish. The solvent is allowed to evaporate under the hood. The film which is formed is then dried under a vacuum to ensure that all of the solvent has evaporated. The film can then be evaluated for miscibility.

#### 7.3.2 Haake Mixer

A Haake mixer was used instead of an extruder, or solution cast films, for some of the blends. The mixer is a batch process which uses less material than an extruder, but provides a more homogenous material (i.e., part of the material did not have to be discarded due to possible erroneous conditions) which can be evaluated. The Haake mixer has a volume of 300 cc and was operated at 80% capacity to ensure thorough mixing.

## 7.4 Discussion of Results

# 7.4.1 Blends of PLA with CA, CAP, CAB

CA, CAP, and CAB are commercial polymers which are strong, tough, and have good moisture permeation properties. However, processibility is a common problem for these materials. Plasticizers are usually added to these resins to improve processibility, but in a polylactide blend, the PLA may act as a plasticizer.

Since CA has a very high processing temperature (> 240°C), it was eliminated as a possible blend material with PLA. CAP and CAB can be extruded at a temperature of 210°C. Initial studies were done with blends of 70% CAP and Transparent extrudate was observed for this composition at a 30% PLA. processing temperature of 230°C. However, SEM studies show that two phases are present, i.e., CAP and PLA are not miscible. This phenomenon can be seen in Figure 7.3. Solution casting of PLA with CAP/CAB in THF and methylene chloride did not result in transparent films. The 70/30 blend was also run in the Haake mixer at a set temperature of 210°C for 30 minutes. The actual recorded temperature was ~ 220°C. This increase in temperature may be due to the shear forces in the mixer. The resulting resin was not transparent. Further analysis via SEM also revealed two phases. The transparent extrudate obtained from extrusion is presumably due to PLA degradation.

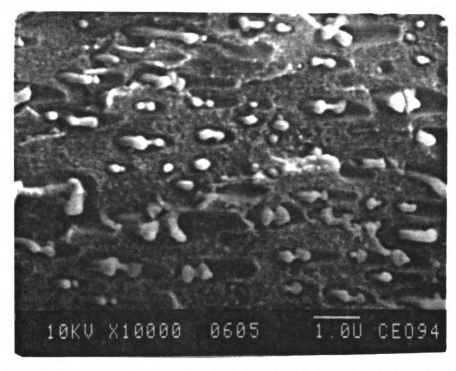


Figure 7.3: SEM micrograph of 70% CAP and 30% PLA showing immiscibility.

#### 7.4.2 Blend of PLA with PP

A blend of 70% PP with 30% PLA was attempted in the Haake mixer at 190°C for 20 minutes. The blend showed no miscibility.

#### 7.4.3 Blends of PLA with PVA

Solution casting was conducted for a range of PLA/PVA compositions. The resulting films were transparent. Initial SEM results show compatibility and possible miscibility at some compositions. These films are not very stable under the electron beam, so care must be taken to avoid charging. The 70% PLA/30%

PVA blend appeared to be miscible, i.e. two distinct phases are not apparent, by SEM.

The 40% PVA/ 60% PLA blend; however, was immiscible as two phases were present when viewed by SEM. Small circles of PVA were apparent in the polylactide polymer matrix. DSC studies show a reduced glass transition temperature (T<sub>G</sub>) of the blends; however, the T<sub>G</sub>s for both PLA and PVA are very close (58°C and 42°C, respectively) so it is difficult to tell if there is really only one T<sub>G</sub> which would indicate miscibility or if there are two T<sub>G</sub>s which would be indicative of immiscibility. Table 7.2 shows the T<sub>G</sub>s as given by DSC.

Table 7.2: Glass transition temperatures for PLA/PVA blends.

Sample	T <sub>G</sub> (°C)
Pure PLA	57.8
Pure PVA	42.0
70% PLA, 30% PVA	47.2
60% PLA, 40% PVA	46.3

# 7.4.4 Blends of PLA with EVAC Copolymers

Blends of 70% PLA with 30% ELVAX 150 and 350 were dissolved in CH<sub>2</sub>Cl<sub>2</sub> and then cast. The resulting films were not transparent; however, they appeared to be exceptionally strong. SEM analysis revealed two phases; however, the compatibility between PLA and ELVAX 350 was very good.

### 7.4.5 Blends of PLA with Starch

This set of experiments was done to compare the interfacial adhesion properties between starch and (1) PLA, (2) PLA with Lupersol 101, and (3) PLA, Lupersol 101, and maleic anhydride. Figure 7.4 is an SEM micrograph of a 60% PLA/40% starch blend showing poor interfacial adhesion. Figure 7.5 is of a 30% starch/70% PLA blend with 0.5% L101 (PLA wt. basis). This micrograph shows some interfacial adhesion, but separation of the blend is readily apparent.

The addition of MA provides end groups which should improve the interfacial adhesion. Figure 7.6 is an SEM micrograph of a 30% starch/70% maleated PLA blend. The maleated PLA consists of PLA, 2% MA, and 0.5% L101. The interfacial adhesion seen here is very good.

It is thus concluded that the addition of even a small amount of maleic anhydride onto the polylactide backbone will improve the interfacial adhesion of polylactide blends. These blends may be incorporated into single-use biodegradable disposable items in the future.

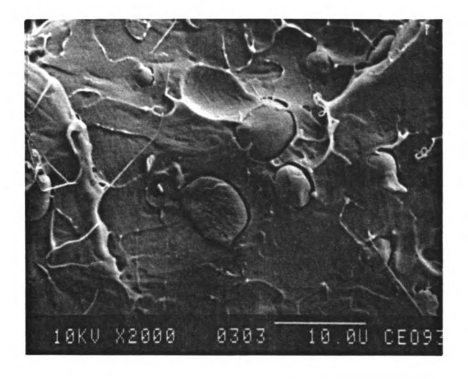


Figure 7.4: SEM micrograph of 60% PLA and 40% starch blend showing poor interfacial adhesion.

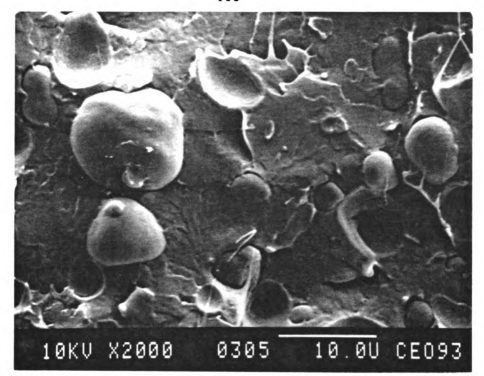


Figure 7.5: SEM micrograph of 30% starch and 70% PLA blend with 0.5% L101 showing partial interfacial adhesion.

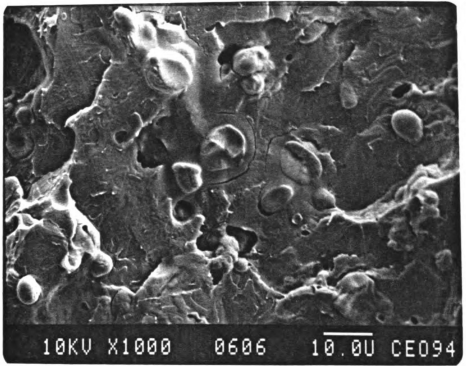


Figure 7.6: SEM micrograph of 30% starch and 70% maleated PLA showing good interfacial adhesion.

# **RELATED WORK**

Preliminary work was done to evaluate the potential of Laser Scanning Confocal Microscopy (LSCM) in studying polymer blend systems. Traditionally, Scanning Electron Microscopy (SEM) has been done to study the morphology of a polymer. The application of LSCM to polymer systems is a fairly novel approach, but it is one which should be considered as LSCM provides a non-invasive technique to study a polymer blend system. In this investigation, two polymer systems were studied: (1) a starch matrix with a protein filler, and (2) an extruded modified starch matrix with a talc filler. A Zeiss 10 LSCM located at the Laser Scanning Microscope Laboratory at Michigan State University was used.

# 8.1 LSCM Background

Laser Scanning Confocal Microscopy is a technique which originated with Young and Roberts (1951) and Minsky (1957) in the form of a confocal scanning optical microscope (CSOM). A working CSOM with a laser as its light source was developed in 1969 by Davidovits and Egger. In the past twenty years the LSCM has been

improved upon by numerous researchers. The equipment has been commercially available since the late 1980's.

The LSCM has been used mainly for biological science. The LSCM can be used to image both surface and subsurface features of lucid samples without the need to section them. For biological and medicinal applications this allows the subsurface viewing of living samples. In an optical microscope, images which are out of focus (possibly due to the difference in specimen thickness) appear blurry and distort the true image. In the LSCM; however, images which are not in focus disappear as the lenses are set up in such a way so that only the image at the specified laser depth is observed. This results in sharper image edges and more image contrast.

The laser confocal microscope or laser scanning confocal microscope is named for its constituents. Laser refers to the light source used to illuminate the sample. Most LSCM's also have conventional light sources such as a tungsten and/or a mercury lamp. Scanning means that only one point is illuminated at a time: the sample must be scanned and the image constructed pixel by pixel. Confocal means that the objective lens of the microscope is used twice, to illuminate the sample and to image it [Kino et al (1989)].

Several viewing modes are available on the LSCM: transmission, reflection, and fluorescence. The transmission mode, used for translucent samples, detects the laser after it has passed through the sample; however, this mode is not confocal. In both the reflection and fluorescence modes, the laser goes to a specified depth into the sample and then is bounced back up into the detection device. A fluoroprobe or a naturally fluorescing material is required in the fluorescent mode. The fluoroprobe is used as a signal for different polymer constituents in blend systems.

The Laser Scanning Confocal Microscope works by scanning a sample via a laser point by point. The laser beam hits the beam splitter which causes a wide beam to pass through the objective lens where it narrows and samples the specimen. The beam is then deflected off of the specimen and heads towards the detector. However, the beam must first pass through a pinhole before it is detected. The pinhole succeeds in blocking out wide-spread beams which would result in unfocused images in a conventional optical microscope. Figure 8.1 shows how a focused image is produced. Figure 8.1 also shows the path of the out-of-focus light Once detected, the image is stored, point-by-point and shown on a high resolution computer screen.

As mentioned early, LSCM has had its use in mainly biological applications. LSCM has also been used in the metrology of various structures including line-widths on integrated-circuit wafers [Lindow et al (1985), Zapf et al (1986)], diameters of fibers

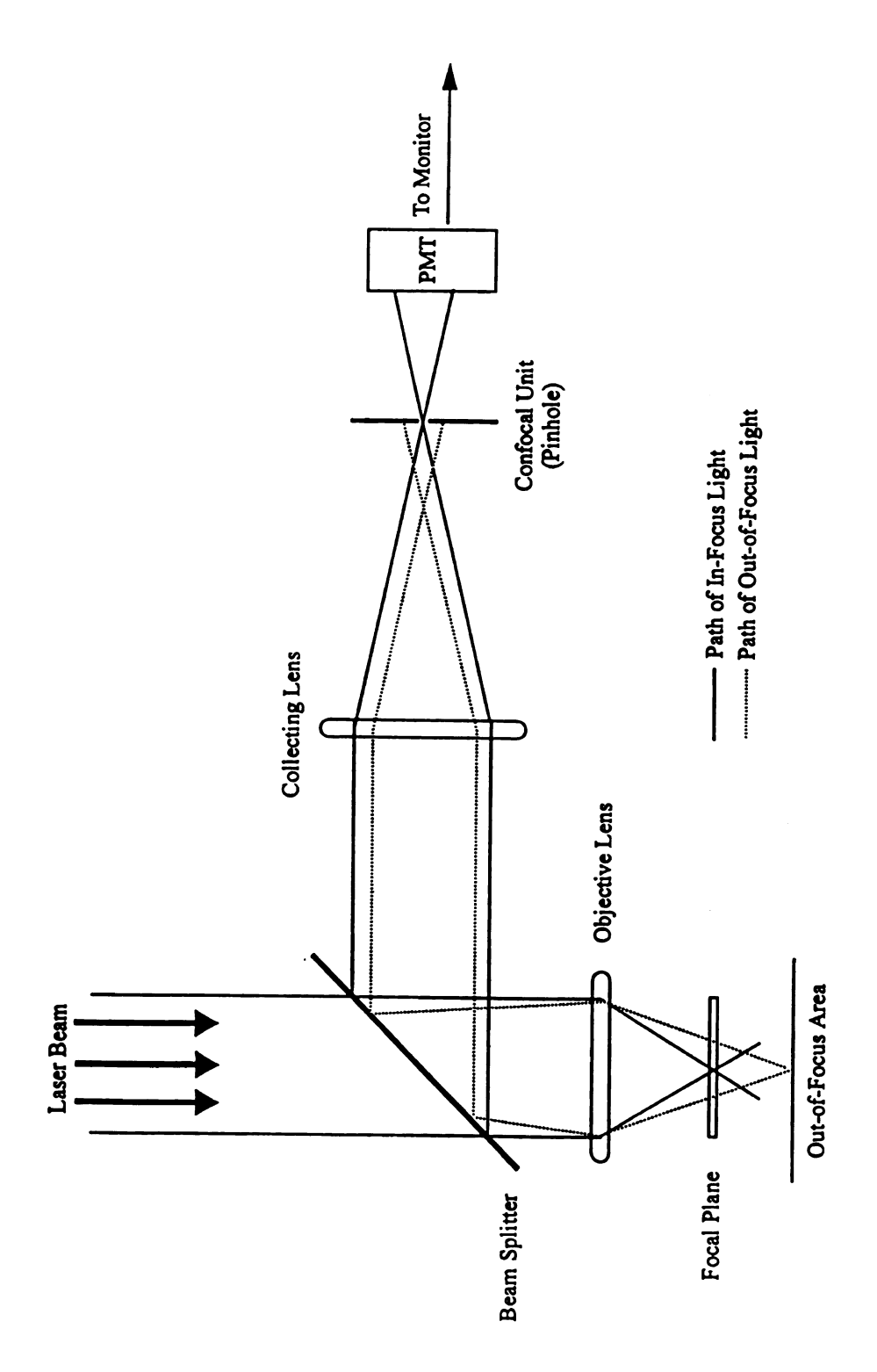


Figure 8.1: LSCM imaging method (modified after Carl Zeiss, Inc., Oberkochen).

[Mechels et al], and particle sizing in metallography, geology, and biology. Laser scanning confocal microscopy is very advantageous for metrology because the scanning stage can be accurately calibrated by using laser inferometry if a scanning stage is used. The image is electronically produced and is visible on a computer screen. The distance between two points on a sample can be readily determined just by selecting the points and pushing a button.

The laser scanning confocal microscope is now being used by material scientists, polymer chemists and chemical engineers because of its ease in use and its imaging capabilities to study polymer and polymer blend morphologies. LSCM provides a non-invasive viewing technique in which little or no sample preparation is necessary to obtain valuable information. The image can viewed directly on a computer screen and can be electronically filtered for sharper detail. The LSCM has improved resolution capabilities over conventional viewing mechanisms (i.e., wide field microscope) and is capable of a transverse (X-Y) resolution of about 0.1 micron. Longitudinal (Z-axis) resolution is also improved as the confocal scope eliminates any unfocused light.

Like any technique, the LSCM does have some limitations. Depth into the specimen is limited by the intensity of the reflected light or fluorescence signal, which to a greater or lesser degree is sample dependent. One other disadvantage of the LSCM is that in its laser mode, some specimens can be destroyed by the intense laser light. This may

occur with any laser application; however, no problems were detected with our samples.

## 8.2 Starch Matrix with Protein Filler

#### Methods and Materials

The focus of this investigation is on the morphology of polymer blends, specifically starch and zein (a corn protein). To illustrate the capability of LSCM to distinguish between starch and protein phases, we impregnated a potato (continuous starch matrix) with the zein protein. To distinguish the zein from the starch matrix, the zein was first treated with 1000 ppm of fluorescein isothiocyanate (FITC), a protein-specific dye commonly used in fluorescence applications. This stained zein was used in only the LSCM applications; for SEM, unstained zein was used. The isothiocyanate of this fluoroprobe reacts with the amines of the proteins and becomes a protein "tag". The zein was then dissolved and allowed to diffuse through the starch matrix. The exact densification method is covered under a confidentiality agreement with Grand Met, and therefore can not be disclosed. After 3 hours, the sample was dried. A BCA protein assay was also done to quantify the amount of protein impregnation. The results of this analysis showed that there was approximately 2 mg of zein protein per gram of starch.

#### Scanning Electron Microscopy

SEM analysis was initially done; however, it was impossible to distinguish the zein protein. SEM sample preparation requires a vigorous drying method in various grades of ethanol which might redissolve the protein. This drying method may also have the ability to alter the structure of the starch matrix. Figure 8.2 is an SEM micrograph of the potato, showing the cell walls and starch granules.

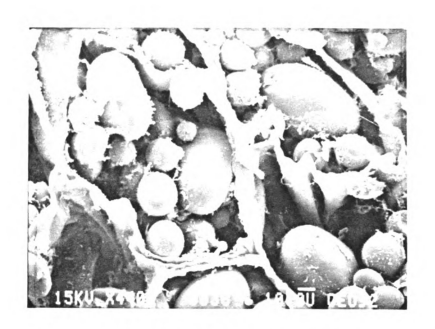


Figure 8.2: SEM micrograph of potato showing cell wall and starch granules.

LSCM was then done on the densified samples. A double-edged razor blade was used to cut a cross-section of the sample approximately 6 mm square. This cross-section was then viewed with the LSCM in all three modes: transmission, reflection, and fluorescence. An argon-ion laser was used (wavelength 488 nm) to fluoresce the tagged protein. Figure 8.3 shows a fluorescent image of the starch matrix impregnated with protein. The bright areas are the fluorescing protein while the darker areas constitute the starch. There is a dense border of protein along the outer edge of the matrix. If no protein were present, the fluorescent image with the laser which was used (488 nm) would appear completely black. Figure 8.4 shows another part of the matrix which has a fracture. As expected, the concentration of the protein along the fracture appears to be much greater than that elsewhere in the matrix, as the protein was able to permeate the matrix in this area faster and easier.

Since the protein border gave such a strong fluorescent signal, it was necessary to trim away the border to see if it was masking the true internal signal. The sample was trimmed down to about 3 mm square and then observed under the LSCM. A transmitted image of the specimen showed that it was still intact; however, the protein and the starch were indistinguishable. Figure 8.5 is a fluorescent image of the same specimen. Large clumps of protein can be identified throughout the matrix; therefore, it is apparent that protein diffusion has indeed occurred.

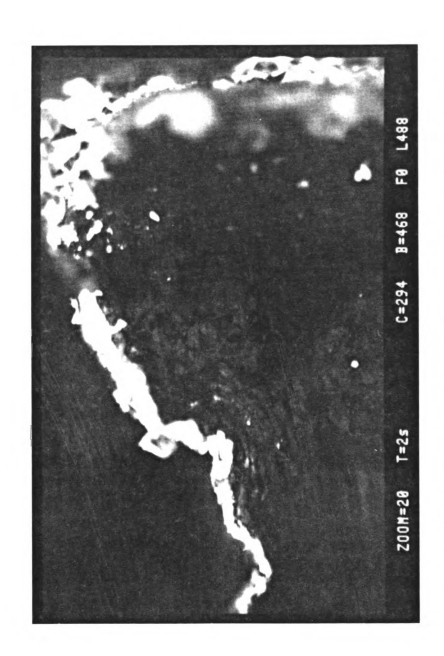


Figure 8.3: LSCM photograph of densified potato showing zein penetration.

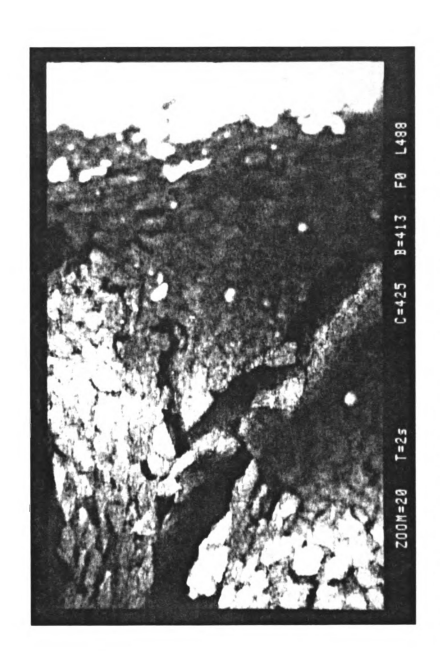


Figure 8.4: LSCM photograph of densified potato showing diffusion of zein along crack.

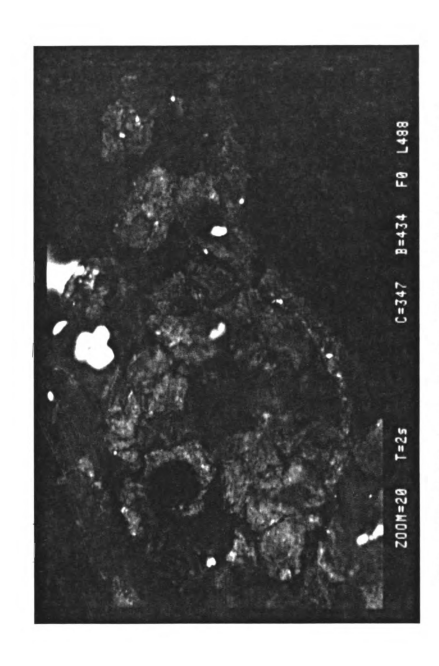


Figure 8.5: LSCM photograph of densified potato (inner cross-section).

### 8.3 Extruded Modified Starch with Talc Filler

As LSCM provided good results for the starch/protein system, it was also initially tried on the extruded modified starch/talc system. This system is currently classified under a confidentiality agreement between Michigan Biotechnology Institute and Japan Corn Starch; hence, specific components and/or compositions may not be given.

### Laser Scanning Confocal Microscopy

A series of samples were viewed via LSCM to check for specific fluorescence. The objective was to find one component of the sample which would fluoresce exclusively in a controllable manner. No distinction could be made between the talc and the modified starch in the transmitted mode. Two types of talc were tested: (1) MSU talc which fluoresced, and (2) Van talc which did not fluoresce. The plasticizer (T comp) which is used to aid in the extrusion process, did not fluoresce. Modified starch (powder form) did not fluoresce. To simulate the extrusion process, some of the modified starch was compression molded at temperatures from 160 to 190° C. Modified starch which had been compression molded fluoresced for the most part, but some areas did not fluoresce (those which may not have melted entirely). Modified starch with T comp in the form of an injection molded bar fluoresced strongly covering the spectrum from red to green. Theoretically, all of the starch in this sample has been melted to a phase which

fluoresces. If this is indeed the case, the parts which do not fluoresce are either air, plasticizer, or contaminants; however, there currently is not a way to make a positive identification. In samples containing tale, the non-fluorescent parts could be tale (unless MSU tale is used which does fluoresce), air, plasticizer, or contamination. Because the fluorescence is so strong, there is no way to be sure that the signal which is viewed truly originated from a specific spot on the sample; i.e., secondary fluorescence may be occurring which means that the fluorescing modified starch signal may be "bouncing" off of the tale which would then appear to fluoresce and may be erroneously mistaken for modified starch. Therefore, at the present time, the use of LSCM has been ruled out in the characterization of modified starch samples.

# Scanning Electron Microscopy:

A method of X-ray analysis may be used to detect the silicon (Si) and magnesium (Mg) components of talc. X-rays from these elements may be mapped to a corresponding surface. Figure 8.6 shows the Si and Mg peaks obtained from a modified starch/talc polymer blend. Figure 8.7 is an SEM micrograph showing the morphology of the starch/talc blend. A dot-mapping of the strongest peak (Si) shows a good dispersion of talc (see Figure 8.8). This analysis was done at an accelerating voltage of 20KV which corresponds to a depth penetration in the sample of about 10 microns.

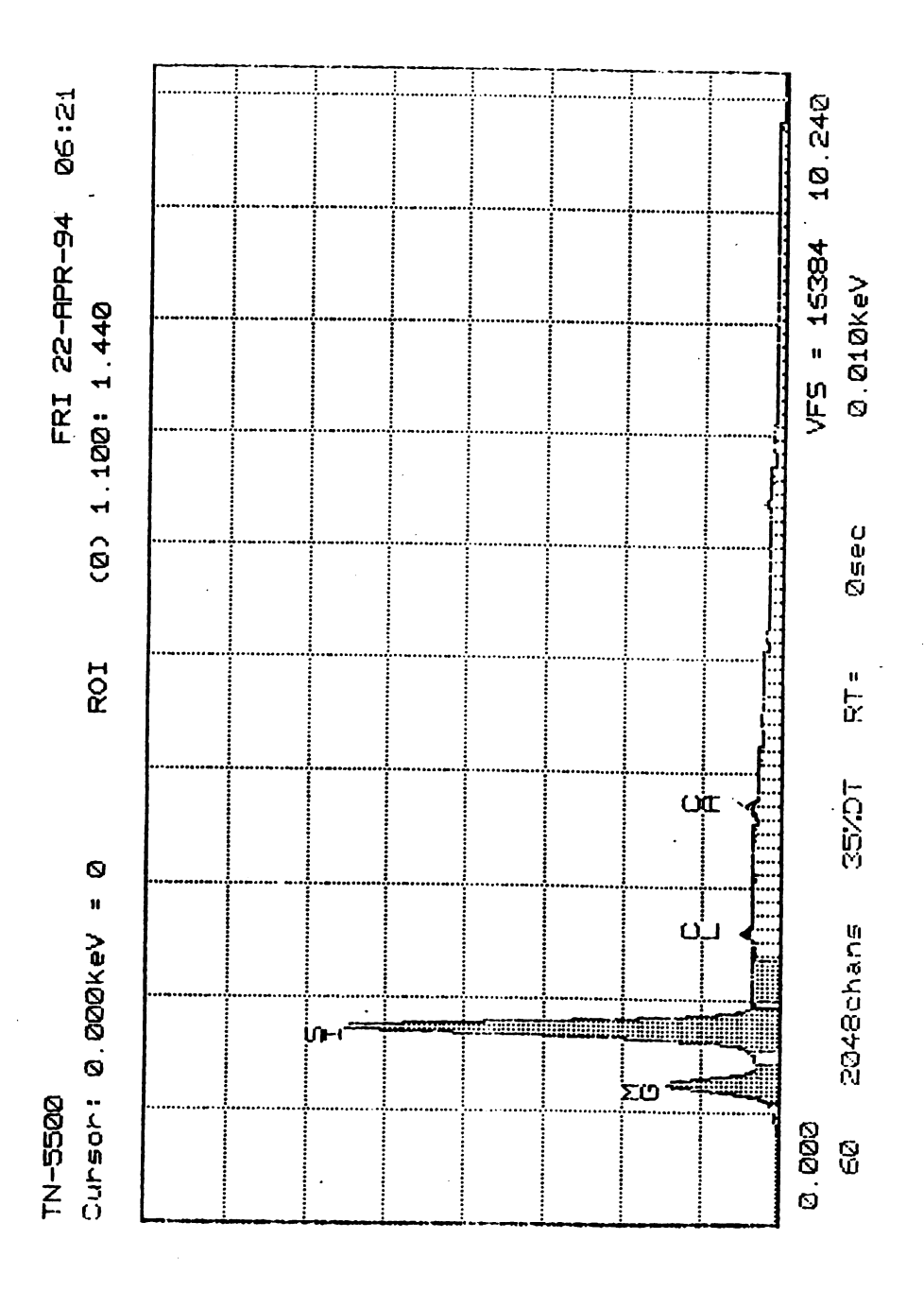


Figure 8.6: SEM X-ray peaks for modified starch with talc.



Figure 8.7: SEM micrograph showing the surface of the modified starch with talc blend.



Figure 8.8: SEM dot map of the X-ray analysis for silicon.

# **CONCLUSIONS AND RECOMMENDATIONS**

## 9.1 Conclusions

### Branching

The free radical branching of polylactide via reactive extrusion is a novel concept which has been applied in the past to polylactides such as polypropylene and polyethylene, but it has never been applied to polylactides. The branching of PLA by reactive extrusion provides an in-situ method of improving the processibility of PLA which could then be used in blow molding and injection molding applications.

The results of this investigation indicate that polylactide branching is favored at temperatures around 170°-180°C with an initiator concentration of about 0.1 - 0.25 %. Highly branched systems, which may include microgelation, are favored at initiator concentrations of 0.5% at about the same temperature range. Chain scission is favored at higher temperatures (T >190°C). Without the presence of initiator, PLA undergoes rapid degradation which may be attributed to chain

scission due to thermohydrolysis and back-biting. This degradation may hinder the applicability of PLA to blow molding and injection molding processes.

The goal of this research has been met. The molecular weight of extruded/processed PLA has been increased with results that are comparable to unextruded, unprocessed PLA. The melt flow index is also increased, i.e., an increase in the melt viscosity is observed which may improve the blow molding processibility of PLA.

#### Maleation

The successful branching of PLA encouraged us to study the maleation of PLA by reactive extrusion processes involving free radicals. Such maleated PLA is of prime interest in order to promote good interfacial adhesion between inorganic fillers and PLA resins. Back-titration analysis of the maleated PLA showed that between 0.066 and 0.672 % maleic anhydride was grafted to the polylactide backbone. Increasing the amount of peroxide initiator led to an increase in the grafting of MA; whereas, extrusion temperature had little effect on the maleation reaction as was expected from the branching study.

Polymer blends are increasingly important from an industrial standpoint as they allow for the tailoring of resin properties. An attempt was made to blend PLA with several different substances including: (1) cellulose acetate derivatives, (2) polypropylene, (3) poly(vinyl alcohol) and ethylene vinyl alcohol copolymers (EVAC), and (4) starch. The PLA and starch blend proved to be most interesting. The interfacial adhesion between the extruded starch and PLA blend was poor; however, the addition of maleic anhydride, which grafts onto the PLA backbone, resulted in good interfacial adhesion between the substances.

#### Related Work

Laser scanning confocal microscopy is a non-invasive tool which can be used to study polymer blend morphology. LSCM is especially useful for biopolymers and their blends as many of the readily available fluoroprobes are designed for biological applications. LSCM can be beneficial in the identification of some of the characteristics in polymer blends including distribution and/or adhesion of the constituents and flow patterns without introducing artifacts usually associated with sample preparation. The LSCM which was done showed how a protein filler could be distinguished from a starch matrix. Characterization of an extruded modified starch matrix with a talc filler was also attempted by LSCM. Theoretically, all of the starch in this sample has been melted to a phase which fluoresces. If this is indeed the

case, the parts which do not fluoresce are either air, plasticizer, or contaminants; however, there currently is not a way to make a positive identification. Therefore, LSCM was not a viable option in the extruded starch/talc blend.

Scanning electron microscopy is another important fundamental tool in studying polymer blend systems. Not only were we able to evaluate the morphology of several polymer blends using SEM, we were also able to use X-ray analysis, in conjunction with dot mapping, to view the dispersion of talc in an extruded modified starch matrix.

# 9.2 Recommendations

## Branching

A patent application which covers the branching and maleation of polylactide via reactive extrusion is currently in progress. Two papers (Carlson, D.L., P. DuBois, R. Narayan, L. Nie, "Free Radical Branching of Polylactide by Reactive Extrusion" and "Maleation of Polylactide by Reactive Extrusion") are to be submitted to *Polymer* pending review of the patent application.

The following recommendations are made for further research on the modification of polylactide via reactive extrusion. Optimization of the extrusion conditions, temperature and % initiator, should be done to maximize the processibility of

PLA. To aid in controlling the reaction, the maximum amount of initiator which can be added before the occurrence of crosslinking should also be determined.

Various maleic anhydride concentrations should be tried in the grafting of MA to PLA. The PLA samples should be injection molded so that tensile strength and other mechanical testing can be done. Of specific interest might be polymer blend samples which compare the interfacial adhesion as related to strength.

### Film Extrusion

A preliminary study on the feasibility of PLA film extrusion was conducted. Further work needs to be done in evaluating the temperature and initiator concentrations which will yield an optimum product.

### Starch / Talc System

X-ray analysis via scanning electron microscopy could prove to be a useful tool in evaluating the dispersion of talc filler in a starch matrix. However, lower accelerating voltages may need to be employed in the SEM so that depth penetration into the sample is minimized. A higher magnification also may need to be used to exploit the resolution of the instrument and utilize the size of the talc particles (about 6 microns).

## **LSCM**

The LSCM has the capability of distinguishing several constituents of a polymer blend. To accomplish this, different fluoroprobes, which signal at different frequencies, must be used for each component. Using different lasers, one has the ability to single out each constituent. These images may then be overlaid to get the complete picture of the blend system. The LSCM may be a useful tool in evaluating polymer blend systems as discussed previously in the Conclusions. Avenues for utilizing LSCM in other polymer blend systems should be addressed.

# **APPENDIX - RAW DATA**

Table A.1: Branched data from TriSEC (triple detector size exclusion chromatography)

Pd = polydispersity	a = Mark-Houwink parameter	Log K = log of Mark-Houwink parameter	
n = number average	w = weight average	z = third moment	peak = peak
LS = light scattered	M = molecular weight	IV = intrinsic viscosity	Rg = radius of gyration

PLA	PLA   LS-Mn LS-Mw	LS-Mw	LS-Mz	Mpeak	Mw-Pd	LS-IVn	Mpeak Mw-Pd LS-IVn LS-IVw LS-IVz IV-Pd Rgn	LS-IVz	IV-Pd		Rgw	Rgz	Rg-Pd	æ	Log K
1	117800	163700	228700	133200	1.39	0.863	1.009		1.17	1.159 1.17 15.76 17.49	17.49	19.32	1.11	0.707	0.707 -3.658
7	131400	190300	449000 138200	138200	1.45	0.931	1.102	1.344	1.18	1.18 16.7 18.65	18.65	21.64	1.12	0.733	0.733 -3.791
က	120800	168700	275400 133500	133500	1.4	0.888	1.046	1.225	1.18	1.18 16.02 17.8	17.8	19.94	1.11	0.734	0.734 -3.79
<b>+</b>	114100	161200	229000	229000 133000	1.41	0.856	1.006	1.158	1.18	1.18 15.58	17.36	19.24	1.11	0.71	-3.671
ν.	123800	173700	332900	134400	1.4	0.897	1.053	1.242	1.17	1.17 16.17	17.95	20.31	1.11	0.736	-3.803
Average	121580	171520	303000	134460	1.41	0.89	1.04	1.23	1.18	16.05	17.85	20.09	1.11	0.72	-3.74
stand.dev.	6561	11544	92152	2158	0.02	0.03	0.04	0.08	0.01	0.43	0.51	0.97	0.00	0.01	0.07
% dev.	5.40	6.73	30.41	1.61	1.66	3.37	3.75	6.23	0.47	2.69	2.83	4.84	0.40	1.97	1.91
160/0.00	LS-Mn LS-Mw	LS-Mw	LS-Mz	Mpeak	Mw-Pd	LS-IVn	Mpeak Mw-Pd LS-IVn LS-IVv LS-IVz IV-Pd Rgn	LS-IVz	IV-Pd		Rgw	Rgz	Rg-Pd	а	Log K
1	90100	116500	243600	93900	1.29	0.719	0.812		1.13	0.953 1.13 13.41 14.49	14.49	16.19	1.08	0.765	0.765 -3.939
7	87300	115200	233800	91100	1.32	0.732	0.838	1.003	1.14	1.14 13.38 14.56	14.56	16.42	1.09	0.757	0.757 -3.882
3	89000	113700	193500	90700	1.28	0.711	0.805	0.92	1.13	13.32	14.39	15.82	1.08	0.771	-3.966
Average	88800	115133	223633	91900	1.30	0.72	0.82	96.0	1.13	13.37	14.48	16.14	1.08	0.76	-3.93
stand.dev.	1411	1401	26552	1744	0.02	0.01	0.02	0.04	0.01	0.05	0.09	0.30	0.01	0.01	0.04
% dev.	1.59	1.22	11.87	1.90	1.61	1.47	2.12	4.36	0.51	0.34	0.59	1.88	0.53	0.92	1.09

Table A.1 cont.

Log K	-2.916	0.611 -3.178	-3.252	-3.12	0.18	5.67		Log K	-3.707	-3.597	-3.701	-3.67	90.0	1.69		Log K	-3.417	-3.523	-3.42	-3.45	90.0	
ત્વ	0.562 -2.916	0.611	0.63	09.0	0.04	5.84		а	0.718 -3.707	0.697 -3.597	0.714	0.71	0.01	1.57		а	0.656 -3.417	0.676 -3.523	0.659	99.0	0.01	
Rg-Pd	1.49	1.34	1.27	1.37	0.11	8.22		Rg-Pd	1.14	1.24	1.13	1.17	90'0	5.20		Rg-Pd	1.27	1.22	1.18	1.22	0.05	
Rgz	65.05	45.6	35.04	48.56	15.22	31.35		Rgz	22.7	32.58	20.86	25.38	6.30	24.83		Rgz	36.92	32.19	23.94	31.02	6.57	
Rgw	26.06	22.77	20.49	23.11	2.80	12.12		Rgw	18.7	20.67	18.01	19.13	1.38	7.22		Rgw	21.36	20.99	19.13	20.49	1.20	
Rgn	1.52 17.44 26.06	16.93	16.16	16.84	0.64	3.83		Rgn	16.44	16.7	15.87	16.34	0.42	2.60		Rgn	16.88	17.21 20.99	16.16	16.75	0.54	•
Pd-VI		1.4	1.34	1.42	0.09	6.45		IV-Pd	1.21	1.35	1.21	1.26	0.08	6.43		IV-Pd	1.32	1.28	1.25	1.28	0.04	
LS-IVz	3.283	2.547	2.242	2.69	0.54	19.89		LS-IVz	1.397	2.263	1.274	1.64	0.54	32.77		LS-IVz	1.91	1.741	1.426	1.69	0.25	
NAI-S	1.462	1.297	1.219	1.33	0.12	9.36		NAI-S	1.103	1.262	1.041	1.14	0.11	10.04		NAI-S-	1.202	1.189	1.104	1.17	0.05	
S-IVn J	96.0	0.926	0.91	0.93	0.03	2.74		S-IVn	0.915	0.935	0.859	0.90	0.04	4.36		S-IVn I	0.91	0.928	0.881	0.91	0.02	,
Mw-Pd ]	6.94	4.1	2.85	4.63	2.10	45.27		Mw-Pd	1.59	2.33	1.5	1.81	0.46	25.21		Mw-Pd 1	3.21	2.54	1.86	2.54	0.68	;
Mpeak Mw-Pd LS-IVn LS-IVw LS-IVz IV-Pd Rgn	144700	142200	126800	137900	9694	7.03		Mpeak Mw-Pd LS-IVn LS-IVw LS-IVz IV-Pd	129500	132500	134400	132133	2470	1.87		Mpeak Mw-Pd LS-IVn LS-IVv LS-IVz IV-Pd	141300	143100	134100	139500	4762	;
LS-Mz	15450000 144700	7713000 142200	3500000 126800	8887667 137900	6060982	68.20		LS-Mz	739700 129500	2255000 132500	353500 134400	1116067	1005069	90.08		LS-Mz	8375000 141300	5692000 143100	877000 134100	4981333 139500	3799182	
LS-Mw	917000	526300	332100	591800	297900	50.34		LS-Mw	201200	296700	180500	226133	61983	27.41		LS-Mw	424700	353500	222800	333667	102401	•
LS-Mn	132200	128500	116700	125800	8095	6.43	_	LS-Mn	126300	127300	120100	124567	3900	3.13		LS-Mn	132200	139300	119700	130400	9923	•
160/0.05	-	2	3	Average	stand.dev.	% dev:	-	160/0.14	_	2	3	Average	stand.dev.	% dev.	•	160/0.26	-	2	3	Average	stand.dev.	

Table A.1 cont

170/0.0	LS-Mn	LS-Mw	LS-Mz	Mpeak	Mw-Pd	LS-IVn	Mpeak Mw-Pd LS-IVn LS-IVw LS-IVz IV-Pd	LS-IVz	IV-Pd	Rgn	Rgw	Rgz	Rg-Pd	m	Log K
-	82300	109800	176500	00806	1.33	0.723	0.825	1.028	1.18	13.11	14.44	16.21		0.769	-3.924
7	61700	102600	239500	83200	1.66	0.691	0.834	1.074	1.21	11.94	13.75	16.41	1.15	0.614	-3.129
٣	84600	128100	301200	00666	1.51	0.713	0.848	1.042	1.19	13.28	14.97	17.45	1.13	0.703	-3.627
Average	76200	113500	239067	91300	1.50	0.71	0.84	1.05	1.19	12.78	14.39	16.69	1.13	0.70	-3.56
stand.dev.	12610	13146	62351	8361	0.17	0.03	0.01	0.02	0.02	0.73	0.61	0.67	0.03	0.08	0.40
% dcv.	16.55	11.58	26.08	9.16	11.02	2.31	1.39	2.25	1.28	5.71	4.25	3.99	2.23	11.19	11.28
170/0.1	LS-Mn	LS-Mw	LS-Mz	Mpeak	Mw-Pd	LS-IVn	Mw-Pd LS-IVn LS-IVv LS-IVz IV-Pd	LS-IVz	IV-Pd	Rgn	Rgw	Rgz	Rg-Pd	ત્વ	Log K
1	126400	170700	370700 126000	126000	1.35	0.947	1.079	1.244	1.14	16.48	17.98	20.2	1.09	0.737	0.737 -3.782
7	126200	163500	249900 125400	125400	1.3	0.972	1.094	1.239	1.13	16.6	17.96	19.75	1.08	0.729 -3.731	-3.731
3	123200	159400	241300 126700	126700	1.29	0.947	1.072	1.219	1.13	16.33	17.69	19.46	1.08	0.736	-3.767
Average	125267	164533	287300 126033	126033	1.31	96.0	1.08	1.23	1.13	16.47	17.88	19.80	1.08	0.73	-3.76
stand.dev.	1793	5720	72354	651	0.03	0.01	0.01	0.01	0.01	0.14	0.16	0.37	0.01	0.00	0.03
% dev.	1.43	3.48	25.18	0.52	2.45	1.51	1.04	1.07	0.51	0.82	0.91	1.88	0.53	0.59	0.70
	-														
170/0.5	LS-Mn	LS-Mw	LS-Mz	Mpeak	Mw-Pd	LS-IVn	Mpeak Mw-Pd LS-IVn LS-IVw LS-IVz IV-Pd	LS-IVz	IV-Pd	Rgn	Rgw	Rgz	Rg-Pd	а	Log K
-	131600	1.15E+08	4.83E+09 192000	192000	870.29	0.825	2.057	24.12	2.49	17.39	1712	209036.2 98.45	98.45	0.405	0.405 -2.189
7	137300	88730000	4.92E+09 183700	183700	646.25	0.783	1.535	9.081	1.96	17.18	535.2	57880.07	31.15	0.457	-2.477
3	151900	53010000	4.88E+09 185000	185000	348.98	0.801	1.369	6.629	1.71	17.56	310.5	51751.16	17.68	0.525	-2.844
7	114700	38690000	3.93E+09 162600	162600	337.31	0.77	1.174	1.908	1.52	16.21	37.99	481.95	2.34	0.505	-2.718
Average	133875	73740000	4.64E+09	180825	550.71	0.79	1.53	10.43	1.92	17.09	649	79787	37	0.47	-2.56
stand.dev.	15378	34383909	4.75E+08	12685	256.58	0.02	0.38	9.60	0.45	09.0	737	89927	45	0.05	0.29
% dev:	11.49	46.63	10.23	7.02	46.59	3.00	24.69	91.97	21.90	3.53	114	113	113	11.32	11.29

Table A.1 cont.

Log K	-3.891	-3.907	-3.89	-3.90	0.01	0.24	Log K	-3.711	-3.815	-3.851	-3.79	0.07	1.92		Log K	0.695 -3.626	0.689 -3.586	-3.608	-3.61	0.02	
æ	0.764 -3.891	0.767	0.764	0.77	0.00	0.23	В	0.726 -3.711	0.745	0.751	0.74	0.01	1.76		а	0.695	0.689	0.692	69.0	0.00	
Rg-Pd	1.08	1.09	1.08	1.08	0.01	0.53	Rg-Pd	1.09	1.1	1.09	1.09	0.01	0.53		Rg-Pd	1.12	1.12	1.11	1.12	0.01	
Rgz	16.24	15.95	14.98	15.72	99.0	4.20	Rgz	18.15	17.93	18.53	18.20	0.30	1.67		Rgz	20.82	21.06	20.69	20.86	0.19	
Rgw	14.55	14.21	13.65	14.14	0.45	3.21	Rgw	16.44	16.11	16.61	16.39	0.25	1.55		Rgw	18.01	18.24	18.17	18.14	0.12	
Rgn	1.14 13.42	13.07	12.61	13.03	0.41	3.12	Rgn	1.14 15.07 16.44	14.67 16.11	15.19 16.61	14.98	0.27	1.82		Rgn	16.02 18.01	16.3	16.31	16.21	0.16	
IV-Pd	1.14	1.14	1.14	1.14	0.00	0.00	IV-Pd	1.14	1.15	1.15	1.15	0.01	0.50		IV-Pd	1.18	1.17	1.16	1.17	0.01	
LS-IVz	1	0.983	0.907	96.0	0.05	5.14	LS-IVz	1.133	1.101	1.146	1.13	0.02	2.06		LS-IVz	1.186	1.209	1.181	1.19	0.01	
S-IVw	0.862	0.837	0.795	0.83	0.03	4.07	S-IVw	0.991	0.956	0.988	0.98	0.02	1.98		S-IVw	0.999	1.022	1.011	1.01	0.01	
S-IVn I	0.759	0.733	0.7	0.73	0.03	4.05	S-IVn I	0.867	0.828	0.859	0.85	0.02	2.42		S-IVn I	0.847	0.874	0.868	0.86	0.01	
Mw-Pd	1.31	1.32	1.28	1.30	0.02	1.60	Mw-Pd	1.32	1.35	1.33	1.33	0.02	1.15		Mw-Pd	1.51	1.49	1.45	1.48	0.03	
Mpeak Mw-Pd LS-IVn LS-IVw LS-IVz IV-Pd Rgn	89500	85400	82800	85900	3378	3.93	Mpeak Mw-Pd LS-IVn LS-IVv LS-IVz IV-Pd	107800	106800	111000	108533	2194	2.02		Mpeak Mw-Pd LS-IVn LS-IVv LS-IVz IV-Pd	129700	129900	133000	130867	1850	
LS-Mz	229100	227900	156000	204333	41862	20.49	LS-Mz	216900 107800	242000 106800	267200 111000	242033	25150	10.39		LS-Mz	460700 129700	494100 129900	386000	446933	55349	
LS-Mw	111500	107400	98100	105667	9989	6.50	LS-Mw	138700	136400	144700	139933	4285	3.06		LS-Mw	190300	193300	190200	191267	1762	
LS-Mn	85300	81400	76400	81033	19++	5.51	 LS-Mn	104700	100800	108600	104700	3900	3.72		LS-Mn	126400	129700	130900	129000	2330	
0.0/081	2	3	7	Average	stand.dev.	% dev.	 180/0.1	1	7	3	Average	stand.dev.	% dev.	·	180/0.25	-	2	3	Average	stand.dev.	

Table A.1 cont.

190/0.0	LS-Mn	LS-Mw	LS-Mz	Mpeak	Mw-Pd	LS-IVn	Mpeak Mw-Pd LS-IVn LS-IVv LS-IVz IV-Pd	LS-IVz	IV-Pd	Rgn	Rgw	Rgz	Rg-Pd	ત્વ	Log K
2	78400	99100	131500	84900	1.26	0.678	0.765	0.86	1.13	0.86 1.13 12.58 13.58	13.58	14.71	1.08	0.738	0.738 -3.787
6	87100	121400	304800	91400	1.39	0.702	0.825	1.047		13.19 14.58	14.58	17.1	1.1	0.776	0.776 -3.987
<b>→</b>	83300	104800	141500	89300	1.26	0.682	0.771	0.865			12.86 13.86	15.01	1.08	0.761	-3.913
Average	82933	108433	192600	88533	1.30	69.0	0.79	0.92	1.14	12.88 14.01	14.01	15.61	1.09	0.76	-3.90
stand.dev.	4362	11585	97297	3317	0.08	0.01	0.03	0.11	0.02	0.31	0.52	1.30	0.01	0.02	0.10
% dev:	5.26	10.68	50.52	3.75	5.76	1.87	4.20	11.53	2.02	2.37	3.68	8.34	1.06	2.52	2.60
190/0.1	LS-Mn	LS-Mw	LS-Mz	Mpeak	Mw-Pd	LS-IVn	Mpeak Mw-Pd LS-IVn LS-IVw LS-IVz IV-Pd	LS-IVz	IV-Pd	Rgn	Rgw	Rgz	Rg-Pd	а	Log K
-	116800	151300	226800 114700	114700	1.3	0.902	1.026	1.17	1.14	15.8 17.15	17.15	18.85	1.09	0.745	-3.82
. 2	117600	158300	293000 120700	120700	1.35	0.895	1.028	1.192	1.15	15.81	17.31	19.38	1.09	0.746	-3.83
2	109200	146800	224000 112100	112100	1.34	0.873	0.999	1.137	1.14	15.33	16.79	18.55	1.09	0.716	-3.671
Average	114533	152133	247933	115833	1.33	0.89	1.02	1.17	1.14	15.65	17.08	18.93	1.09	0.74	-3.77
stand.dev.	1636	5795	39054	4411	0.03	0.02	0.02	0.03	0.01	0.27	0.27	0.42	0.00	0.02	0.09
% dev:	4.05	3.81	15.75	3.81	1.99	1.70	1.59	2.37	0.50	1.75	1.56	2.22	0.00	2.32	2.36
190/0.5	LS-Mn	LS-Mw	LS-Mz	Mpeak	Mw-Pd	LS-IVn	Mpeak Mw-Pd LS-IVn LS-IVv LS-IVz IV-Pd	LS-IVz	IV-Pd	Rgn	Rgw	Rgz	Rg-Pd	ત્વ	Log K
	157200	1.02E+08	4.87E+09 165700	165700	650.13	0.925	2.076	25.72	2.24	18.29 1911	1911	266070 104.5	104.5	0.403	-2.138
2	150300	150300 31330000	4.85E+09 160200 208.45	160200	208.45	0.877	1.224	2.903	1.4	17.56 63.19	63.19	2609	3.6	0.577	-3.06
3	153400	153400 1.09E+08	4.85E+09 160900	160900	709.78	0.85	1.874	19.36	2.2	17.65 1252	1252	142995 70.96	70.96	0.399	0.399 -2.144
Avcrage	153633	80803333	4.86E+09 162267	162267	522.79	0.88	1.72	15.99	1.95	17.83	1075	138387	59.67	0.46	-2.45
stand.dev.	3456	42975151	10208387	2994	273.85	0.04	0.45	11.77	0.47	0.40	936	130048	51.36	0.10	0.53
% dev.	2.25	53.18	0.21	1.85	52.38	4.30	25.81	73.62	24.34	2.23	87	94	80.98	22.11	21.68

Table A.1 cont.

200/0.0	LS-Mn	LS-Mw	LS-Mz	Mpeak	Mpeak Mw-Pd LS-IVn LS-IVw LS-IVz IV-Pd Rgn	LS-IVn	LS-IVw	LS-IVz	IV-Pd	Rgn	Rgw	Rgz	Rg-Pd	В	Log K
<b>→</b>	103000	125000	165400	165400 103000	1.21	0.827	0.917	1.019	1.11	1.11 14.65 15.62	15.62	16.77	1.07	0.768 -3.934	-3.934
S	101800	123300	159300	101900	1.21	0.834	0.927	1.031	1.11	1.11 14.65 15.61	15.61	16.75	1.07	0.766	0.766 -3.914
9	103000	124600	162900	162900 103800	1.21	0.818	0.91	1.014	1.11	1.11 14.61 15.57	15.57	16.71	1.07	0.778	-3.989
Average	102600	124300	162533	162533 102900	1.21	0.83	0.92	1.02	1.11	14.64	15.60	16.74	1.07	0.77	-3.95
stand.dev.	693	889	3066	954	0.00	0.01	0.01	0.01	0.00	0.02	0.03	0.03	0.00	0.01	0.04
% dev.	89.0	0.72	1.89	0.93	0.00	0.97	0.93	98.0	0.00	0.16	0.17	0.18	0.00	0.83	0.98
	_														
200/0.1	LS-Mn	LS-Mw	LS-Mz	Mpeak	Mpeak Mw-Pd LS-IVn LS-IVv LS-IVz IV-Pd	LS-IVn	LS-IVw	LS-IVz	IV-Pd	Rgn	Rgw	Rgz	Rg-Pd	а	Log K
_	105600	138100	215600 114300	114300	1.31	0.798	0.933	=	1.17	1.17 14.69 16.08	16.08	17.92	1.09	0.816	0.816 -4.195
2	105600	136400	201800	110400	1.29	0.857	696.0	1.1	1.13	15.01	16.26	17.84	1.08	0.744	-3.805
3	105200	137200	203100	111200	1.3	0.853	0.972	1.115	1.14	1.14 14.99	16.3	17.96	1.09	0.739	-3.784
Average	105467	137233	206833 111967	111967	1.30	0.84	96.0	1.11	1.15	14.90	16.21	17.91	1.09	0.77	-3.93
stand.dev.	231	820	7620	2060	0.01	0.03	0.02	0.01	0.02	0.18	0.12	90.0	0.01	0.04	0.23
% dev.	0.22	0.62	3.68	1.84	0.77	3.94	2.27	0.78	1.82	1.20	0.72	0.34	0.53	5.62	5.89
200/0.25	LS-Mn	LS-Mw	LS-Mz	Mpeak	Mw-Pd LS-IVn LS-IVv LS-IVz IV-Pd	LS-IVn	LS-IVw	LS-IVz	IV-Pd	Rgn	Rgw	Rgz	Rg-Pd	æ	Log K
1	112100	158700	286400 116400	116400	1.42	0.836	0.97	1.131	1.16	1.16 15.26 16.91	16.91	19.15	1.11	0.713	-3.682
2	115500	164100	313200 119400	119400	1.42	0.833	0.965	1.121	1.16	1.16 15.39 17.05	17.05	19.33	1.11	0.714	-3.696
3	114500	160600	291200 117000	117000	1.4	0.832	96.0	1.116	1.15	15.33	16.94	19.14	1.1	0.702	-3.631
Average	114033	161133	296933	117600	1.41	0.83	0.97	1.12	1.16	15.33	16.97	19.21	1.11	0.71	-3.67
stand.dev.	1747	2739	14290	1587	0.01	0.00	0.01	0.01	0.01	0.07	0.07	0.11	0.01	0.01	0.03
% dev:	1.53	1.70	4.81	1.35	0.82	0.25	0.52	0.68	0.50	0.42	0.43	0.56	0.52	0.94	0.93

Table A.2: Ubbelhode viscometry experiments.

t = time

nrel = relative viscosity

to = initial time

nsp = specific viscosity

c = concentration

Pure PLA

concentration	ì
concentiation	

g/dL	time (sec.)	nrel = t/to	nsp = nrel - 1	ln(nrel)/c	nsp/c
0.5001	85.17	1.617	.617	.961	1.234
0.25	68.05	1.292	.292	1.026	1.169
0.1	59.16	1.123	.123	1.164	1.234
0.05	55.66	1.057	.057	1.108	1.139
0.025	54.19	1.029	.029	1.146	1.162
	•				
extrapolation	to zero using	linear regre	ession	1.156	1.164

170/0.5

concen	tration

oonoona aaon	1				
g/dL	time (sec.)	nrel = t/to	nsp = nrel - 1	ln(nrel)/c	nsp/c
0.5011	93.91	1.783	.783	1.154	1.563
0.2505	71.16	1.351	.351	1.202	1.402
0.1002	59.84	1.136	.136	1.276	1.361
0.0501	56.63	1.075	.075	1.449	1.503
0.025	54.73	1.039	.039	1.539	1.569
	•				
extrapolation	to zero using	linear regre	ession	1.459	1.463

Table A.3: Polylactide film results.

Conditions used:

10" gage length
1.25" sample width

1.0 in/min rate of grip separation 0.1 in/in\*min initial strain rate

0.1 lb preload

pure pla at 170C (340F)

sample thickness: .005"

L L	( ,						
sample #	max lbs	max psi	break lbs	break psi	break %	break region	tensile modulus (psi)
pla.200	17.43	2789	16.6	2656	4.87	grip	174.4
pla.201	17.05	2729	17	2721	2.67	center	149.7
pla.202	19.87	3180	19.72	3155	2.44	grip	184.5
pla.203	18.28	2925	18.22	2915	2.55	center	168.4
pla.204	18.77	3004	17.66	2826	3.24	grip	185
pla.205	17.56	2810	15.42	2467	4.63	center	169.2
pla.206	20.18	3229	18.75	3000	5.81	grip	175.3
pla.207	19.65	3145	19.65	3144	2.52	center	187.6
Average	18.60	2976.38	17.88	2860.50	3.59		174.26
stand.dev	1.21	193.13	1.51	241.08	1.32		12.32
% dev.	6.49	6.49	8.43	8.43	36.71		7.07

pla at 170C (340F) with 0.1%L101

sample thickness: .003"

	•	•			•			
	1	,						tensile
	sample #	max lbs	max psi	break lbs	break psi	break %	break region	modulus (psi)
	pla01.100	9.68	2581	9.393	2505	4.21	center	136
	pla01.101	9.619	2565	8.496	2266	3.52	grip (top)	147.5
	pla01.102	10.17	2713	9.698	2586	2.94	grip (top)	151.3
	pla01.103	9.43	2515	6.226	1660	3.46	grip (bottom)	157.5
	pla01.104	10.99	2931	10.19	2718	4.35	center	163.8
	pla01.105	10.14	2703	10.14	2703	2.23	grip (top)	152.9
	pla01.106	10.08	2687	9.833	2622	3.22	center	130.9
	pla01.107	10.03	2676	4.504	1201	8.89	center	139.1
•	Average	10.02	2671.38	8.56	2282.63	4.10		147.38
	stand.dev	0.48	127.81	2.09	558.16	2.05		11.26
	% dev.	4.78	4.78	24.45	24.45	49.94		7.64

Table A.4: Maleation data from TriSEC.

Pd = polydispersity	a = Mark-Houwink parameter	Log K = log of Mark-Houwink parameter	
n = number average	w = weight average	z = third moment	peak = peak
LS = light scattered	M = molecular weight	IV = intrinsic viscosity	Rg = radius of gyration

180/0/2 LS-Mn	LS-Mn	LS-Mw	LS-Mw LS-Mz Mpeak Mw-Pd LS-IVn LS-IVw LS-IV IV-Pd Rgn Rgw Rgz Rg-Pd a	Mpeak	Mw-Pd	LS-IVn l	LS-IVw	LS-IV	IV-Pd	Rgn	Rgw	Rgz	Rg-Pd	ಡ	Log K
	86200		104700 138200 87000	87000		1.21 0.864 0.945 1.043 1.09 14 14.9 16 1.06 0.71 -3.57	0.945	1.043	1.09	14	14.9	16	1.06	0.71	-3.57
7	77800	00666	135000	85800		0.786	0.891	1.006	1.13	13.2	14.3	15.6	1.08	0.74	-3.73
8	79700	101600	139600	87900	1.27	0.804	0.911	1.033	1.13	13.4	14.5	15.8	0.911 1.033 1.13 13.4 14.5 15.8 1.08	0.75	-3.77
Average	81233	102067	137600	86900	1.25	0.82	0.92	1.03	1.12	13.53	1.12 13.53 14.55 15.77	15.77	1.07	0.73	-3.69
stand.dev.	1105	2434	2358	1054	0.04	0.04	0.03	0.02	0.02	0.42	0.02 0.42 0.29 0.20	0.20	0.01	0.02	0.11
% dev.	5.42	2.38	1.71	1.21	3.02	4.99	2.98	1.86		3.08	2.07 3.08 1.99 1.27	1.27	1.08	2.81	2.92
180/0.1/2 LS-Mn		LS-Mw	LS-Mw LS-Mz Mpeak Mw-Pd LS-IVn LS-IV WLS-IV IV-Pd Rgn Rgw Rgz Rg-Pd a	Mpeak	Mw-Pd	LS-IVn l	LS-IVw	LS-IV	IV-Pd	Rgn	Rgw	Rgz	Rg-Pd	а	Log K
1	009†6		120800 162900 99300	99300	1.28	1.28 0.7 0.813 0.936 1.16 13.6 14.8 16.2 1.09	0.813	0.936	1.16	13.6	14.8	16.2	1.09	0.82	0.82 -4.22
7	96300	121400	121400 166900 102600	102600	1.26	0.736	0.836	0.95	1.14	13.8	15	16.3	0.836 0.95 1.14 13.8 15 16.3 1.08		0.78 4.03
ĸ	006+6	120200	120200 169300 100700	100700	1.27	0.743	0.848	0.97	1.14	13.8	15	16.3	1.08	0.79	4.07
Average	95267		120800 166367 100867	100867	1.27	0.73	0.83	0.95		13.74	1.15 13.74 14.89 16.26	16.26	1.08	0.80	4.10
stand.dev.	200	009	3233	1656	0.01	0.02	0.02	0.02	0.01	0.15	0.15 0.10 0.10	0.10	0.01	0.02	0.10
% dev.	0.95	0.50	1.94	1.64	0.79	3.18	2.14	1.79		1.01 1.11	0.70	09.0	0.53	2.33	2.47

Table A.4 cont.

180/0.25/2   LS-Mn LS-Mw	LS-Mn	LS-Mw	LS-Mz	Mpeak	Mpeak Mw-Pd LS-IVn LS-IV IV-Pd Rgn	LS-IVn I	S-IVw	LS-IV	IV-Pd	Rgn	Rgw	Rgz	Rg-Pd	В	Log K
-	92600	92600 119100	177700	99700	1.29	0.74	0.856	0.856 0.998 1.16 13.7 14.9	1.16	13.7	14.9	16.5	1.09	0.81	4.15
3	86900	86900 112700	161600	94100	1.3	0.723	0.832		0.955 1.15	13.3	14.5	16	1.06	0.77	-3.95
<b>→</b>	87600	87600 113800	162800	94700	1.3	0.73	0.838	96.0	1.15	13.4	14.6	16	1.09	0.76	-3.9
Average	89033	89033 115200	167367	96167	1.30	0.73	0.84	0.97	1.15	13.47	13.47 14.67 16.15	16.15	1.08	0.78	<b>4</b> .00
stand.dev.	3109	3422	8968	3075	0.01	0.01	0.01	0.02	0.01	0.19	0.21	0.28	0.02	0.03	0.13
% dev:	3.49	2.97	5.36	3.20	0.45	1.17	1.48	2.42	0.50	1.45	1.43	1.73	1.60	3.37	3.35
	,														
180/0.5/2	LS-Mn	LS-Mw	LS-Mn LS-Mw LS-Mz	Mpeak	Mpeak Mw-Pd LS-IVn LS-IVv LS-IV IV-Pd	LS-IVn I	S-IVw	LS-IV	IV-Pd	Rgn	Rgw	Rgz	Rg-Pd	а	Log K
_	85300	85300 111100	156900	92500	1.3	0.658	0.75	0.75 0.848	1.14 12.8	12.8	71	15.3	1.09	0.74	-3.83
2	82700	82700 108400	158800	90200	1.31	0.687	0.79	0.912	1.15	12.9	14.1	15.5	1.09	0.75	-3.87
~	87300	87300 114100	164100	94900	1.31	0.67	0.775	0.892	1.16	13	14.2	15.7	1.09	0.78	4.01
Average	85100	85100 111200	159933	92533	1.31	0.67	0.77	0.88	1.15	12.91	12.91 14.08	15.48	1.09	0.76	-3.90
stand.dev.	2307	2851	3731	2350	0.01	0.01	0.02	0.03	0.01	0.10	0.13	0.20	0.00	0.02	0.10
% dev:	2.71	2.56	2.33	2.54	0.44	2.17	2.62	3.70	0.87	0.76	0.93	1.28	0.00	2.47	2.45
200/0.1/2	LS-Mn LS-Mw LS-Mz	LS-Mw	LS-Mz	Mpeak	Mpeak Mw-Pd LS-IVn LS-IVw LS-IV IV-Pd	LS-IVn I	S-IVw	LS-IV	IV-Pd	Rgn	Rgw	Rgz	Rg-Pd	а	Log K
-	104400	104400 128800	174300 105500	105500	1.23	0.768	0.871	0.982	1.13	14.4	15.5	16.8	1.07	0.82	4.23
2	97500	97500 122200	164700 101700	101700	1.25	0.763	0.869	0.981	1.14	14.1	15.2	16.5	1.08	0.8	4.09
3	98500	98500 124700	165100	165100 101800	1.27	0.792	0.888	0.978	1.12	14.3		16.6	1.08	0.71	-3.66
Average	100133	100133 125233	168033	168033 103000	1.25	0.77	0.88	0.98	1.13	14.26	14.26 15.35 16.60	16.60	1.08	0.78	-3.99
stand.dev.	3729	3332	5431	2166	0.02	0.05	0.01	0.00	0.01	0.17	0.15	0.14	0.01	90.0	0.30
% dev.	3.72	2.66	3.23	2.10	1.60	2.00	1.19	0.21	0.88	1.17	1.00	0.85	0.54	7.28	7.46

Table A.4 cont.

Log K	-3.83	1.09 0.8 -4.04	-3.87	-3.91	0.11	2.83	Log K	-3.83	4.	4.13	-4.02	0.17	4.16
В	0.76	0.8	0.77	0.78	0.02	2.57	В	0.74	<b>8</b> .0	0.8	0.78	0.03	4.24
Rg-Pd	1.09	1.09	1.09	1.09	0.00	0.00	Rgz Rg-Pd a	1.07	1.1 0.8 -4.11	1.1	1.09	0.02	1.59
Rgz	15.6	15.7	15.3	15.53	0.22	1.39	Rgz	15.1	14.9	15.1	14.99	0.10	0.65
Rgw	14.2	14.4	13.9	1.16 12.98 14.17 15.53	0.01 0.23 0.22 0.22	0.50 1.78 1.57 1.39	Rgw	13.9	13.5	13.6	1.15 12.55 13.66 14.99	0.03 0.37 0.22 0.10	2.50 2.98 1.65 0.65
Rgn	13	13.2	12.7	12.98	0.23	1.78	Rgn	13	12.3	12.4	12.55	0.37	2.98
IV-Pd	1.15	1.16	1.16	1.16	0.01	0.50	IV-Pd	1.12	1.17	1.17 12.4 13.6 15.1	1.15	0.03	2.50
S-IV	1.012	0.999	1.011	1.01	0.01	0.72	S-IV	0.831	0.719 0.832 1.17 12.3 13.5 14.9	0.828	0.83	0.00	0.25
S-IVw	1.31 0.765 0.883 1.012 1.15 13 14.2 15.6 1.09 0.76 -3.83	0.873 0.999 1.16 13.2 14.4 15.7	0.879	0.88	0.01	0.57	S-IVw	1.25 0.665 0.743 0.831 1.12 13 13.9 15.1 1.07 0.74 -3.83	0.719	0.715	0.73	0.02	2.09
LS-IVn l	0.765	0.754	0.758	0.76	0.01	0.73	LS-IVn I	0.665	0.613	0.612	0.63	0.03	4.81
Mw-Pd	1.31	1.28	1.3	1.30	0.02	1.18	Mw-Pd	1.25	1.33	1.32	1.30	0.04	3.35
Mpeak	81400	86000	26800	81400	4600	5.65	Mpeak Mw-Pd LS-IVn LS-IVw LS-IV IV-Pd Rgn Rgw	91000	88900	90700	90200	1136	1.26
LS-Mz	76200 99500 138300 81400	81000 103700 141500	129800	136533	6047	4.43	LS-Mz	88100 109700 149500 91000	79000 104700 152800	82500 108800 164000	155433	2009	4.89
LS-Mw	99500	103700	72200 94200	76467 99133	4761	4.80	LS-Mw	109700	104700	108800	83200 107733	4590 2665	5.52 2.47
LS-Mn	76200	81000	72200	76467	7 90++	5.76	LS-Mn	88100	79000	82500	83200	<b>12</b> 80	5.52
200/0.25/2 LS-Mn LS-Mw LS-Mz Mpeak Mw-Pd LS-IVn LS-IV WLS-IV IV-Pd Rgn Rgw Rgz Rg-Pd a Log K	-	2	е	Average	stand.dev.	% dev.	200/0.5/2 LS-Mn LS-Mw LS-Mz	-	2	3	Average	stand.dev.	% dev.

Table A.5: Titration results of maleated samples.

Titrating against 0.004 M NaOH

Normality of morpholine 0.05238 Normality of HCl 0.007179

Temperature			sample		moles of	grams	
ID#	(°C)	%L101	wt (g)	mL HCl	anhydride	anhydride	% anhydride*
1	180	0.5	1.07	4.628	7.154E-05	0.007	0.6556
2	180	0.5	1.077	4.65	7.138E-05	0.007	0.6499
3	180	0	1.021	13.63	6.91E-06	0.0007	0.0664
4	180	0.25	0.914	7.792	4.882E-05	0.0048	0.5238
5	180	0.25	0.868	9.341	3.77E-05	0.0037	0.4259
6	180	0.1	1.01	11.173	2.455E-05	0.0024	0.2383
7	180	0.1	0.9	11.836	1.979E-05	0.0019	0.2156
8	200	0.1	0.996	10.651	2.83E-05	0.0028	0.2786
9	200	0.1	1.051	10.387	3.019E-05	0.003	0.2817
10	200	0.25	0.796	9.421	3.713E-05	0.0036	0.4574
11	200	0.25	0.849	8.927	4.067E-05	0.004	0.4698
12	200	0.5	1.004	5.445	6.567E-05	0.0064	0.6414
13	200	0.5	1.13	3.314	8.097E-05	0.0079	0.7026

<sup>\*</sup> weight percent of sample which is anhydride, i.e., that has maleic anhydride functional group

# **BIBLIOGRAPHY**

## **BIBLIOGRAPHY**

Akkapeddi M.K., et al, Polymer Preprints 29, 567 (1988).

Argyropoulos, D.C., L. Nie, and R. Narayan, "Amylose-Styrene Maleic Anhydride Copolymer Blends", paper presented at AICHE meeting (1991).

Barakat, I., Ph. DuBois, R. Jerome, Ph. Teyssie, Journal of Polymer Science: Part A: Polymer Chemistry, 31, 505 (1993).

Brown, S.B. and C.M. Orlando, in <u>Encyclopedia of Polymer Science and Engineering</u>, John Wiley & Sons, Vol.14 p169 (1988).

Callais, P.A. and R.T. Kazmierczak, ANTEC'90, p1921 (1990).

Conn, J., R. Oyasu, M. Welsh, J.M. Beal, Am. J. Surg., 128, 19 (1974).

Dalvag H., C. Klason, H.E. Stromvall, *International Journal of Polymeric Material*, 11, 9 (1985).

Damani, N.C., US Patent 5,198,220 (1993).

Davidovits, P., M.D. Egger, Nature, 233, 831 (1969).

De Roover, B., M. Sclavons, V. Carlier, J. Devaux, R. Legras, A. Momtaz, Journal of Polymer Science: Part A: Polymer Chemistry, 33, 829 (1995).

Doane, W.M., C.L. Swanson, G.F. Fanta, "Emerging Polymeric Materials Based on Starch", in *Emerging Technologies for Materials and Chemicals from Biomass*, ACS Symp. Ser. 476, R.M. Rowell, T.P. Schultz, and R. Narayan, Eds., p197 (1992).

Eitenmuller, J., H. Rackur, W. Wimmer, M. Weiss, US Patent 4,610,692 (1986).

Flory, P.J., Principles of Polymer Chemistry, Cornell University Press (1967).

Fritz, H.G. and B. Strohrer, Intern. Polym. Proc. 1, 31 (1986).

Gaylord, N.G. and J.Y. Koo, J. Polym. Sci. Polym. Lett. Ed., 19, 107 (1981).

Gaylord, N.G. and M. Mehta, J. Polym. Sci. Polym. Lett. Ed., 20, 481 (1982).

Gaylord, N.G. and P. Elayaperumal, Die Angewandte Makromolekulare Chemie, 117, 195 (1983a)

Gaylord, N.G. and M.K. Mishra, J. Polym. Sci. Lett. Ed., 21, 23 (1983b).

Gaylord, N.G., M. Mehta, R. Mehta, J. Appl. Polym. Sci., 33, 2549 (1987).

Gaylord, N.G. and R. Mehta, J. Polym. Sci. Polym. Chem. Ed., 26, 1189 (1988).

Gaylord, N.G., R. Mehta, V. Kumar, M. Tazi, J. Appl. Polym. Sci., 38, 359 (1989).

Gaylord, N.G., R. Mehta, D.R. Mohan, V. Kumar, J. Appl. Polym. Sci., 44, 1941 (1992).

Gilding, D.K., in <u>Biocompatibility of Clinic Implant Materials</u>, D.F. Williams, Ed., CRS Press, Boca Raton, Vol. 2, 9 (1982).

Glassner, W.G. 'Novel Structural Materials from Lignin', in *Wood Processing and Utilization*, J.F. Kennedy, G.O. Phillips, and P.A. Williams, Eds., p163 (1989).

Gogolewski, S., M. Jovanovic, S.M. Perren, J.G. Dillon, M.K. Hughes, *Polym. Degrad. and Stab.*, 40, 313 (1993).

Goodson, J.M., US Patent 4,764,377 (1988).

Hamielic, A.E., P.E. Gloor, S. Zhu, Y. Tang, COMPALLY'90, p85 (1990).

Heller, J., CRC Crit. Rev. Ther. Drug Carrier Syst., 1, 39 (1985).

Hogt, A., ANTEC'88, p1478 (1988).

Jacobs, C., P. Dubois, R. Jerome, P. Teyssie, *Macromolecules*, 24(11), 3027 (1991).

Jamshidi, K., S-H Hyon, Y. Ikada, Polymer., 29, 2229 (1988).

Johnson, J.B., G.L. Funk, Analytical Chemistry. 27(9), 1464 (1955).

Kino G.S., T.R. Corle, Physics Today, 55 (Sept. 1989).

Krishnan, M., R. Narayan, 'Compatibilization of Biomass Fibers with Hydrophobic Materials', in Materials Interactions Relevant to Recycling of Wood-Based Materials, Mat. Res. Soc. Symp. Proc., R.M. Rowell, T.L. Laufenberg, and J.K. Rowell Eds., 266, 93 (1992).

Lambla, M., R.X. Yu, S. Lorek, "Coreactive Polymer Alloys", in *Multiphase Polymers: Blends and Ionomers*, ACS symp. ser.395, Utracki, L.A. and Weiss, R.A., Eds., p67 (1989).

Lindow J.T., S.D. Bennet, I.R. Smith, Proc. Soc. Photo-Opt. Instrum. Eng. 565, 81 (1985).

McNeill, I.C., H.A. Leiper, Polymer Degradation and Stability, 11, 267 (1985).

Mechels S., M. Young, Proc. Soc. Photo-Opt. Instrum. Eng. 1556, 164 (1991).

Mehta, R.C., R. Jeyanthi, S. Calis, B.C. Thanoo, K.W. Burton, P.P. DeLuca, *Journal of Controlled Release*, 29, 375 (1994).

Meier, D.J., Heterophase Polymer Systems, Michigan Molecular Institute, notes for course 702 (1991).

Minsky M., US Patent 3,013,346 (1961).

Mizuno S., et al., US Patent 4,085,086 (1978).

Morita, H., T. Akagawa, Y. Kita, US Patent 4,694,031 (1987).

Murayama, T., <u>Dynamic Mechanical Analysis of Polymeric Material</u>, Elsevier Scientific Publishing Co. (1978).

Narayan, R., 'Biomass (Renewable) Resources for Production of Materials, Chemicals, and Fuels - A Paradigm Shift', in *Emerging Technologies for Materials and Chemicals from Biomass, ACS Symp. Ser. 476*, R.M. Rowell, T.P. Schultz, and R. Narayan, Eds., p1 (1992).

Pabedinskas, A., W.R. Cluett, S.T. Balke, *Polymer Engineering and Science*, 29(15), 993 (1989).

Pabedinskas, A., W.R. Cluett, S.T. Balke, *Polymer Engineering and Science*, 34(7), 585 (1994a).

Pabedinskas, A., W.R. Cluett, *Polymer Engineering and Science*, **34(7)**, 598 (1994b).

Rauwendaal, C., Polymer Extrusion, Hasner Publishers, (1986).

Russell, K.E., Journal of Polymer Science: Part A: Polymer Chemistry, 33, 555 (1995).

Schmitt, E.E. and R.A. Polistina, US Pat. 3,297,033 (1967).

Schneider, A.K., US Patent 3,797,499 (1974).

Schneider, A.K., US Patent 3,636,956 (1972).

Schneider, A.K., Canadian Patent 863,673 (1971).

Siggia, S., J.G. Hanna, Analytical Chemistry., 23(11), 1717 (1951).

Sneller, J.A., Mod Plast. Int., 42 (1985).

Sperling, L.H., <u>Introduction to Physical Polymer Science</u>, John Wiley & Sons, Inc. (1992).

Sperling, L.H., Carraher, <u>Concise Encyclopedia of Polymer Science and Engineering</u>, J.I. Kroschwitz, ed., Wiley Interface (1990).

Stassen, S., N. Nihant, V. Martin, C. Grandfils, R. Jerome, P. Teyssie, *Polymer*, 35(4), 777 (1994).

Suwanda, D., S.T. Balke, ANTEC'89, Conf. Proc. 589 (1989).

Suwanda D., R. Lew, S.T. Balke, Journal of Applied Polymer Science, 35, 1019 (1988a).

Suwanda D., R. Lew, S.T. Balke, Journal of Applied Polymer Science, 35, 1033 (1988b).

Tian D., P. Dubois, R. Jerome, P. Teyssie, Macromolecules, 27, 4134 (1994).

Triacca, V.J., P.E. Gloor, S. Zhu, A.N. Hrymak, A.E. Hamielec, *Polymer Engineering and Science*, 33(8), 445 (1993).

Tzoganakis, C., J. Vlachopoulos, A.E. Hamielec, Polym. Eng. Sci., 28, 170 (1988).

Tzoganakis, C., Y. Tang, J. Vlachopoulos, A.E. Hamielec, *Polym. Plast. Technol. Eng.*, 28, 319 (1989).

Udding, A.C., US Patent 4,921,914 (1988).

Van Dijk, J.A.P.P., J.A.M. Smit, Journal of Polymer Science: Polymer Chemistry Edition, 21, 197 (1983).

Viscotek Right Angle Laser Light Scattering Operations Manual (1992).

Yau, W.W., J.J. Kirkland, D.D. Bly, <u>Modern Size-Exclusion Liquid</u> <u>Chromatography</u>, John Wiley and Sons (1979).

Young J.Z., F. Roberts, *Nature*, 167, 231 (1951).

Yves, M.T., US Patent 3,531,561 (1970).

Zapf T., R.W. Wijnaendts-van-Resandt, Microelectron. Eng. 5, 573 (1986).

